Physics Lib

APR 28 1947

REGISTERED NO. M 3121

PROCEEDINGS

OF THE

INDIAN ACADEMY

OF SCIENCES

VOL. XXV] *SECTION A* [NO. 2

FEBRUARY, 1947

Price Rs. 2 or 3 Sh. *Annual Subscription Rs. 18*

PRINTED AT THE BANGALORE PRESS, BANGALORE CITY, BY G. SRINIVASA RAO, SUPERINTENDENT, AND PUBLISHED BY THE INDIAN ACADEMY OF SCIENCES, BANGALORE.

DIFFERENTIATION TRENDS IN THE DECCAN TRAPS

By N. A. Vemban, M.Sc.

Received July 1, 1946
(Communicated by Prof. C. Mahadevan, F.N.I., F.A.SC.)

Abstract.—In this study the author has critically reviewed the existing literature on the Deccan traps, brought together all the published analyses (55 in number) and studied their petro-chemical relationships. The material under study has come from four regions, *viz.*, the Central Provinces, Pavagad Hills, the Bombay Coast and Kathiawar. The analyses are first grouped according to the major rock types which they represent and the peculiarities in each group studied. A regional grouping of the rocks is adopted for studying the differentiation trends graphically using the variation diagram as also Prof. Niggli's QLM diagram. It is deduced from these studies that the original magma is probably an ultrabasic (essexitic or picritic) type which proceeds during differentiation towards both the calc-alkaline and alkaline fields, the former predominating. There does not seem to be much evidence for the existence of two separate primary basic magmas (tholeiitic and olivine-basaltic) as advocated by Kennedy. A single magma-type more basic than plateau basalts would appear to be adequate for the evolution of rocks in the Deccan trap assemblage, as shown by Kuno.

The study reveals also that much more petrological and chemical work should be done on some of the differentiated groups and attention should be focussed on the solution of the mechanism of differentiation and the localisation of the resultant products in certain regions.

Introduction

Towards the close of the Mesozoic era and during the early part of the Tertiary period a series of highly fluid lavas were extruded from fissures and cracks in the earth's crust as a result of movements connected with the disruption of the great southern continent, Gondwanaland. They spread over a large part of Peninsular India in thick horizontal sheets of basalts and dolerites, inundating and filling up the pre-trappean valleys and the topographic irregularities of the country. This volcanic rock-formation which covers at the present day a total area of some 200,000 sq. miles in Bombay, Kathiawar and Cutch, Central Provinces, Central India and parts of the

Deccan and occupies about one-seventh of the Indian Peninsula is known in Indian Geology as the Deccan traps. The present distribution of the Deccan traps does not give us a clear idea of their past extent, as denudation has continuously been at work through long ages since their consolidation, and it is possible that extensive stretches of this formation might have been removed by the agents of weathering. Small outlying patches of the Deccan traps are found in the west in Sind, in the east in Sirguja and Jashpur, and in the south-east near Rajahmundry in the Madras Presidency, these being separated from the main mass of the formation by long distances.

The geology and petrographic characters of the rock-types comprising the Deccan traps have been described and their chemical characters and petrogenesis discussed by several eminent geologists. As many as sixty quantitative chemical analyses of the Deccan traps have been made by different investigators dating from 1922 when Dr. H. S. Washington published a series of eleven analyses of these rocks supplied by the Geological Survey of India, and gave an account of their mineralogical characters. In 1926 Dr. M. S. Krishnan described the rocks of the Girnar and Osham Hills of the Kathiawar Peninsula and made a chemical study of them. About the same time the interesting dyke rocks from the West Gir Forest, Kathiawar, were studied by S. K. Chatterjee and his studies were published in 1932. This was followed by the work of Prof. K. K. Mathur and P. R. J. Naidu (1932), and Prof. A. S. Kalapesi and G. P. Contractor (1935, 1936) on the petrology of the Deccan traps in the Bombay Island and neighbouring areas. Sir L. L. Fermor gave, in 1934, an admirable account of the chemical characters of the Linga traps, which he had mapped in collaboration with Dr. C. S. Fox several years previously. In 1936 Dr. H. Crookshank gave an account of the geology of the northern slopes of the Satpura Hills in which there is only one analysis of a porphyrite from near Jamundhonga. Apart from the analyses given in the above literature, four analyses of Deccan traps from the Pavagad Hills given by V. S. Dubey (1929) in his thesis for the Ph.D. Degree of the London University and two analyses of traps from Kathiawar and Pavagad Hills made by Dubey and published by M. P. Bajpai (1935) are also available and are included in the present study. The present paper is based entirely on a study of these analyses compiled from the literature cited.

The object of this paper is to study the petrochemistry of the Deccan traps and the history and evolution of the magma in the formation of the various types using the methods developed by Prof. Dr. P. Niggli of Zürich. As a knowledge of the petrology of the different types, their field characters, mode of occurrence, genetic relationship and geological history is essential

for presenting the petrochemistry, a brief recapitulation of these features is given below. Every effort has been made to consult all the papers published so far on the Deccan traps and it is hoped that no important paper has been omitted.

Field Characters of the Deccan Traps

The Deccan traps occur as extrusive flows and as intrusive sills and dykes. The flows are in the form of sheets of extensive dimensions, and have been poured out subaerially, evidences for which are found in the vesicular surface of the flows and the cooling cracks which have occasionally given rise to columnar jointing. The flows are remarkably horizontal throughout their extent; but a deviation from horizontally is noticeable in the Bombay Coast where the sheets are found to exhibit a gentle dip towards the sea. Slight inclination, folding and even faulting are seen in the Satpura and the Linga region of the Central Provinces, Kandesh and the Rajpipla hills near Broach. The dips and folds are believed to have been brought about by post-trappean disturbances due to tectonic causes, for the inter-trappean lacustrine beds which must originally have been deposited horizontally have also been affected by them similarly.

The lavas have spread out intermittently in a series of sheets, the successive flows being often marked off from each other by beds of volcanic ash or scoriæ and by intertrappean horizons of sedimentary limestones, chert and 'green earth'. The fresh-water deposits with remains of plants and animals intervening between the flows and the atmospheric weathering and denudation of the surface of the flows provide evidences of the lapse of long intervals of time between succeeding flows of lavas. The flows attain a maximum thickness of more than 7,000 ft. near the coast of Bombay, but become thinner away from it and are only about 500 ft. on the eastern edge at Amarkantak, 200 ft. near Belgaum in the south and 100 to 200 ft. in Sind in the north-west. The average thickness in the entire area may be estimated at about 2,000 ft. The thickness of individual flows varies from a few feet to as much as 120 ft. with an average of about 40-60 ft. At Bhusawal, a bore-hole which penetrated a depth of 1,217 ft. showed the existence of 29 flows, the average thickness of each flow being 40 ft. In the Linga region of the Chhindwara district in the Central Provinces, five flows with an average thickness of 60 ft. were encountered in a section whose total thickness was 300 ft.

A typical individual flow consists of a thin, porous or vesicular base which, passing up into non-vesicular columnar basalt, becomes by gradational increase in the grain-size of the minerals a coarse-grained dolerite in

the centre, and further up basaltic again and finally vesicular and amygdaloidal. There are deviations from this general succession in many places and the flows may be amygdaloidal, porphyritic or fine-grained and dense throughout their thickness.

The flows often pass into sills. The sills contain no open cavities or amygdales and are mostly compact, although occasionally vesicular. Underneath the sills and flows, but visible only in those localities where the formation is quite thin as in the marginal areas, there are numerous ramifying and massive dykes of all sizes and thicknesses. They are found in Cutch, in the Rajpipla hills near Broach, in the West Gir Forest in Kathiawar, and in the Narbada Valley as intrusions in the Gondwana rocks. The dykes may be regarded as the feeders of the flows and sills. Variation is noticed in the grain-size of mineral constituents of these dykes and sills from fine-grained basalts to coarse-grained dolerites and gabbros, and they may be also of composite nature and of porphyritic habit.

The Deccan traps have been divided into three groups as follows:—

Upper Traps (1,500 ft.).—Bombay and Kathiawar; with numerous inter-trappean horizons and layers of volcanic ash.

Middle Traps (4,000 ft.).—Central India and Malva; with numerous ash beds above and devoid of inter-trappeans.

Lower Traps (500 ft.).—Central Provinces and eastern areas; with inter-trappean beds and rare occurrences of ash beds.

The volcanic activity that built up the plateau of the Deccan is thought to have occurred in three distinct cycles. The first cycle of eruptive activity was marked by long periods of quiescence between flow and flow when sedimentary deposits were laid down in lakes that had collected in minor depressions and corrugations in the bedded basalts. The main area of activity was situated in the eastern tracts in the earlier period, gradually shifting towards the west. The second period of activity was more pronounced and powerful than the first and enormous volumes of lava were ejected at such frequent intervals that there was little or no time for the formation of sedimentary beds. Then after an interval of long quiescence, the third cycle operated in a limited area around Bombay (presumably extending westwards into the area now occupied by the sea) and the eruptions were intermittent as they represented the later phases in the decline of volcanic activity.

The ash beds associated with the lower and upper traps and to some extent with the middle traps indicate that at times the activity attained an

appreciable degree of explosive violence. This explosive phenomenon was not only short and temporary but also confined to limited areas.

Petrology of the Deccan Traps

The Deccan traps exhibit a remarkable uniformity of mineralogical characters and chemical composition. The normal trap is basaltic or doleritic with an average specific gravity of 2·90, the maximum being 3·05 and the minimum 2·58. Specimens with the higher specific gravity are sometimes to be found in the lower parts of the flows and sills where olivine and augite seem to have accumulated on account of gravitative crystal settling. The vesicular and amygdaloidal types are always less dense than the average compact varieties.

The normal compact doleritic to basaltic type extends over very large areas. This normal type is black to dark-greenish grey in colour with brownish or purplish tint and varies in grain-size from dense, compact aphanites through fine-grained basalts to rather coarse-grained dolerites. In the western part of the formation, near Bombay, ultrabasic as well as acid types are associated with the main basalt with intrusive relationship. The ultrabasic types which are chiefly in the form of dykes in the main mass of basalt are confined to the western edge of the trap formation in Bombay and Kathiawar, while the acid and sub-acid types are found mainly along two zones, one running from the Pavagad Hills to Bombay and the other from the Narbada Valley to Porbandar State in Kathiawar. The ultrabasic types comprise oceanite, ankaramite and limburgite; the intermediate types, andesite, trachyte and syenite; and the acid types, granophyre, felsite, rhyolite, obsidian and pitchstone. In the Girnar and Osham Hills in Kathiawar, monzonite, nepheline syenite and lamprophyres occur as intrusives in the basalts.

Microscopic characters.—Under the microscope the normal Deccan trap varies from dense crypto-crystalline or hyalitic basalt to a coarse-crystalline dolerite. The main mineral constituents are feldspars, augite, and iron-ore, while the minor ones are olivine, biotite, hornblende, quartz, palagonite, zeolite and apatite. In addition to these minerals, there is always a certain amount of interstitial glass showing varying degrees of devitrification.

Feldspars.—The feldspar is the dominant constituent of the normal rocks, forming about 40 to 45 per cent. of the volume. It occurs as small idiomorphic laths and prisms, and phenocrysts which may be in glomeroporphyritic aggregates. The equant tables may be in ophitic to subophitic intergrowth with augite. The laths are generally twinned according to the

Albite law and vary in composition from 40% An to 80% An with an average value of 60% An. The phenocrysts exhibit Albite as well as Carlsbad laws and are also sometimes zoned with a maximum variation of 20% An between the core and the rim, the centre being the most basic part. The feldspar is to a certain extent the earlier mineral to crystallise, but it is soon joined by augite so that both the minerals are found crystallised simultaneously evidenced by subophitic and doleritic textures.

Augite.—The next abundant mineral after feldspar is augite, forming about 30 to 35 per cent. It belongs to the enstatite-augite or pigeonite group. It is greenish or brownish grey in hand specimens, but colourless in thin sections. The optic axial angle ($+2V$) varies between 20° and 45°. The augite is ophitic, subophitic or granular and exhibits intersertal relationship to feldspar. It is often intergrown with magnetite.

Glass.—A certain amount of interstitial glass is often present in the basaltic types. The glass is deep brown or straw yellow in colour and may also be nearly opaque, being dusted with numerous grains of incipient minerals. In some specimens the glass is cryptocrystalline, while in others it is finely crystalline with the development of microlites of feldspar and of idiomorphic quartz grains and augite. The percentage of glassy matter varies greatly bearing an inverse proportion to augite and magnetite. In some cases the glass is highly altered to chlorophaeite, celadonite and delessite with dusty magnetite inclusions.

Iron ores.—The iron ores are in irregular grains, thin needles and skeletal crystals. They may have been formed directly from crystallisation of the magma, but some grains are due to the secondary alteration of glass. They are mostly titaniferous as confirmed by the appreciable amount of titanium revealed in the analysis.

Quartz and Micropegmatite.—Quartz and micropegmatite are common in some types, found in the upper part of the sills. Quartz in the micropegmatitic portions sometimes shows inclusions of apatite indicating that the micropegmatite is of primary origin.

Olivine.—The mineral is found only occasionally in the coarser-grained varieties, such specimens coming mostly from the lower portions of sills and flows. The mineral is altered to iddingsite and serpentine.

Biotite and Hornblende.—These minerals are absent in normal types, but may be found in specimens of advanced differentiation. In some cases they appear to have resulted from the alteration of augite.

Secondary minerals.—Several secondary minerals are found in the Deccan traps as cavity fillings during the later stages of igneous activity and as pro-

ducts of alteration and replacement. The zeolites are typical of these, the most common ones being stilbite, apophyllite, heulandite, laumontite, scolecite and chabazite. Calcite, chalcedony (and its varieties) are also found in the amygdales. The cavities may be lined with chlorophaeite and delessite and sometimes filled with them. The alteration products are palagonite, iddingsite and serpentine, these minerals being formed from the main constituents such as feldspar, augite, olivine and glass.

Chemical Characters of the Deccan Traps

From field observations it has been found that a diverse assemblage of rock-types occurs in the Deccan trap formation even though the main bulk consists of undifferentiated basalt and dolerite. From the tables given later (Tables I, II, IV, V and VI) it will be seen that SiO_2 which plays an important rôle in the determination of several rock-types varies from 42·21% to 73·24% with a range of 31·03%. According to the degree of saturation they may be undersaturated, saturated or oversaturated, showing olivine or nepheline at one end and quartz at the other. Based on mineralogical characters which have a direct bearing on the conditions obtaining during the consolidation of the magma, the rocks fall into the following groups, each including several types of allied chemical or mineralogical characters:— (1) Peridotites, (2) Dolerites and Basalts, (3) Andesites, (4) Syenites and trachytes, (5) Rhyolites, granophyres, etc. The peridotites and pyroxenites are all undersaturated ultrabasic rocks rich in pyroxene and olivine and low in feldspar. Dolerites and basalts may be either undersaturated or oversaturated, but they are essentially basic with predominant calcic plagioclase and ferromagnesians. The difference between the basaltic group and the peridotites is the higher percentages of calcium oxide, alumina and alkalis, with dominant soda and lower magnesia and iron-oxides in the former. The silica percentage in the basic types varies from 45% to 52%. The intermediate rocks comprise andesites, syenites and trachytes in which the silica percentage is between 52% and 61% with corresponding increase in calcium and alkalis, and decrease in magnesia and iron-oxides. This difference is reflected in the rocks in their having more plagioclase and orthoclase and less ferromagnesians. In certain of the syenites the silica may not be sufficient to saturate all alkalis so that nepheline is formed in preference to plagioclase. The last group, containing over 61% silica, is oversaturated with the result that it shows free quartz.

Peridotites

This group comprises limburgite, oceanite and ankaramite. These rocks are ultrabasic, rich in olivine, augite and iron-ores with subordinate

TABLE I

Chemical Analyses of Peridotites

		1	2	3
SiO_2	..	42·21	43·26	44·90
Al_2O_3	..	15·27	10·85	11·00
Fe_2O_3	..	7·72	3·01	1·65
FeO	..	8·75	7·80	9·57
MnO	..	Tr.	..	..
MgO	..	6·58	18·32	15·98
CaO	..	9·15	10·31	10·97
Na_2O	..	5·37	1·23	1·47
K_2O	..	1·49	0·53	0·75
TiO_2	..	0·54	2·12	2·88
P_2O_5	..	0·15	..	..
H_2O	..	2·56	3·60	..
		99·79	101·03	99·17
Sp. Gr.	..	2·91	3·02	2·98
NIGGLI VALUES				
si	..	88·16	78·59	84·45
al	..	18·79	11·61	12·19
fm	..	47·89	65·55	62·14
c	..	20·48	20·07	22·09
alk	..	12·84	2·77	3·58
ti	..	0·85	2·89	4·08
p	..	0·14	..	..
k	..	0·154	0·220	0·252
mg	..	0·427	0·756	0·720
C. I. P. W. NORM				
Or	..	8·74	2·78	3·89
Ab	..	7·34	9·96	12·05
An	..	13·12	22·80	18·90
Ne	..	20·62	..	..
Di	..	25·33	22·38	28·17
Ol	..	9·37	30·73	27·45
Mt	..	11·21	4·41	2·32
Il	..	1·03	3·95	5·32
Ap	..	0·37	..	..
Water	..	2·56	3·60	..
		99·69	100·61	98·10
Q	..	14·6	19·2	21·3
L	..	43·0	22·0	23·2
M	..	42·4	58·8	55·5
n	..	0·19	0·61	0·55
y	..	0·23	0·15	0·18
Total alk. feldspars	..	15·08	12·74	15·94
Total feldspars	..	29·20	35·54	34·84
Total ferromagnesians	..	34·70	53·11	55·62
Total iron ores	..	12·24	8·36	7·64

feldspar. The minor constituents are chlorite, biotite and serpentine formed from the main constituents by alteration. When olivine is the predominant ferromagnesian mineral the rock is termed oceanite, while a rock corresponding to oceanite but rich in glass is designated limburgite. With predominant augite the rock-type is known as ankaramite. The chemical composition, Niggli values and the C.I.P.W. norm of these rocks are given in Table I. A short account of the mineralogical characters of these rocks is given in the descriptions of these rocks given below in the table.

From the chemical composition it will be seen that oceanite and ankaramite have more or less similar composition, while limburgite differs greatly from these two rock-types. Compared with the other two types, limburgite has lower silica, magnesia, calcium oxide and titania, and higher alumina, iron oxides and alkalis. This difference in composition is reflected in both the Niggli values and the norm. The norm shows the rocks to be comparatively higher in orthoclase and lower in plagioclase. The total alkali feldspars are higher, but the total feldspars are lower than in the other two types. Nepheline is peculiar to this rock compared to the other two in which it is not found. There is no marked difference in the diopside molecule which is intermediate between the values for oceanite and ankaramite, but in the case of olivine, it will be seen that its percentage is very low compared to the other two types. Magnetite is comparatively high while ilmenite is low. When we compare the QLM and $\pi\gamma$ values, we see that quartz is lower and that the leucocratic and melanocratic constituents are in about equal proportions, which is not so in the case of the other two types. The proportion of normative anorthite to the total normative feldspars represented by the value π is lower, while the proportion of normative wollastonite to the total normative ferromagnesians is higher than in the other two types.

Even though oceanite and ankaramite do not differ greatly from each other, the latter is richer in silica, alumina, ferrous oxide, calcium oxide and alkalis, and poorer in ferric oxide, magnesia and titania than the former. This difference in chemical composition expresses itself in the ankaramite by the higher amounts of alkali feldspars (the total feldspars in the two are about the same with a higher percentage of 0·70 in oceanite), diopside and ilmenite and lower amounts of olivine and magnetite. More over, diopside is higher in percentage than olivine, as is the case also mineralogically. The above differences as well as the QLM and $\pi\gamma$ values clearly indicate that differentiation has been at work in enriching the ankaramite in quartz and leucocratic constituents, with concomitant impoverishment in melanocratic minerals.

TABLE

Chemical Analyses of

	4	5	6	7	8	9	10
SiO_2 ..	46·14	46·80	46·82	46·90	47·02	47·30	47·50
Al_2O_3 ..	20·93	7·86	14·70	14·29	12·46	14·33	17·12
Fe_2O_3 ..	3·80	4·26	2·53	1·82	5·80	14·31	2·77
FeO ..	6·27	7·89	11·58	8·31	9·25		7·68
MnO ..	*n.d.*	0·30	0·12	0·27	0·19	*n d.*	0·15
MgO ..	3·70	14·79	6·90	8·95	4·51	5·93	4·00
CaO ..	11·30	10·96	10·10	13·29	9·90	11·00	8·37
Na_2O ..	2·90	2·93	3·60	1·59	4·92	3·10	5·75
K_2O ..	0·60	0·83	0·50	0·56	1·50	0·97	0·64
TiO_2 ..	3·50	1·80	3·30	0·82	2·56	2·16	1·37
P_2O_5 ..	0·42	0·19	0·15	0·40	0·69	*n.d.*	Tr.
H_2O^+ ..	0·11	0·86	0·32	2·89	1·54	1·09	1·96
H_2O^- ..	..	1·10	0·24	..			1·04
	99·67	100·57	100·86	100·19[1]	100·34	100·19	99·85[2]
Sp. Gr. ..	2·83	2·97	3·00	..	2·90	3·00	..
Tem. C. ..	..	..	..	..	..	..	..

[1] Includes 0·10 CO_2 [2] Includes 1·50 CO_2

si ..	111·87	90·31	103·49	101·0	110·27	108·87	119·87
al ..	29·90	8·94	19·14	18·13	17·21	19·44	25·45
fm ..	33·01	61·91	48·53	47·12	44·51	45·11	36·83
c ..	29·34	22·65	23·91	30·65	24·86	27·12	22·63
alk ..	7·75	6·50	8·42	4·10	13·42	8·33	15·09
ti ..	6·38	2·61	5·48	1·33	4·51	3·73	2·61
p ..	0·44	0·15	0·15	0·36	0·69	..	..
k ..	0·120	0·157	0·084	0·189	0·167	0·171	0·069
mg ..	0·405	0·687	0·468	0·609	0·354	0·451	0·408
Q ..	..	..	..	..	..	..	..
Or ..	3·56	4·90	2·95	3·34	8·86	..	3·78
Ab ..	24·54	15·49	24·59	13·48	24·18	..	35·50
An ..	42·31	5·84	22·47	30·18	7·48	..	18·95
Ne ..	..	5·04	3·19	..	9·42	..	7·22
Di ..	9·00	37·73	21·94	26·65	30·73	..	10·81
Hy ..	6·00	..	..	8·16	..	..	..
Ol ..	1·19	19·61	14·91	10·20	3·29	..	10·63
Mt ..	5·51	6·18	3·65	2·64	8·40	..	3·99
Il ..	6·65	3·42	6·27	1·57	4·86	..	2·61
Ap ..	1·01	0·45	0·37	0·94	1·68	..	..
Cal ..	..	..	..	0·23	..	..	3·41
H_2O ..	0·11	1·96	0·56	2·89	1·54	..	3·00
	99·88	100·62	100·90	100·28	100·43	..	99·90
Q ..	32·4	18·7	26·0	28·0	22·8	..	27·2
L ..	44·0	22·2	34·9	29·6	37·2	..	47·2
M ..	23·6	59·1	39·1	42·4	40·0	..	25·6
n ..	0·59	0·16	0·39	0·63	0·12	..	0·26
y ..	0·15	0·24	0·21	0·24	0·30	..	0·16
Total alk. feldspars ..	28·10	20·39	27·54	16·82	33·03	..	39·28
Total feldspars ..	70·41	26·23	50·01	47·00	40·51	..	58·23
Nepheline ..	..	5·04	3·19	..	9·42	..	7·22
Total ferromag. ..	16·19	57·34	36·85	45·01	34·02	..	21·44
Total iron ores ..	12·16	9·60	9·92	4·21	13·26	..	6·60

II

Basalts and Dolerites

11	12	13	14	15	16	17	18	19	20	21
47·72	48·92	48·18	48·43	48·53	48·62	48·64	48·72	48·74	48·84	49·06
14·54	16·12	13·51	15·06	13·81	14·12	14·22	16·70	11·52	14·37	11·66
1·83	5·86	3·26	3·35	1·90	2·29	2·64	7·79	5·71	2·63	3·26
8·79	7·63	8·29	11·74	7·69	12·40	10·52	7·51	7·16	10·00	11·31
..	..	0·46	*n.d.*	0·90	0·21	..	*n.d.*	0·17	0·22	0·22
5·57	4·01	7·01	3·56	11·20	5·29	5·36	2·05	7·25	5·33	5·01
14·09	9·64	10·67	9·42	10·46	9·49	11·51	10·36	10·83	9·82	10·44
2·99	4·13	2·65	3·10	1·83	2·95	2·67	3·90	3·45	2·26	2·27
1·62	2·83	0·50	0·75	0·59	0·60	1·04	1·03	0·70	0·52	0·70
2·56	0·95	2·98	3·10	0·06	0·88	1·42	0·50	1·07	2·63	3·20
..	..	0·60	0·31	Nil	0·30	..	*n.d.*	0·53	0·36	0·37
0·99	1·70	1·14 0·37	0·65 0·23	2·91 0·39	2·28 0·63	2·70	*n.d.*	2·70	2·50 0·44	1·82 1·08
100·70	100·89	99·65[3]	99·70	100·27	100·06	100·72	98·56	99·83	99·92	100·40
3·03	2·94	..	2·90	..	3·050	2·99	3·00	..	2·927	2·935
..	..	..	..	..	22·8°	..	..	..	22°	..

[3] Includes 0·03 Cl

									Niggli Values	
106·95	113·29	113·39	120·83	103·71	116·12	113·89	120·14	112·29	122·18	121·89
19·20	22·41	18·73	22·13	17·39	19·87	19·61	24·26	15·64	21·18	17·07
38·17	39·55	47·57	44·01	54·07	48·11	43·92	37·46	48·91	46·20	48·58
33·83	24·35	26·90	25·17	23·94	24·27	28·86	27·35	26·72	26·31	27·78
8·80	13·69	6·80	8·69	4·60	7·75	7·61	10·93	8·73	6·31	6·57
4·31	1·69	5·27	5·82	0·10	1·58	2·50	0·93	1·85	4·94	5·98
..	..	0·59	0·33	..	0·43	..	..	0·51	0·38	0·39
0·263	0·311	0·110	0·138	0·176	0·119	0·203	0·148	0·117	0·131	0·16
0·487	0·357	0·517	0·301	0·659	0·391	0·426	0·201	0·509	0·430	0·3828
									CIPW Norm	
..	..	0·80	0·92	..	..	..	..	..	4·17	5·40
9·56	16·74	2·95	4·45	3·51	3·34	6·17	6·07	4·12	3·07	3·89
9·28	15·56	22·44	26·22	15·47	25·15	22·58	32·14	29·21	19·13	19·39
21·46	17·04	23·48	24·95	27·73	23·35	23·69	25·03	13·90	27·54	19·46
8·66	10·48	..	..	..	..	..	0·45	..	..	..
39·68	25·23	21·00	16·61	19·55	18·40	17·73	21·98	29·55	15·75	24·18
..	..	15·76	14·11	15·54	13·68	12·69	..	4·00	17·75	13·70
3·56	3·83	..	..	12·29	7·49	8·62	0·94	4·92	..	..
2·65	8·49	4·72	4·86	2·76	3·25	3·82	11·30	8·29	3·82	4·64
4·86	1·81	5·66	5·89	0·12	1·67	2·69	0·96	2·03	4·99	6·08
..	..	1·42	..	..	0·67	..	..	1·25	0·84	0·93
..	..	..	0·75	..	..	..	..	..	..	..
0·99	1·70	1·51	0·88	3·30	2·91	2·70	..	2·70	2·99	2·90
100·70	100·88	99·74	99·64	100·27	99·91	100·69	98·87	99·97	100·05	100·57
26·3	23·9	30·6	31·8	27·5	29·5	29·0	28·7	26·3	33·8	32·7
35·1	43·1	31·1	35·8	29·2	33·7	33·5	41·2	30·5	32·3	28·1
38·6	33·0	38·3	32·4	43·3	36·8	37·5	30·1	43·2	33·9	39·2
0·37	0·24	0·47	0·44	0·58	0·44	0·44	0·38	0·28	0·54	0·44
0·38	0·28	0·22	0·22	0·17	0·19	0·28	0·27	0·27	0·18	0·25
18·84	32·30	25·39	30·67	18·98	28·49	28·75	38·21	33·33	22·20	23·28
40·30	49·34	48·87	55·62	46·71	51·84	52·44	63·24	47·23	49·74	42·74
8·66	10·48	..	..	..	..	..	0·45	..	..	..
43·24	29·06	36·76	30·72	47·38	39·57	39·04	22·92	38·47	33·50	37·88
7·51	10·30	10·38	10·75	2·88	4·92	6·51	12·26	10·32	0·81	10·72

TABLE

	22	23	24	25	26	27	28
SiO_2 ..	49·08	49·20	49·20	49·34	49·38	49·60	49·78
Al_2O_3 ..	11·79	11·50	17·52	13·30	13·49	16·10	11·80
Fe_2O_3 ..	2·98	3·11	6·20	5·01	3·67	4·73	2·83
FeO ..	11·72	11·35	10·73	7·85	8·94	9·17	11·86
MnO ..	0·22	0·24	*n.d.*	0·20	0·21	..	0·24
MgO ..	4·79	4·91	2·80	5·63	6·48	5·15	5·13
CaO ..	10·54	10·60	9·23	9·37	11·26	10·85	10·36
Na_2O ..	2·46	2·25	3·46	4·04	1·68	2·28	2·75
K_2O ..	0·78	0·63	0·76	0·88	0·72	0·87	0·63
TiO_2 ..	3·18	3·34	0·70	2·19	2·16	2·12	3·20
P_2O_5 ..	0·33	0·25	*n.d.*	0·99	0·46	..	0·28
H_2O^+ ..	1·40	1·70	*n.d.*	1·44	1·42	1·00	1·08
H_2O^- ..	0·80	0·92	*n.d.*	..	0·24		0·52
	100·07	100·30	100·60	100·24	100·11	101·87	100·46
Sp. Gr. ..	3·00	2·948	3·00	2·90	2·926	2·91	3·007
Tem. C. ..	..	..	..	..	22°	..	..

[4] Includes SO_3 0·09 [5] Includes SO_3 0·09; BaO 0·03

si ..	121·23	121·94	117·57	119·65	117·14	115·98	211·40
al ..	17·16	16·79	24·67	19·01	18·85	22·18	16·96
fm ..	47·83	47·96	42·54	45·80	47·60	44·18	48·50
c ..	27·89	28·13	23·62	24·34	28·61	27·18	27·05
alk ..	7·12	7·12	9·17	10·85	4·94	6·46	7·49
ti ..	5·90	6·22	1·26	3·99	3·85	3·72	5·84
p ..	0·34	0·27	..	1·02	0·46	..	0·29
k ..	0·173	0·140	0·127	0·125	0·219	0·20	0·131
mg ..	0·369	0·378	0·234	0·444	0·481	0·406	0·384
Q ..	3·18	3·66	..	..	5·24	3·00	2·46
Or ..	4·45	3·89	4·51	5·17	4·23	5·00	3·89
Ab ..	20·96	21·48	29·26	34·18	14·21	18·86	23·06
An ..	18·90	18·07	30·04	15·58	27·15	30·30	18·07
Ne ..	..	..	..	..	..	..	..
Di ..	26·35	27·19	13·32	20·30	21·22	18·18	26·54
Hy ..	13·00	12·00	9·36	6·74	15·99	13·38	14·12
Ol ..	..	..	3·21	3·22	..	..	..
Mt ..	4·41	4·41	8·98	7·27	5·33	6·73	4·18
Il ..	6·08	6·23	1·34	4·16	4·10	3·95	6·08
Ap ..	0·62	0·62	..	2·35	1·06	..	0·62
Cal ..	..	..	..	..	..	..	..
H_2O ..	2·20	2·62	..	1·44	1·66	1·00	1·60
	100·15	100·17	00·02	100·41	100·90	100·40	100·62
Q ..	32·0	32·1	29·7	28·4	32·8	31·8	31·6
L ..	28·9	28·4	40·2	35·0	29·1	34·6	29·1
M ..	39·1	39·5	30·1	36·6	38·1	33·6	39·3
π ..	0·41	0·41	0·46	0·27	0·58	0·55	0·39
ν ..	0·26	0·27	0·16	0·22	0·22	0·21	0·26
Total alk. feldspars ..	25·41	25·37	33·77	39·35	18·44	23·86	26·95
Total feldspars ..	41·31	43·44	63·81	54·93	45·59	54·16	45·02
Nepheline ..	..	..	..	..	..	..	..
Total ferromag ..	39·35	39·19	25·89	30·26	37·43	31·56	40·66
Total iron ores ..	10·49	10·64	10·32	11·43	9·21	10·68	10·26

II—(*Contd.*)

29	30	31	32	33	34	35	36	37	38	39
49·83	49·90	49·98	50·12	50·12	50·47	51·39	52·98	53·46	49·28	50·61
11·83	11·98	12·51	12·33	13·52	13·10	15·06	14·53	15·50	11·69	13·58
3·14	4·55	2·83	4·53	3·99	0·43	3·24	3·38	2·81	3·04	3·19
10·92	9·83	11·71	8·04	9·19	10·06	7·97	10·05	10·17	11·56	9·92
0·21	0·15	0·23	0·14	0·18	0·35	0·27	0·04	0·07	0·23	0·16
5·60	5·89	5·42	7·54	5·42	11·06	6·66	3·66	3·59	4·96	5·46
9·66	9·80	10·00	9·57	9·97	10·94	8·49	7·49	7·61	10·49	9·45
2·39	2·23	2·65	2·20	2·42	0·97	2·17	3·43	3·37	2·51	2·60
0·52	0·47	0·30	0·92	0·56	1·24	1·14	1·34	0·84	0·68	0·72
2·29	3·76	2·27	3·06	2·46	0·98	0·62	0·62	0·40	3·23	1·91
0·30	0·21	0·37	0·22	0·29	tr.	0·20	0·64	0·31	0·31	0·39
3·09	0·87	0·95	0·70	1·46	0·24	1·51	1·88	1·87	1·50	1·70
0·35	0·33	0·24	0·81	0·14	0·06	..	0·48	0·63	0·83	0·43
100·13	99·97	99·55[4]	100·18	99·84[5]	100·02[6]	100·07[7]	100·12	100·63	100·31	100·12
3·006	2·986	2·975	2·954	2·903	..	..	2·831	2·855	2·972	2·916
22°	22·8	22·8°	23°	23°	..	..	22·8°	22°	..	..

[6] Includes 0·08 NiO & 0·8 Cr_2O_3 [7] Includes 0·03 Cl & 1·32 CO_2

124·62	123·03	121·84	120·12	124·52	107·91	128·33	142·44	144·05	121·63	126·34
17·44	17·40	17·96	17·42	19·79	16·57	22·15	23·01	24·62	17·00	19·97
50·06	50·64	49·19	51·49	46·97	54·67	48·07	44·20	43·18	48·18	47·35
25·88	25·89	26·11	24·57	26·53	25·05	22·71	21·57	21·96	27·74	25·26
6·62	6·07	6·74	6·52	6·71	3·71	7·07	11·22	10·24	7·07	7·42
4·31	6·98	4·16	5·51	4·60	1·58	1·17	1·26	0·81	5·99	3·58
0·32	0·22	0·38	0·23	0·30	..	0·21	0·73	0·36	0·33	0·42
0·125	0·122	0·070	0·216	0·133	0·457	0·257	0·204	0·141	0·151	0·154
0·417	0·427	0·400	0·523	0·427	0·644	0·515	0·332	0·334	0·378	0·429
4·90	7·74	3·27	5·46	5·77	..	6·21	4·38	5·01	3·60	4·14
3·07	2·78	1·78	5·56	3·34	7·35	6·73	7·78	4·95	3·89	4·45
20·24	18·86	22·44	18·34	20·45	8·23	18·35	28·82	28·52	20·96	22·01
20·03	21·40	21·33	21·13	24·37	27·70	27·98	20·29	24·70	18·90	23·07
..	..	..	..	..	..	..	..	..	..	..
21·64	20·73	21·71	19·55	19·18	21·64	3·77	10·74	9·45	26·28	17·41
17·28	12·49	18·51	15·53	13·93	27·04	26·16	18·58	19·99	13·20	17·78
..	..	..	..	..	5·16	..	..	..	..	..
4·56	6·50	4·10	6·50	5·79	0·63	4·70	4·87	4·07	4·41	4·64
4·36	7·14	4·31	5·93	4·67	1·87	1·18	1·22	0·76	6·08	3·65
0·70	0·62	0·87	0·67	0·67	..	0·47	1·51	0·74	0·62	1·01
..	..	..	..	..	..	3·00	..	..	..	..
3·44	1·20	1·19	1·51	1·60	0·30	1·51	2·36	2·50	2·41	2·13
100·22	99·46	99·51	100·18	99·77	99·92	100·06	100·55	100·69	100·35	100·29
33·0	33·7	32·3	32·1	33·5	29·9	35·4	34·1	35·5	32·1	33·2
28·5	27·8	29·4	28·7	31·0	26·4	34·4	36·8	37·3	28·6	31·8
38·5	38·5	38·3	39·2	35·5	43·7	30·2	29·1	27·2	39·3	36·0
0·45	0·48	0·45	0·46	0·49	0·63	0·52	0·34	0·41	0·41	0·46
0·22	0·22	0·22	0·20	0·21	0·18	0·05	0·15	0·13	0·26	0·19
23·31	21·64	24·22	23·90	23·79	15·58	25·08	36·60	33·47	24·85	26·46
43·34	43·04	45·55	45·03	48·16	43·28	53·06	56·89	58·17	43·75	49·53
..	..	..	..	..	..	..	..	..	..	..
38·92	33·22	40·22	35·08	33·11	53·84	29·93	29·32	29·44	39·48	35·19
8·92	13·64	8·41	12·43	10·46	2·50	5·88	6·09	4·83	10·49	8·29

Dolerites and Basalts

By far the most dominant rock-types forming the bulk of the Deccan trap formation are dolerites and basalts. These two types are distinguished by the grain-size of the minerals but there is every gradation and no clear demarcation between them. At some places as in the Bombay coast and in parts of Kathiawar, rocks which are coarsely crystalline and gabbroidal in texture occur as small patches in the main basaltic types. These are to be regarded as the plutonic phase of the basic magma intruded into basalts or as differentiated portions formed as a result of crystal settling. There are as many as 35 analyses of these basic rocks recorded by different investigators, these being listed in Table II according to the order of increasing silica percentage.

From the series of analyses it will be seen that at the low silica end of the series, the rocks are rich in olivine and grade into peridotites, but with increase of silica olivine is gradually replaced by augite and free quartz appears in the norm, suggesting andesitic affinities. These types are, however, typical basalts and dolerites as they are distinguished by the presence of augite and iron ores and absence of hornblende.

From this list of chemical analyses (Table II) a selected number of 12 analyses representing certain well-defined types are given for the purpose of examination of chemical characters and normative mineral composition.

From Table III it will be seen that the silica percentage varies from 46·14% to 53·46%. The alumina percentage is uniform in the majority of types within the range of 12·46% to 15·50% (except in Nos. 4 and 5 which contain 20·93% and 7·86% respectively. The iron oxides vary from about 9·5% to 15·5% with an average of 12·2%. The iron oxides in the Deccan traps are generally higher than in most other basalts. The more silicic types have higher iron oxides but it will be seen that 6 and 23 are higher in iron oxides compared to the other types. The MgO is low compared to the FeO percentage, but in 5 and 15 it is quite high. CaO is uniform in most of the rocks varying from 7·61% to 11·26%, but in one type, No. 11, it is as much as 14·09%. Soda and potash are higher in 6, 8, 10 and 11 than in others and these rocks are from Kathiawar and Pavagad Hills where alkali and acid rocks are associated. Titanium and phosphorus are seen in normal amounts, but in 15 and 37 titanium is low.

When we examine the norms of these rocks we are able to distinguish two major groups, the unsaturated types and oversaturated types. The unsaturated types are divisible into two divisions according to the presence of olivine only or of olivine and nepheline. No. 4 is a rock with predomi-

TABLE III

Selected Analyses of Basalts and Dolerites from Table II

	4	5	6	8	10	11	15	19	23	26	33	37
SiO_2 ..	46·14	46·80	46·82	47·02	47·50	47·72	48·53	48·74	49·20	49·38	50·12	53·46
Al_2O_3 ..	20·93	7·86	14·70	12·46	17·12	14·54	13·81	11·52	11·50	13·49	13·52	15·50
Fe_2O_3 ..	3·80	4·26	2·53	5·80	2·77	1·83	1·90	5·71	3·11	3·67	3·99	2·81
FeO ..	6·27	7·89	11·58	9·25	7·68	8·79	7·69	7·16	11·35	8·94	9·19	10·17
MnO ..	*n.d.*	0·30	0·12	0·19	0·15	..	0·90	0·17	0·24	0·21	0·18	0·07
MgO ..	3·70	14·79	6·90	4·51	4·00	5·57	11·20	7·25	4·91	6·48	5·42	3·59
CaO ..	11·30	10·96	10·10	9·90	8·37	14·09	10·46	10·83	10·60	11·26	9·97	7·61
Na_2O ..	2·90	2·93	3·60	4·92	5·75	2·99	1·83	3·45	3·55	1·68	3·42	3·37
K_2O ..	0·60	0·83	0·50	1·50	0·64	1·62	0·59	0·70	0·63	0·72	0·56	0·84
TiO_2 ..	3·50	1·80	3·30	2·56	1·37	2·56	0·06	1·07	3·34	2·16	2·46	0·40
P_2O_5 ..	0·42	0·19	0·15	0·69	tr.	..	nil	0·53	0·25	0·46	0·29	0·31
H_2O^+ ..	0·11	0·86	0·32	1·54	1·96	0·99	2·91	2·70	1·70	1·42	1·46	1·87
H_2O^-	..	1·10	0·24		1·04		0·39		0·92	0·24	0·14	0·63
..	99·67	100·57	100·86	100·34	99·85†	100·70	100·27	99·83	100·30	100·11	99·84‡	100·63
Sp. Gr. ..	2·83	2·97	3·00	2·90	..	3·03	..	..	2·948	2·926	2·903	2·855
Temp. C. ..	..	..	..	..	..	..	..	..	..	22°	23°	22°

† Includes 1·50 CO_2 ‡ Includes SO_3 0·09 ; BaO 0·03

si ..	111·87	90·31	103·49	110·27	119·87	106·95	103·71	112·29	121·94	117·14	124·52	144·05
al .	29·90	8·94	19·14	17·21	25·45	19·20	17·39	15·64	16·79	18·85	19·79	24·62
fm ..	33·01	61·91	48·53	44·51	36·83	38·17	54·07	48·91	47·96	47·60	46·97	43·18
c ..	29·34	22·65	23·91	24·86	22·63	33·83	23·94	26·72	28·13	26·61	26·53	21·96
alk ..	7·75	6·50	8·42	13·42	15·09	8·80	4·60	8·73	7·12	4·94	6·71	10·24
ti ..	6·38	2·61	5·48	4·51	2·61	4·31	0·10	1·85	6·22	3·85	4·60	0·81
p ..	0·44	0·15	0·15	0·69	..	..	..	0·51	0·27	0·46	0·30	0·36
k ..	0·120	0·157	0·084	0·167	0·069	0·263	0·176	0·117	0·140	0·219	0·133	0·141
mg ..	0·405	0·687	0·468	0·354	0·408	0·487	0·659	0·509	0·378	0·481	0·427	0·334
Q ..	..	..	..	..	..	..	..	..	3·66	5·24	5·77	5·01
Or ..	3·56	4·90	2·95	8·85	3·78	9·56	3·51	4·12	3·89	4·23	3·34	4·95
Ab ..	24·54	15·49	24·59	24·18	35·50	9·28	15·47	29·21	21·48	14·21	20·45	28·52
An ..	42·31	5·84	22·47	7·48	18·95	21·46	27·73	13·90	18·07	27·15	24·37	24·70
Ne ..	..	5·04	3·19	9·42	7·22	8·66	..	..	..	..	..	..
Di ..	9·00	37·73	21·94	30·73	10·81	39·68	19·55	29·55	27·19	21·22	19·18	9·45
Hy ..	6·00	..	..	..	..	..	15·54	4·00	12·00	15·99	13·93	19·99
Ol ..	1·19	19·61	14·91	3·29	10·63	3·56	12·29	4·92	..	..	..	..
Mt ..	5·51	6·18	3·65	8·40	3·99	2·65	2·76	8·29	4·41	5·33	5·79	4·07
Il ..	6·65	3·42	6·27	4·86	2·61	4·83	0·12	2·03	6·23	4·10	4·67	0·76
Ap ..	1·01	0·45	0·37	1·68	..	..	..	1·25	0·62	1·06	0·67	0·74
Cal ..	..	..	..	..	3·41	..	..	..	..	..	..	..
H_2O ..	0·11	1·96	0·56	1·54	3·00	0·99	3·30	2·70	2·62	1·65	1·60	2·50
	99·88	100·62	100·90	100·43	99·90	100·70	100·27	99·70	100·17	100·19	99·77	100·69
Q ..	32·4	18·7	26·0	22·8	27·2	26·3	27·5	26·3	32·1	32·8	33·5	35·5
L ..	44·0	22·2	34·9	37·2	47·2	35·1	39·2	30·5	28·4	29·1	31·0	37·3
M ..	23·6	59·1	39·1	40·0	25·6	38·6	43·3	43·2	39·5	38·1	35·5	27·2
n ..	0·59	0·16	0·39	0·12	0·26	0·37	0·58	0·28	0·41	0·58	0·49	0·41
y ..	0·15	0·24	0·21	0·30	0·16	0·38	0·17	0·27	0·27	0·22	0·21	0·13
Total alk. feldspars ..	28·10	20·39	27·54	33·03	39·28	18·84	18·98	33·33	25·37	18·44	23·79	33·47
Total feldspars	70·41	26·23	50·01	40·51	58·23	40·80	46·71	47·23	43·44	45·59	48·16	58·17
Nepheline ..	..	5·04	3·19	9·42	7·22	8·66	..	..	..	..	..	..
Total ferromag.	16·19	57·34	36·85	34·02	21·44	43·24	47·38	38·47	39·19	37·21	33·11	29·44
Total iron ores	12·16	9·60	9·92	13·26	6·60	7·51	2·88	10·32	10·64	9·43	10·46	4·83

TABLE IV

Analyses of Andesites

	40	41	42
SiO_2 ..	53·12	53·57	58·11
Al_2O_3 ..	15·72	17·16	17·92
Fe_2O_3 ..	3·72	3·50	2·82
FeO ..	9·10	10·22	4·56
MnO ..	..	..	0·11
MgO ..	2·74	2·04	2·70
CaO ..	9·34	8·93	6·75
Na_2O ..	3·54	3·65	3·93
K_2O ..	0·75	1·15	2·07
TiO_2 ..	1·40	1·23	1·12
P_2O_5 ..	0·36	..	0·42
H_2O^+ ..	0·15	0·40	0·18
H_2O^- ..	0·21		..
	100·15	101·85	100·69
Sp. Gr. ..	2·82	2·83	..
si ..	141·02	140·39	176·20
al ..	24·59	26·49	32·02
fm ..	38·47	37·26	30·50
c ..	26·56	25·06	21·93
alk ..	10·38	11·19	15·55
ti ..	2·79	2·42	2·55
p ..	0·40	..	0·55
k ..	0·123	0·172	0·258
mg ..	0·281	0·214	0·400
Q ..	5·51	3·54	9·18
Or ..	4·45	6·67	12·24
Ab ..	29·94	30·39	33·24
An ..	24·79	27·24	25·14
Di ..	16·39	14·19	4·57
Hy ..	9·89	11·55	8·80
Mt ..	5·40	5·10	4·10
Il ..	2·66	2·28	2·12
Ap ..	0·84	..	1·04
Water ..	0·36	0·40	0·18
	100·23	101·36	100·61
Q ..	35·1	34·6	39·9
L ..	37·5	40·3	43·6
M ..	27·4	25·1	16·5
π ..	0·41	0·41	0·35
γ ..	0·23	0·21	0·11
Total alk. feldspars ..	34·39	37·06	45·48
Total feldspars ..	59·18	64·30	70·62
Total pyroxenes ..	26·28	25·74	13·37
Total iron-ores ..	8·06	7·38	6·22

nant feldspars, while 15 and 19 have the same amount of total feldspars. The types 5, 6, 8 and 10 and 11 have nepheline in their norms. From an examination of the norms of these types it will be seen that the total alkali

feldspars increase with the increase of silica. The total feldspars also tend to increase correspondingly. Pyroxene molecules do not show any definite relationship to the increase of silica but vary greatly within these types.

The oversaturated types are 23, 26, 33 and 37. Of these 23, 26 and 33 belong to the Lower Traps, while 37 comes from the Upper Traps. These types show a striking increase in total feldspars from types 23 to 37. On the other hand the pyroxene molecules are decreased. Thus with the increase in silica we are able to notice progress of differentiation in the enrichment of feldspars and decrease of pyroxenes.

Andesites

This group of rocks is found mainly in Bombay Islands, Kathiawar and Pavagad Hills. These rocks are black in colour and carry phenocrysts of feldspar. The plagioclase feldspars are predominant and are arranged in groundmass, composed of glass, augite and iron ores, in parallel position exhibiting flow-banding. These rocks differ from basalts in the higher proportion of felsic constituents which are more than 60% of the rock whereas in the basalts the ratio between felsic and mafelsic constituents is around 1 : 1. The chemical composition, Niggli values and norms of the three andesites from the Bombay Islands are given in Table IV.

From an examination of the chemical composition and other values of the rocks, we see that 40 and 41 are similar in composition and that the type 42 differs from these two types. The analysis of 41 is unsatisfactory owing to the high summation. The higher percentages of alumina and alkalis in No. 41 results in the higher proportion of feldspars in the norm of this rock. The lower percentages of MgO, CaO and TiO_2 are expressed in lower diopside and ilmenite. The iron oxides in the two rocks are about the same. Even though the silica content in 41 is slightly higher than in 40 the normative quartz is lower in 40.

When we compare the third type with 40 and 41 we see that the silica is higher by 5%. Alumina and alkalis are also higher, iron oxides, calcium oxide and titanium are lower. As a result the norm shows higher percentages of alkali feldspars and lower percentages of anorthite, pyroxenes and iron-ores.

Syenites, Trachytes and Nepheline Syenites

These sub-acid rocks are confined to the Bombay Coast, Kathiawar and Pavagad Hills and occur either as flows or as intrusive masses in the main body of dolerites. The rocks are all cream coloured or buff in appearance. The available chemical analyses of nepheline syenite and trachytes

TABLE V

Chemical Analyses of Syenite and Trachytes

	43	44	45	46
SiO_2 ..	56·11	61·12	61·54	62·91
Al_2O_3 ..	21·35	19·38	15·82	14·97
Fe_2O_3 ..	2·41	8·82	0·26	0·72
FeO ..	0·97	1·48	3·79	3·80
MnO ..	0·75	0·41	*n·d*	..
Mgo ..	0·59	Tr.	Tr.	0·43
Cao ..	2·55	Tr.	3·36	4·40
Na_2O ..	8·64	4·60	6·21	5·85
K_2O ..	3·39	3·53	4·61	4·91
TiO_2 ..	0·84	*n·d*	Tr.	0·23
P_2O_5 ..	0·31	*n·d*	0·71	..
CO_2 ..	..	..	0·96	..
H_2O^+) ..	1·24	0·82	1·59)	2·00
H_2O^-)		0·35	0·24)	
	99·15	100·51	100·79†	100·22
Sp. Gr. ..	2·69	2·38	2·431	2·56
		† Includes 1·70 FeS_2		
si ..	187·14	232·03	243·84	235·66
al ..	41·95	43·34	36·94	33·05
fm ..	13·80	31·19	13·33	16·33
c ..	9·11	..	14·25	17·66
alk ..	35·14	25·47	35·48	32·96
ti ..	2·10	..	..	0·85
p ..	0·44	..	1·19	..
k ..	0·205	0·336	0·328	0·356
mg ..	0·212	..	..	0·147
Q ..	..	20·87	2·94	1·80
Or ..	20·07	20·87	27·24	28·91
Ab ..	51·98	38·90	52·40	49·25
An ..	7·70	..	2·50	..
Ne ..	0·17	..	..	..
Sodalite ..	9·59	..	..	..
Corundum ..	1·63	7·99	..	..
Perofskite ..	1·43	..	..	..
Di ..	..	..	8·25	15·08
Wo ..	..	..	..	1·86
Ol ..	1·04	..	..	..
Mt ..	3·13	6·11	0·46	0·93
Hae ..	0·26	4·60	..	..
Il ..	..	..	..	0·46
Pyrite ..	..	..	1·70	..
Ap ..	0·76	..	1·55	..
Calcite ..	..	..	2·20	..
Water ..	1·24	1·17	1·83	2·00
	99·00	100·51	101·17	100·29
Q ..	30·4	42·0	39·7	38·1
L ..	62·9	44·0	52·6	49·2
M ..	6·7	14·0	7·7	12·7
n .	0·09	0·00	0·02	0·002
γ ..	0·07	0·00	0·23	0·52
Total alk. fels. ..	72·05	59·77	79·64	78·16
Total feldspars ..	79·75	59·77	82·14	78·16
Nepheline ..	0·17	..	..	
Total ferromag. ..	1·04	..	8·35	16·94
Total iron ores ..	3·39	10·71	2·16	1·39

are given in Table V. The nepheline syenite comes from Kathiawar and the trachytes from Bombay.

When the chemical analysis of nepheline syenite (No. 43) is examined, it is seen that it has higher alumina and alkalis and lower iron oxides, and calcium oxide. The norm shows high alkali feldspars. There is a small amount of nepheline and olivine. The excess of soda and alumina and silica goes into sodalite. It is interesting to note that there are no pyroxenes in the norm.

The three trachytes do not differ much in their silica content. No. 44 has higher alumina and iron oxides than the others. There are only traces of magnesia and calcium oxides and consequently the excess of alumina is released as corundum and the silica as quartz in large amount.

When we examine types 45 and 46 we see that 45 has higher alumina and soda and lower iron oxides, calcium oxide and potash. Type 46 has a small amount of magnesia, while in 45 magnesia is only in traces. In the norm, quartz is lower than in 45; there is no anorthite in type 46, but instead wollastonite is formed.

Rhyolites, Granophyres, etc.

This group of rocks is found on the Bombay Coast, Pavagad Hills and Kathiawar. They are white to pale grey or black in colour and are granulitic or cryptocrystalline or glassy. The glass in some of the specimens is divitrified, giving rise to felsitic texture. Quartz and feldspar are the predominant constituents with micropegmatitic relationship. The feldspars are orthoclase albite and oligoclase. They differ mineralogically from andesites in having an abundance of quartz and feldspar and low proportion of ferromagnesians; and from syenites in being rich in quartz and having lower proportion of alkali feldspars. The chemical composition, norm and other values of these rocks are given in Table VI.

From the table it is seen that this group contains generally low percentages of iron-oxides, magnesia and calcium oxide and high percentages of silica, alumina and alkalis. As a result they show small amounts of ferromagnesian minerals and are predominantly rich in quartz and feldspar. In some of the rocks the alumina is in excess after combining with alkalis and calcium oxide, and appears in the norm as free Al_2O_3, *i.e.*, corundum. In type 48 we get also acmite as a result of the excess of Na which is highest in this rock.

Petrochemistry

The number of rock analyses given in the preceding tables is large and covers several rock groups from ultrabasic through basic and intermediate

TABLE VI

Chemical Analyses of Rhyolites, Granophyres, etc.

	47	48	49	50	51	52	53	54	55
SiO_2 ..	63·03	66·20	66·86	67·00	68·90	70·86	71·00	71·84	73·24
Al_2O_3 ..	16·51	13·12	14·33	14·55	15·46	14·41	16·35	12·51	11·75
Fe_2O_3 ..	4·68	3·00	1·94	1·06	1·09	1·20	2·73	3·80	2·20
FeO ..	2·29	1·10	3·47	3·05	1·85	1·87	1·03	0·85	2·07
MnO ..	0·21	..	0·16	..	0·14	..	..	..	..
MgO ..	0·38	1·19	0·59	1·37	0·26	0·64	0·52	1·15	Tr.
CaO ..	3·05	1·90	2·01	5·40	2·29	1·63	1·41	1·70	Tr.
Na_2O ..	2·43	6·01	4·54	3·78	3·66	3·02	4·32	4·10	5·10
K_2O ..	2·50	4·65	3·01	2·60	3·03	4·56	3·05	2·20	3·20
TiO_2 ..	1·10	0·75	0·68	0·60	1·08	0·45	0·59	..	..
P_2O_5 ..	0·20	..	0·50	..	1·00	..	..	..	..
H_2O^+ ..	1·95	3·20	2·41	1·20	0·95	2·02	*n.d*	1·05	0·51
H_2O^- ..	1·12							0·92	0·26
	99·45	101·12	100·50	100·61	99·71	100 66	101·00	101·05*	98·80†
Sp. Gr. ..	2·59	2·26	2·51	2·25	2·45	2·59	2·42	2·44	2·67
		* Includes CO_2 0·93			† Includes CO_2 0·47				
si ..	272·60	281·60	299·89	267·34	345·96	363·57	338·74	362·02	423·44
al ..	42·08	32·88	37·88	34·19	45·75	43·58	45·96	37·14	40·04
fm ..	26·73	21·05	24·14	21·50	14·45	17·53	17·59	26·60	19·58
c ..	14·13	8·66	9·64	23·08	12·30	8·97	7·19	9·17	..
alk ..	17·06	37·41	28·34	21·23	27·50	29·92	29·26	27·09	40·38
ti ..	3·58	2·40	2·29	1·80	4·07	1·73	2·12	..	..
p ..	0·36	..	0·94	..	2·11	..	..	..	..
k ..	0·403	0·337	0·304	0·312	0·353	0·498	0·317	0·262	0·292
mg ..	0·091	0·358	0·163	0·379	0·136	0·279	0·210	0·324	..
Q ..	32·76	11·47	23·24	22·56	32·81	30·64	30·84	36·77	31·50
Or ..	14·74	27·49	17·81	15·57	17·92	26·94	17·79	13·02	18·90
Ab ..	20·55	41·58	38·38	31·44	30·93	25·53	36·15	34·66	42·97
An ..	13·94	..	7·03	15·01	5·50	8·10	6·95	2·56	..
Cor ..	4·70	..	1·03	..	4·15	1·55	3·47	2·45	..
Acmite ..	..	8·17	..	..	..	..	..	..	..
Di ..	0·94	7·53	5·42	9·68	1·64	3·30	..	2·86	..
Hy ..	..	..	..	2·29	..	..	1·30	..	..
Mt ..	4·87	0·26	2·83	1·39	1·59	1·74	1·62	2·73	3·94
Il ..	2·09	1·43	1·29	1·22	2·05	0·85	1·06	.	..
Hae ..	1·31	..	..	..	..	..	1·60	1·92	..
Ap ..	0·47	..	1·18	..	2·35	..	..	..	..
H_2O ..	3·07	3·20	2·41	1·20	0·95	2·02	*n.d*	1·97	0·77
	99·44	101·13	100·62	100·36	99·89	100·67	100·78	101·05*	101·38†
Q ..	53·8	43·8	49·9	49·6	55·5	55·5	53·8	57·4	..
L ..	32·6	46·4	40·5	39·2	35·4	38·3	38·9	32·8	..
M ..	13·6	9·8	9·6	11·2	9·1	6·2	7·3	9·8	..
n ..	0·28	0·00	0·11	0·24	0·10	0·13	0·11	0·05	..
γ ..	0·00	0·29	0·00	0·32	0·00	0·00	0·00	0·00	..
		* Includes 2·11 calcite			† Includes 3·30 pyrites				
Total alk. fels. ..	35·29	69·07	56·19	47·01	48·85	52·47	53·94	47·68	61·87
Total fels. ..	49·23	69·07	63·22	62·02	54·35	60·57	60·89	50·24	..
Total ferromag. ..	0·94	15 70	5·42	11·97	1·64	3·30	1·30	2·86	..
Total iron ores ..	8·27	1·69	4·12	2·61	3·64	2·59	4·23	4·65	3·94

to acid types. Even though these types are distributed widely in the Deccan trap formation, yet in some places different varieties are closely associated. As the rocks come mainly from four regions, mentioned below, it is proposed to examine the types found in each of these regions separately:

1. Central Provinces
2. Bombay Coast
3. Pavagad Hills
4. Kathiawar

In the study of differentiation trends, the rocks from the Pavagad Hills have been grouped with those of the Bombay Coast, as the analyses available from this region are small, numbering only five.

The types from the Central Provinces are undifferentiated basalts and dolerites belonging to the Lower Traps. They show only very slight progressive differentiation from bottom flow upwards, and the rocks from different flows appear at first sight to be very similar both mineralogically and chemically. The regular change in composition is detected only when the norms of these rocks are calculated, as has been shown by Sir L. L. Fermor. An exception to the general uniformity of the trap flows is, however, found in the northern slopes of the Satpuras, where composite dykes and sills with acid cores are occasionally met with, though only one analysis of such an acid rock is available. The Niggli values, QLM and $\pi\gamma$ values of all rocks from this area are grouped together in Table VII for ready reference.

TABLE VII

Niggli and Other Values of the Deccan Traps from the Central Provinces

	20	21	22	23	26	28	29	31	47
si ..	122·18	121·89	121·23	121·94	117·14	121·40	124·62	121·84	272·60
al ..	21·18	17·07	17·16	16·79	18·85	16·96	17·44	17·96	42·08
fm ..	46·20	48·58	47·83	47·96	47·60	48·50	50·06	49·19	26·73
c ..	26·31	27·78	27·89	28·13	28·61	27·05	25·88	26·11	14·13
alk ..	6·31	6·57	7·12	7·12	4·94	7·49	6·62	6·74	17·06
k	0·131	0·168	0·173	0·140	0·219	0·131	0·125	0·070	0·403
mg ..	0·430	0·382	0·369	0·378	0·481	0·384	0·417	0·400	0·091
Q ..	33·8	32·7	32·0	32·1	32·8	31·6	33·0	32·3	53·8
L ..	32·3	28·1	28·9	28·4	29·1	29·1	28·5	29·4	32·6
M ..	33·9	39·2	39·1	39·5	38·1	39·3	38·5	38·3	13·6
π ..	0·54	0·44	0·41	0·41	0·58	0·39	0·45	0·45	0·28
γ ..	0·18	0·25	0·26	0·27	0·22	0·26	0·22	0·22	0·00

In the Bombay Coast the lavas belong to the Upper Traps. The rocks here show a deviation from the uniformity of traps ordinarily found, in that

TABLE

Niggli and Other Values of Deccan

	2	3	4	6	9	14	16	18	24	27	32
si ..	78·59	84·45	111·87	103·49	108·87	120·83	116·12	120·14	117·57	115·98	120·12
al ..	11·61	12·19	29·90	19·14	19·44	22·13	19·87	24·26	24·67	22·18	17·42
fm ..	65·55	62·14	33·01	48·53	45·11	44·01	48·11	37·46	42·54	44·18	51·49
c ..	20·07	22·09	29·34	23·91	27·12	25·17	24·27	27·35	23·62	27·15	24·57
alk ..	2·77	3·58	7·75	8·42	8·33	8·69	7·75	10·93	9·17	6·46	6·52
k ..	0·220	0·252	0·120	0·084	0·171	0·138	0·119	0·148	0·127	0·20	0·216
mg ..	0·756	0·720	0·405	0·468	0·451	0·301	0·391	0·201	0·234	0·406	0·523
Q ..	19·2	21·3	32·4	26·0	..	31·8	29·5	28·7	29·7	31·8	32·1
L ..	22·0	23·2	44·0	34·9	..	35·8	33·7	41·2	40·2	34·6	28·7
M ..	58·8	55·5	23·6	39·1	..	32·4	36·8	30·1	30·1	33·6	39·2
π ..	0·61	0·55	0·59	0·39	..	0·44	0·44	0·38	0·46	0·55	0·46
y ..	0·15	0·18	0·15	0·21	..	0·20	0·19	0·27	0·16	0·21	0·20

the ultrabasic, intermediate and acid types are associated with basalts and dolerites. The magma has undergone extensive differentiation as is well brought out by the si values which range from 78 to 423 units (Table VIII).

The traps from the Pavagad Hills also belong to the Upper Traps. Acid and alkaline rocks occur in this area, but no analysis of alkaline rocks is available and the five analyses that were compiled from the literature range in si from 90 to 345 units, showing thereby that a fair degree of differentiation has taken place in the magma. The Niggli and other values of these analyses are given in Table IX.

TABLE IX

Niggli and Other Values of Deccan Traps from the Pavagad Hills

	5	8	25	49	51
si ..	90·31	110·27	119·65	299·89	345·96
al ..	8·94	17·21	19·01	37·88	45·75
fm ..	61·91	44·51	45·80	24·14	14·45
c ..	22·65	24·86	24·34	9·64	12·30
alk ..	6·50	13·42	10·85	28·34	27·50
k ..	0·157	0·167	0·125	0·304	0·353
mg ..	0·687	0·354	0·444	0·163	0·136
Q ..	18·7	22·8	28·4	49·9	55·5
L ..	22·1	37·2	35·0	40·5	35·4
M ..	59·1	40·0	36·6	9·6	9·1
π ..	0·16	0·12	0·27	0·11	0·10
y ..	0·24	0·30	0·22	0·00	0·00

VIII

Traps from the Bombay Coast

36	40	41	42	44	45	46	48	50	53	54	55
142·44	141·02	140·39	176·20	232·03	243·84	235·66	281·60	267·34	338·74	362·02	423·44
23·01	24·59	26·49	32·02	43·34	36·94	33·05	32·88	34·19	45·96	37·14	40·04
44·20	38·47	37·26	30·50	31·19	13·33	16·33	21·05	21·50	17·59	26·60	13·58
221·57	26·56	25·06	21·93	..	14·25	17·66	8·66	13·08	7·19	9·17	..
11·22	10·38	11·19	15·55	25·47	35·48	32·96	37·41	21·23	29·26	27·09	40·38
0·204	0·123	0·172	0·258	0·336	0·328	0·358	0·337	0·312	0·317	0·262	0·292
0·332	0·281	0·214	0·400	..	..	0·147	0·358	0·379	0·210	0·324	..
34·1	35·1	24·6	39·9	42·0	39·7	38·1	43·8	49·6	53·8	57·4	..
36·8	37·5	40·3	43·6	44·0	52·6	49·2	46·4	39·2	38·9	32·8	..
29·1	27·4	25·1	16·5	14·0	7·7	12·7	9·5	11·2	7·3	9·8	..
0·34	0·41	0·41	0·35	0·00	0·02	0·002	0·00	0·24	0·11	0·05	..
0·15	0·23	0·21	0·11	0·00	0·23	0·52	0·29	0·32	0·00	0·00	..

In Kathiawar where the Deccan lavas belong to the Upper Traps, we see that ultrabasic, alkaline, subacid and acid rocks occur as intrusives side by side in basalts. The Niggli and other values of all the available analyses from this area are given in Table X.

Differentiation Trends in the Deccan Traps

1. *Central Provinces.*—We have already seen that the rocks from the Central Provinces comprise undifferentiated basalts and dolerites, showing close resemblance in mineralogical and chemical characters. This feature is amply brought out when we examine the Niggli values in Table VII. We see that, even though the si values vary from 117 to 272, there is a concentration of eight out of nine rocks at the basic end of the series in the si range of 117 and 124, and that there is a well marked large gap between this group and the single remaining specimen with si 272. It is therefore unsatisfactory to construct curves joining the two extreme types with such a large gap between them. The porphyrite which is alone acid rock, comes from the core of a composite dyke cutting across a sill. Even though we can say from the intrusive nature of the dyke that it is younger than the sill in which it is intruded yet, according to Dr. Crookshank, it is of doubtful age.

2. *Bombay Coast and Pavagad Hills.*—When a differentiation diagram is constructed (Fig. 1) from the Niggli values with si as abscissa and the other values as ordinate of all the analysed rocks from these areas, one observes that the rocks which are allied in composition tend to get concentrated together. As a result of this concentration we see well-marked gaps in the distribution of these rocks on the diagram. The largest gap is

TABLE X

Niggli values and other values for the Deccan Traps from Kathiawar

	1	7	10	11	12	13	15	17	19	34	35	43	52
si ..	88·16	101·0	119·87	106·95	113·29	113·39	103·71	113·89	112·29	107·91	128·33	187·14	363·57
al ..	18·79	18·13	25·45	19·20	22·41	18·73	17·39	19·61	15·64	16·57	22·15	41·95	43·58
fm ..	47·89	47·12	36·83	38·17	39·55	47·57	54·07	43·92	48·91	54·67	48·07	13·80	17·53
c ..	20·48	30·65	22·63	33·83	24·35	26·90	23·94	28·86	26·72	25·05	22·71	9·11	8·97
alk ..	12·84	4·10	15·09	8·80	13·69	6·80	4·60	7·61	8·73	3·71	7·07	35·14	29·92
k ..	0·154	0·189	0·069	0·263	0·311	0·110	0·176	0·203	0·117	0·457	0·257	0·205	0·498
mg ..	0·427	0·609	0·408	0·487	0·357	0·517	0·659	0·426	0·509	0·644	0·515	0·212	0·279
Q ..	14·6	28·0	27·2	26·3	23·9	30·6	27·5	29·0	26·3	29·9	35·4	30·4	55·5
L ..	43·0	29·6	47·2	35·1	43·1	31·1	29·2	33·5	30·5	26·4	34·4	62·9	38·3
M ..	42·4	42·4	25·6	38·6	33·0	38·3	43·3	37·5	43·2	43·7	30·2	6·7	6·2
▪ ..	0·19	0·63	0·26	0·37	0·24	0·47	0·44	0·44	0·28	0·63	0·52	0·09	0·13
y ..	0·93	0·24	0·16	0·38	0·28	3·22	0·28	0·28	0·27	0·18	0·05	0·07	0·00

between the si values of 176 and 232. It is seen that except for this large gap, there is a fair uniformity in the distribution of rocks over the whole range.

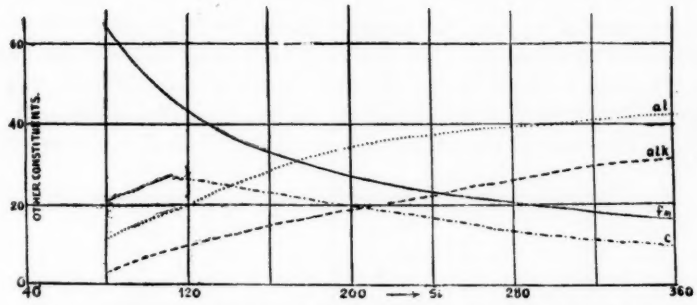

FIG. 1. Differentiation Diagram for the Deccan Traps from the Bombay Coast and Pavagad Hills

The diagram shows that the al and alk curves increase simultaneously with the increase of silica. On the other hand the fm and (in the major portion of the diagram) the c curve decrease correspondingly. The al curve rises more rapidly than the alk curve at the initial stages, but becomes flatter after si = 184. The rise of the alk curve is practically uniform throughout. The difference between al and alk, which is at a minimum at the beginning, attains as a result of the more rapid rise of the al curve a maximum of 15 units at si = 184; then again the difference diminishes with the increase of silica as the al curve becomes flatter. The fm curve is very steep from si = 80 to 160; afterwards the fall becomes less with the increase of si. The c curve is at first sympathetic to al and fm curves, but it becomes anthipathetic to them and changes direction sharply at si = 112, thence becoming roughly parallel to the fm curve. The alk and fm curves which at first show a difference of 63 units between them converge and cross each other at si = 244, diverging again with a difference of 17 units at the acid end. The intersection of fm and al curves, which is called the *isofalic point* falls at si = 176 corresponding to which are the following values.

si = 176, al = fm = 30, c = 22, alk = 15. This isofalic point shows a slight deviation from the calc-alkali suite of rocks. (The other two intersection points of c and alk, and of fm and alk are well above 200 which are usual in calc-alkali suites.)

3. *Kathiawar.*—The differentiation diagram for the magma of Kathiawar drawn from the values of the rocks so far analysed (Table X) shows that the rhyolite is separated by a large gap from the other rocks (gap from

si = 187 to 363). The differentiation diagram (Fig. 2) differs greatly from the tendencies of the curves exhibited in the case of the Bombay Coast. All the curves are steep and increase or fall rapidly with the increase of si. The difference between al and alk curves, which are sympathetic to each other, is greatest (12 units) at the silica low end, as a result of the more rapid rise of the alk curve. The difference is only 7 units at the silica-rich end of the diagram. The curve c is antipathetic to the fm curve till it reaches si = 108; afterwards the value of the c falls with the rise of si so that it is sympathetic

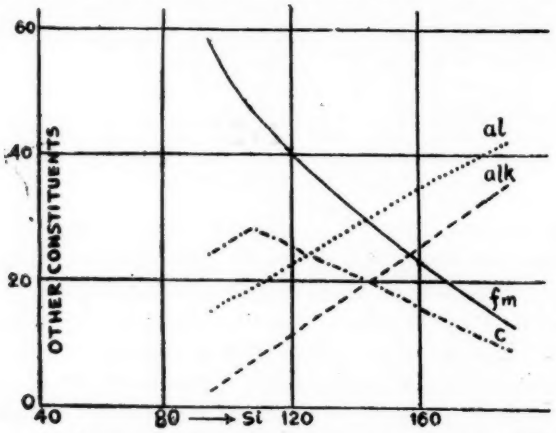

FIG. 2. Differentiation Diagram for the Deccan Traps from Kathiawar

to the fm curve. The curves fm and alk which show a difference of 50 units at the beginning intersect at si = 156 and then diverge giving a difference of 22 units at the end of the diagram. The *isofalic point* represented by the intersection of fm and al curves is situated at si = 140, the other values obtained at this point being as follows:

$$si = 140 \quad al = fm = 29 \quad c = 20 \quad alk = 18$$

All the main points of intersection of the curves lie well below si = 200, a feature which shows that the differentiation tendencies exhibited are characteristic of the alkaline suite of rocks.

The intrapolated values for these two differentiation diagrams are given in Table XI.

The differentiation diagrams based on the Niggli values do not give us an idea of the individual behaviour of soda and potash and of magnesia as they are grouped together in alk and fm values respectively. To study the relationship between potash and magnesia in the differentiation of the magma

TABLE XI

Intrapolated Molecular Values of the Deccan Traps

	Bombay coast and Pavagad Hills				Kathiawar			
si	al	fm	c	alk	al	fm	c	alk
80	10·5	63	20·5	2·5	..	..	..	..
100	16	52	25	6	16	50	26	4
120	20	43	27	9	22·5	39	25	10
140	24	37·5	25·5	11·5	29	29	20	18
160	27	33	24	14	35	22	16	24
180	30	29·5	22	16	40	16	11	32
200	32	27	20	18				
220	34	25	19·5	20				
240	35	23	17	22				
260	36	22	15	24				
280	37	21	14	27				
300	38	19	12	28·5				
320	39	18	10·5	30				
340	40	16	9	31				
360	41	14	7	32				

the k and mg values which are themselves the proportion of the molecules in alk and fm values respectively and which bring out the relationship between the components Na and k and between Fe and Mg, are plotted with k as abscissa and mg as ordinate and the diagrams are given as Figs. 3 and 4.

In the case of the diagram for the Bombay Coast and the Pavagad Hills (Fig. 3) we see that there are two tendencies in the relationship of k and mg values. In the first, the relation between k and mg values are reciprocal to each other, so that a decrease in one value is accompanied by the increase in the other; in the second, the values show simultaneous increase in both. The first condition is characteristic of the calc-alkali suite of rocks and the second is normal to the alkaline suites.

In Fig. 4 we see that when k and mg values are plotted omitting the single acid type, the diagram brings out the alkaline-affinities of the magma of Kathiawar. The k and mg values show a corresponding rise so that the points occupy a zone inclined about 45° to the sides.

THE QLM DIAGRAM

The QLM diagram is very important in the study of differentiation and the order of crystallisation of the rock-types in the history of evolution, as they present at a glance the role of quartz (silica) in the differentiation trends, and also the relative proportions of the leucocratic and melanocratic constituents. These three values, Q, L and M which by their relative pro-

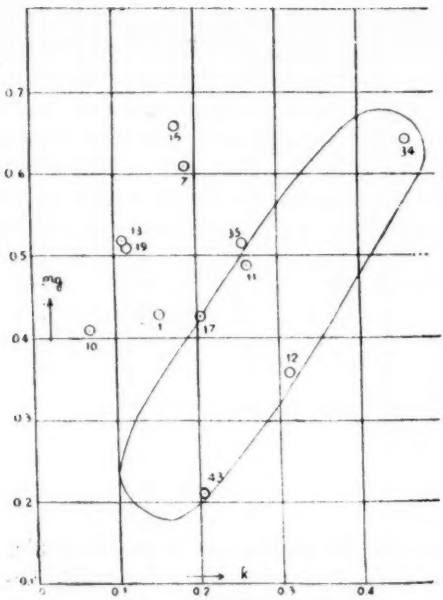

FIG. 3

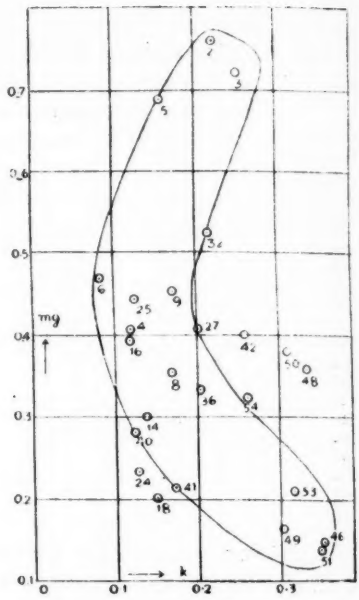

FIG. 4

FIG. 3. *k–mg*. Diagram for the Deccan Traps from the Bombay Coast and Pavagad Hills

FIG. 4. *k–mg*. Diagram for the Deccan Traps from Kathiawar

portions bring out the magmatic affinities of rock-types, represent the three corners of the diagram. The values M and L are the unsaturated ferromagnesian and feldspar molecules respectively. When these molecules are given enough silica for saturation, they form pyroxenes and feldspars. The point P on the side QM and F on the side QL represent the limit of saturation, beyond which pyroxenes and feldspars form respectively. This line PF is the saturation line, dividing the triangle into two areas, the undersaturated PFLM and oversaturated QFP.

The QLM values of the rocks from all the four regions of the Deccan Trap formation, given in Tables VII, VIII, IX and X have been plotted in trilinear diagrams given as Figs. 5, 6 and 7 reproduced from Niggli (1938, Figs. 2*a*, 20 and 21). In the diagrams are shown the 'main basalt field' in which are distinguished the two well-defined areas the 'normal-basalts' and 'alkali basalt' and a well-marked area of calc-alkaline field. We see from these diagrams that most of these types fall within the main-basalt field.

The so-called ' primary basalts ' are encountered in all parts of the world, occupying enormous areas and have been poured out at different geological times without any significance in space and time. These lava flows are all similar in composition, composed chiefly of three principal minerals, pyroxenes, feldspars and iron-ores with or without olivine. From a study of the evidences relating to origin of these basalts, it has been concluded that they represent liquefied portions of the basic shell of the earth underlying the upper layer of granite, and have subsequently been forced up to the surface. It has been estimated that the basic shell extends to many kilometers below the granitic layer. Whether these lavas represent actually the composition of the magma reservoir or whether they have undergone any degree of differentiation in it before being brought to the surface is a matter of controversy.

W. Q. Kennedy (1933), basing his studies on the investigations of the authors of the Mull Memoir, has come to the conclusion " that there exist two great primary basalt magmas, the olivine-basalt type and the tholeiite basalt type....the former being the parent of the alkaline rock and the latter the parent of the calc-alkaline suite....". He maintains, therefore, that a particular late differentiate is determined only by the nature of the 'primary magma ' that gave rise to it and not by the physical conditions of crystallisation during differentiation. He does not discuss the question fully, as according to him there is no evidence to show that either of these ' primary ' magmas is a derivative of the other or that they were the differentiates of a common parent, but simply regards these two magmas as representing primary magmas.

On the other hand, H. Kuno (1937), as a result of a chemical study of the basalts from all over the world, concludes that the plateau-basalts do not represent the composition of the primary magma and that the ultimate primary magma should have been more basic than plateau-basalts, having the composition of olivine-eucrite. He believes that the tholeiitic type has been derived from olivine-basalt type, which in turn originated from the primary olivine-eucrite magma.

The present author is inclined to believe that the lavas of the Deccan trap do not represent the composition of the primary magma and that they may have been derived from deep-seated magma reservoirs containing magma of a more basic composition. It is well known that the Deccan lavas were surprisingly fluid and that a single flow by virtue of its mobility was capable of spreading over long distances, as is well seen in the Nagpur region of the Central Provinces. This fluidity is explained as due to two causes, first that they might have had a special composition, and second that they might have

had a high degree of super-heat. According to those who invoke the first explanation, it was the high percentage of iron-oxides usually present in the lavas that was responsible for the fluidity. But considering the thickness of the crust traversed by the magma, especially through the granitic shell before reaching the surface, it seems reasonable to suppose that the lavas should have possessed a temperature considerably above their melting point. As this shell underlies the superincumbent granitic crust, it should naturally be subjected to great pressure which keeps it in the solid state. Should this pressure from above be reduced considerably over a portion of the magma basin, the magma becomes fluid. Deeper in the basaltic shell, temperature and pressure naturally increase and a zone will be reached where the volume of the rock is at a minimum. In this zone the sesquioxides such as Fe_2O_3, Al_2O_3, Cr_2O_3, etc., present in the rock will tend to form garnet, a high pressure mineral instead of the common ferromagnesians of a more shallow zone. This deep zone has been termed *the infra-plutonic zone* and if melting takes place in this zone due to release of pressure, the resultant chemical changes that take place through the conversion of garnet to other minerals, being exothermic, release a great deal of heat energy which will superheat the magma. This infra-plutonic zone is variously estimated by different investigators to be at depths between 37 Km. and 60 Km. There is also difference of opinion whether the basic shell extends to such depths required for the formation of garnet or whether the peridotitic layer, which is believed to underlie the basic shell has already made its appearance. If there be the peridotitic layer at this zone, it would react in the same way to the volume law and give rise to garnet and alkali-pyroxene. A rock containing these minerals would behave similarly when the hydrostatic pressure is released and the resulting magma will be superheated. If, therefore, we assume the second hypothesis that the magma possessed much superheat, then the lavas should necessarily be regarded as having originated from deep-seated sources, located at a minimum depth of 50 Km. to 60 Km. In the opinion of the author it appears probable that not only the lower layers of the basic shell but also contiguous parts of the peridotitic shell will be melted. It is suggested that the resulting magma would correspond in composition to picrite. This picritic magma may be assumed to represent the primary magma from which the Deccan lavas were differentiated.

In the field we see evidences for the existence of lavas of ultrabasic composition. Ultrabasic rocks such as limburgite, oceanite, etc., occur, and they appear to be intrusive into the basaltic rocks. They are not the result of accumulation of early formed minerals such as olivine and pyroxene but are the direct products of consolidation from liquids of the same

composition. A study of the phenocrysts of some of these ultrabasic rocks by Dr. W. D. West seems to indicate that they and the groundmass crystals are of the same composition and that they have not been formed by crystal settling due to gravitation, but represent the normal constituents of rock formed from lavas of the same composition.

With this primary picritic—magma as the starting point in the differentiation of various types we can follow the trends of differentiation for all the regions in the QLM diagram.

Central Provinces.—When the QLM values of the traps from the Central Provinces are plotted (Fig. 5) we see that most of the traps fall within the main basalt field and that only one type falls outside in the calc-alkaline region of the diagram. The undifferentiated nature of the basalts is well brought out by the grouping of the points of 7 basalts close together. Only the type represented by No. 20, which is slightly differentiated, falls away from this group. However, we see in the diagram that differentiation tendencies, exhibited by the lavas, are towards the calc-alkaline field.

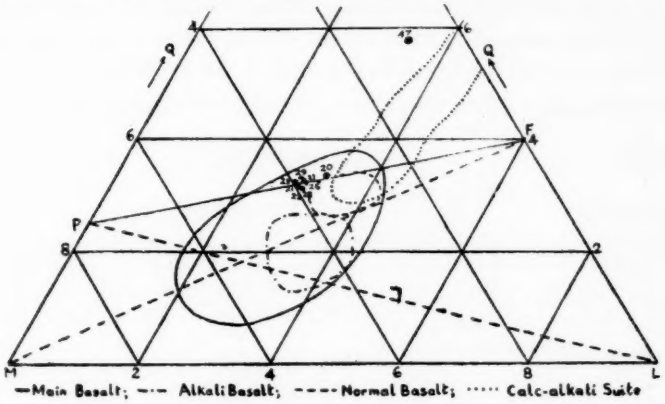

FIG. 5. QLM Diagram for Deccan Traps from the Central Provinces

Bombay Coast and Pavagad Hills.—We have already seen that the rocks of this region cover a wide range from ultra-basic to acid types. When we plot these types in the diagram (Fig. 6) we see that the rocks arrange themselves in a definite sequence along a linear zone both in the main basalt and calc-alkali regions in such a way that we can trace the evolution and sequence of formation of every one of these types. The ultra-basic rock is represented in this region by oceanite and ankaramite which fall in the main basalt field of the diagram towards M. The differentiated types occupy both the

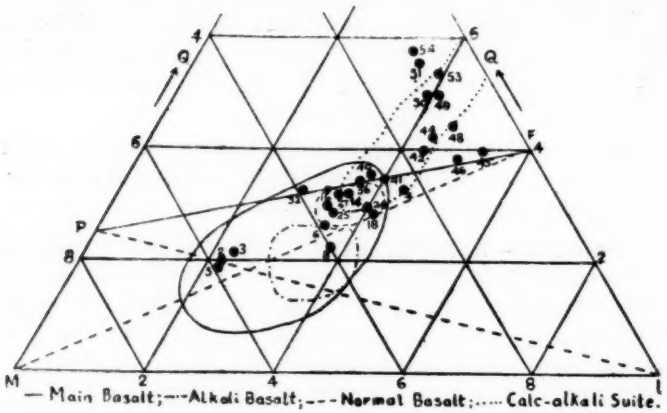

FIG. 6. QLM Diagram for the Deccan Traps from the Bombay Coast and Pavagad Hills

alkaline-basalt and normal basalt fields. The more acid types arrange themselves regularly in the calc-alkaline field. Thus there is only one trend of differentiation towards the calc-alkaline field as shown below:

Olivine-dolerite	(alk-hornblendeperidotitisch)
↓	
Oceanite	(Hornblenditisch)
↓	
Ankaramite	(Hornblenditisch)
↓	
Basalts, Gabbro and Dolerites	(Melatheralithisch, Essexitgabbroid, Normalgabbroid, Normalgabbrodioritisch and Miharaitisch)
↓	
Andesites	(Leukomiharaitisch and Normaldioritisch)
↓	
Trachytes	. . .
↓	
Granophyre and Felsite	(Farsunditisch and Natronrapakiwitisch)

Kathiawar.—The diagram (Fig. 7) for this region differs from the above diagrams in that there are certain types falling outside the main basalt and calc-alkaline fields below the line PF towards F. This region which represents rocks with high percentage of unsaturated leucocratic constituents, is characteristic of the alkaline suite of rocks. There is only one type (Type 52) which falls high up in the calc-alkaline field. The other types fall both in the alkaline basalt and normal basalt regions of the main basalt field.

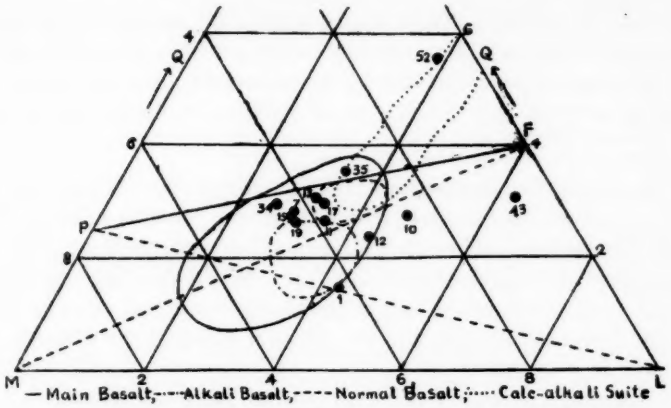

FIG. 7. QLM Diagram for the Deccan Traps from Kathiawar

The differentiation trend can be followed in this diagram along two different lines, one towards the calc-alkaline suite and the other towards the alkaline suite. The sequence of crystallisation of the magma is shown below:

Calc-alkaline trend of differentiation	*Alkaline trend of differentiation*
Basalt (Ankaratritisch)	Basalt (Ankaratritisch)
↓	↓
Dolerites, Basalts and Gabbro (Hornblenditisch, Issitisch, Miharaitisch and Normalgabbroid)	Diorite Gabbro (Normal theralithgabbroid)
↓	↓
Rhyolite (Rapakiwitisch)	Oligoclase-basalt (Lamprodioritisch)
	↓
	Nepheline Syenite (Essexitfoyaitisch)

The ultrabasic type 1 is not taken to represent the original magma as it falls to one side of the main basalt field near its border.

CONCLUSION

From this study of the QLM diagrams constructed for different regions of the Deccan traps we can conclude that the trend of differentiation was generally such as to give rise to calc-alkaline suite of rocks, but in some places as in Kathiawar in addition to the calc-alkaline tendencies there was alkaline trend of differentiation. The rocks so formed contained nepheline and olivine because of inadequate silica available for saturation of these minerals. Thus the Deccan traps give us a clear example of both lines of magmatic differentiation irrespective of whether the 'primary' magma was

olivine-basalt or tholeiite. The primary magma is believed to be ultrabasic in composition corresponding to picrite and the further course of differentiation of this magma was determined by the molecular constitution of the early-formed crystals and the degree of reaction between them and the liquid.

An interesting fact arising out of this study is that though the Deccan traps occupy an enormous area, it is only in the western parts of Bombay and in Kathiawar that differentiated types are present in force. We do not know at present the significance of this fact. Whether it has anything to do with the size and extent of the magma basin, the nature of crust overlying it, the tectonic forces which affected the different parts of the country, or any other factor, is a question which has to receive serious attention in our efforts to elucidate the history and evolution of this great igneous formation.

The author makes grateful acknowledgement to Dr. M. S. Krishnan, Superintending Geologist, Geological Survey of India, for the critical reading of the manuscript of this paper and for many valuable suggestions.

LIST OF WORKS TO WHICH REFERENCE IS MADE

Bajpai, M. P. .. "The Gwalior Trap from Gwalior, India," *Jour. Geol.*, 1935, **43**, No. 1, 61–75.

Chatterjee, S. K. .. "Petrology of the igneous rocks from the West Gir Forest, Kathiawar, India," *ibid.*, 1932, **40**, No. 2, 154–63.

Crookshank, H. .. "Geology of the Northern Slopes of the Satpuras between the Morand and Sher Rivers," *Mem. Geol. Sur. Ind.*, 1936, **46**, pt. 2.

Dubey, V. S. .. "Ph.D. Thesis for the London University," 1929.

Fermor, L. L. .. "On the Chemical Composition of the Deccan Trap Flows of Linga, Chhindwara District, Central Provinces," *Rec. Geol. Sur. Ind.*, 1934, **48**, pt. 3, 344–60.

Kalapesi, A. S., and Contractor, G. P. .. "The Occurrence of Some Acid and Intermediate Rock Types in the Salsette Island, Bombay," *Quart. Jour. Geol. Min. Met. Soc. Ind.*, 1935, **7**, No. 4, 183–91.

———— .. "Petrology of the Salsette Island, Bombay," *Jour. Univer. Bombay*, 1936, **5**, pt. II, 151–71.

———— .. "Variation Diagram of the rocks of the Salsette Island, Bombay," *Quart. Jour. Geol. Min. Met. Soc. Ind.*, **9**, 1937, No. 1, 5–10.

Kennedy, W. Q. .. "Trends of differentiation in Basaltic Magmas," *Amer. Jour. Sci.*, 1933, **25**, 239–56.

Krishnan, M. S. .. "The petrology of rocks from the Girnar and Osham Hills, Kathiawar, India," *Rec. Geol. Sur. Ind.*, 1926, **58**, pt. 4, 380–424.

———— .. "Granophyric Trachyte from Salsette Island, Bombay," *ibid.*, 1929, **62**, pt. 3, 371–76.

Kuno, H. .. "Fractional Crystallisation of Basaltic Magmas," *Jap. Jour. Geol. Geogr.*, 1937, **14**, 189–208.

Mathur, K. K., and Naidu, P. R. J. .. "Volcanic Activity of the Coastal Tracts of Bombay, Salsette and Bassein," *Malaviya Commemoration Volume*, 1932, 154–63.

Niggli, P. .. "Die Komplexe Gravitative Kristallisations-differentiation," *Schweiz. Min. Petr. Mitt.*, 1938, Band **58**, Heft 2, 610–64.

Washington, H. S. .. "Deccan Traps and other Plateau Basalts," *Bull. Geol. Soc. Amer.*, **33**, 765–804.

1. *Limburgite* (Theralithgabbroid).—Lower part of the path near Goraknath, Girnar Hills, Kathiawar. *Rec. Geol. Surv. Ind.*, Vol. LVIII, Pt. 4, 1926, p. 418. Analyst M. S. Krishnan.

   Rock is dull black in colour consisting of glassy groundmass and a few comparatively large crystals of olivine and augite. Under high power, the groundmass reveals a large quantity of brown glassy base, embedded with myriads of microscopic chlorite, magnetite 'dust' and biotite flakes. Microlites of feldspars few. Acicular individuals resembling actinolite in the groundmass. Skeleton-crystals of magnetite.

2. *Oceanite* (Hornblenditisch).—Tramway cutting 1½ miles ENE of Pachkoli village (19° 8′ : 72° 54′), Salsette, Bombay. *Quart. Jour. Geol. Min. Met. Soc. Ind.*, Vol. IX, No. 1, 1937, p. 9. Analyst G. P. Contractor.

   Dark-greenish rock. Holocrystalline and granular with fresh greenish yellow olivine. Groundmass aphanitic, composed of thin laths of plagioclase (Ab 40, An 60), grains of purplish pyroxene and granular iron ores. Pyroxenes are titaniferous. Olivine altered to serpentine and anthophyllite. Feldspar and pyroxene in subophitic relationship.

3. *Ankaramite* (Hornblenditisch).—West of the Vehar lake constituting the Hills (19° 8′ : 72° 55′), Salsette, Bombay. *Quart. Jour. Geol. Min. Met. Soc. Ind.*, Vol. IX, No. 1, 1937, p. 9. Analyst G. P. Contractor.

   Similar to oceanite, but apparently more augite present. Pinkish brown in colour. Porphyritic, olivine crystals. Olivine altered in some parts to typical magnesite.

4. *Vitrophyric Gabbro* (Ossipitisch).—P.W.D. Inspection Bungalow near Bhoyapada (Top of the Mound) Bassein. Malaviya Commemoration Volume 1932, p. 801, Table I, No. 21, Analyst P. R. J. Naidu.

   Plutonic phase of the basic magma; coarsely crystalline and gabbroid in texture. Glass occurring interstially or as groundmass with large crystals of labradorite and augite. Glassy parts contain microlites of feldspar. Colour of the glass varies from reddish brown to deep brown. Iron ores in grains and stout bars. Rock occurs as broad dyke-like intrusion.

5. *Olivine-dolerite* (alk-hornblendeperidotitisch).—Pavagad. V. S. Dubey's unpublished thesis for the Ph.D. degree of the London University, 1929. Analyst V. S. Dubey.

6. *Olivine-Gabbro* (Essexitgabbroid).—Half-way down the western slope of Nale Sopara Hill, Bassein. Malaviya Commemoration Volume, 1932, p. 801, Table I, No. 31. Analyst P. R. J. Naidu.

Occurs as minor intrusion in basaltic rock. Similar to Vitrophyric Gabbro (No. 4) in mineralogical characters. Mode:—Plagioclase 30·9, Pyroxene 30·9, Iron ore 11·2, Glassy Groundmass 27·2.

7. *Olivine-dolerite* (issitisch).—E. of Asodriali Nes, near River Raval. West Gir Forest, Kathiawar. *Jour. Geol.*, Vol. XL, 1932, p. 162, Table I, No. 200 B. Analyst S. K. Chatterjee.

Grayish green and markedly porphyritic with abundant olivine. Pyroxenes exhibit hour-glass structure. Primary magnetite and ilmenite. Chlorite of vermicular form with calcite common.

8. *Alkali-rich Basalt* (Melatheralithisch).—Pavagad. Analyst V. S. Dubey. Given by M. P. Bajpai. *Jour. Geol.*, Vol. XLIII, No. 1, 1935, p. 73, Table VIII, No. 6.

9. *Olivine-dolerite* (normaltheralithisch).—Quarry 2 miles West of Thana Ry. Station, Salsette Island, Bombay. *Quart. Jour. Geol. Min. Met. Soc. Ind.*, Vol. IX, No. 1, 1937, p. 9, App. A. No. 7. Analyst G. P. Contractor.

Composed of feldspar, augite and magnetite. Feldspar and augite are in ophitic relationship. Feldspar is partly altered. Accessories are chlorite, calcite, etc. Rare olivine present.

10. *Oligoclase-Basalt* (Lamprodioritisch).—West of River Raval (2 miles east of Asodriali Nes), West Gir Forest, Kathiawar. *Jour. Geol., Vol.* XL, 1932, p. 162, Table I, No. 200 A. Analyst S. K. Chatterjee.

Greenish-yellow carrying dark glass with magnetite. Feldspar phenocrysts are altered to palagonite. Vesicular silica. Microlites of oligoclase feldspar in the groundmass. Olivine except as phenocrysts.

11. *Olivine-Gabbro* (berondritisch).—North-western end of the long hill near its base, Girnar Hills, Kathiawar. *Rec. Geol. Surv. Ind.*, Vol. LVIII, p. 418, No. 2. Analyst M. S. Krishnan.

Coarse-grained and dark coloured with slight greenish tinge, composed of zoned feldspars, non-pleochroic augite with sub-ophitic structure towards the feldspar and olivine. Biotite at the contact of magnetite and feldspar. Apatite present. Mode: Plagioclase 52·2, Augite 26·2, Olivine 17·5, Biotite 2·0, Apatite 0·4, Iron ore 1·5.

12. *Diorite-Gabbro* (Normaltheralithgabbroid).—Along the path from Bhairao Jap towards Gaomukhi Khund, Girnar Hills, Kathiawar, *Rec., Geol. Surv. Ind.*, Vol. LVIII, p. 418, No. 3. Analyst M. S. Krishnan.

Composed of andesine-labradorite, oligoclase, orthoclase and augite. Augite violet in colour and pleochroic feebly. Colourless non-pleochroic augite also present. Biotite, magnetite and apatite are accessories.

13. *Dolerite* (Normalgabbroid).—From near Khambha, West Gir Forest, Kathiawar. *Jour. Geol.*, Vol. XL, 1932, p. 162, Table I, No. 195 T. Analyst S. K. Chatterjee.

Feldspars are in clusters: pyroxenes are enstatite-augite. Ilmenite, magnetite and rugged flakes of hæmatite present.

14. *Vitrophyric Dolerite* (Normalgabbroidioritisch).—Nale Sopara Hill. Top of 622′ hill, east of the Nale Sopara Rly. Station, Bassein. Malaviya Commemoration Volume, 1932, p. 801, Table I, No. 61. Analyst P. R. J. Naidu.

Dark coloured, compact, breaking with splintry and conchoidal fracture. Occurs as a dyke in a mass of gabbro overflowing it. Half the volume composed of glass. Glass is palagonised and shows microlites of feldspars. Rest of the rock composed of plagioclase, pyroxene and iron ores. Mode: Plagio. 27·0, Pyroxene 20·0, Iron ore 10·1, Glassy groundmass 42·9.

15. *Olivine-Dolerite* (Hornblenditisch).—South of Kapuria Nes, West Gir Forest, Kathiawar, India. *Jour. Geol.*, Vol. XL, 1932, p. 162, Table I, No. 206 C. Analyst S. K. Chatterjee.

Fine-grained dolerite with intergranular to micrographic groundmass of feldspar and augite. Markedly porphyritic with abundant olivine of large size. Pyroxenes are of pale colour exhibiting hour-glass structure. Magnetite and ilmenite are Primary. Ophitic in character.

16. *Dolerite* (Normalgabbroid).—Station Bungalow, Kolhapur State, Bombay. *Bull. Geol. Soc. Amer.*, Vol. 33, 1922, Table I, p. 774, No. 8. Analyst H. S. Washington.

Coarse, holocrystalline, ophitic. Brownish in colour. Labradorite in Tables, 2 mm. in length with anhedral augite intersertal between them. Augite brownish. Magnetite rather abundant, in irregular grains. A few small apatite needles.

17. *Basalt* (Miharaitisch).—Half a mile east of the entrance to the south Gorge, Girnar Hills, Kathiawar. *Rec. Geol. Surv. Ind.*, Vl. LVIII, p. 418, No. 4. Analyst M. S. Krishnan.

Very fine-grained, showing two generations of minerals. Phenocrysts of feldspars larger than those of other minerals. Augite phenocrysts altered to calcite and uralite. Ophitic texture. Groundmass composed of a plexus of minute feldspar laths mingled with augite and magnetite grains.

Greenish mineral probably celadonite. Glass is dark brown, crowded with magnetite dusts.

18. *Basalt* (leukomiharaitisch).—Low level west of the P.W.D. Inspection Bungalow near Bhoyapada, Bassein, Bombay. Malaviya Commemoration Volume, 1932, p. 801, No. 49. Analyst P. R. J. Naidu.

Description of rock not given.

19. *Alkali-rich Basalt* (Ankaratritisch).—Dhanti, Kathiawar, *Jour. Geol.*, Vol. XLIII, No. I, 1935, Table VIII, p. 73, No. 5. Analyst V. S. Dubey.

20. *Dolerite* (Miharaitisch).—Pipardahi station, Seoni, Central Provinces. *Bull. Geol. Surv. Amer.*, Vol. 33, 1922, p. 774, Table I, No. 16. Analyst H. S. Washington.

Coarse, ophitic and sub-hyaline with yellow glass. Greenish black in colour. Composed of labradorite tables and augite with interstitial glass between them. Magnetite is in small amount.

21. *Olivine-Dolerite* (si-pyroxenitisch).—A well 100 yds. east of the B. N. Rly. line at a point WSW of Goreghat village, Linga area, Chhindwara district, Central Provinces. *Rec. Geol. Surv. Ind.*, Vol. LXVIII, pt. 3, p. 350 (Flow 1). Analyst M. Raoult.

Rock dark greyish to brownish black and crystalline. Coarse-grained composed of labradorite laths, brownish grey augite, black iron-ores and dark brown glass, interstitial to principal minerals. Glass primary and contains apatite needles, augite and feldspar. Glass altered to palagonite. A few rounded, olivine phenocrsyts palagonised. Ophitic to sub-ophitic texture.

22. *Olivine-Dolerite* (si-pyroxenitisch).—Kulbehra River, East of Dewardha, Linga area, Chhindwara district, Central Provinces. *Rec. Geol. Surv. Ind.*, Vol. LXVIII, Pt. 3, p. 350 (Flow 2). Analyst M. Raoult.

Dark grayish black, distinctly crystalline; non-porphyritic composed of olivine, labradorite, augite, iron-ore (? ilmenite) and apatite. Augite not in ophitic or sub-ophitic relation, but corrosive towards feldspar. Primary glass grey. Palagonite formed at the expense of feldspar, augite and interstial glass. Olivine largely altered into delessitic pseudomorphs with olivine cores. Occasional calcite.

23. *Basalt* (si-pyroxenitisch).—From an outcrop in the bed of the Kulbehra River, WNW of the village. Bisapur Khurd, Linga area, Chhindwara district, Central Provinces. *Rec. Geol. Surv. Ind.*, Vol. LXVIII, Pt. 3, p. 350 (Flow 2 A). Analyst M. Raoult.

Black fine-grained; scattered phenocrysts of feldspar (sometimes in glomeroporphyritic aggregates) in a groundmass composed of laths of feldspars, augite granules, abundant glass and iron-ores. Glass contains

minute laths, probably apatite. Iron ores are ilmenite and magnetite and are in skeletal shapes and bars and partly in square crystals. Altered olivine also detected. Delessitic palagonite patches with iron-ores.

24. *Dolerite* (Normalgabbrodioritisch).—Half-way down the western slope of the Inspection Bungalow, Bhoyapada, Bassein, Bombay. Malaviya Commemoration Volume, 1932, p. 801, Table I, No. 29. Analyst P. R. J. Naidu.

This is a medium grained phase of gabbro.

25. *Basalt* (Normalgabbrodioritisch).—Pavagad. V. S. Dubey's unpublished thesis for the Ph.D. degree of the London University, 1929 (unpublished). Analyst R. K. Saksena.

26. *Dolerite* (Arriegitisch).—Padmi, Mandla, Central Provinces. *Bull. Geol. Soc. Amer.*, Vol. 33, 1922, p. 774, Table I, No. 15. Analyst H. S. Washington. Coarse, ophitic, subhyaline dolerite with yellow glass. Glass is interstitial to labradorite tables and augite grains. Magnetite is seen in small amount.

27. *Basalt* (Miharaitisch).—From the low lying plain between Kurla and Ghatkoper (19° 5′ : 54° 34′) Rly. Stations, Salsette, Bombay. *Quart. Jour. Geol. Min. Met. Soc. Ind.*, Vol. IX, 1937, p. 9, App. A, No. 6. Analyst G. P. Contractor.

Dark and finely crystalline. Abundant crystals of light brown augite and fairly good amount of magnetite in a groundmass of short laths of labradorite and anisotropic base. Large crystals of feldspar are also seen. Intersertal and ophitic in texture. Iron-ores in irregular pieces.

28. *Basalt* (si-pyroxenitisch).—Shikarpur quarry, ¼ mile east of the Bengal-Nagpur Rly. bridge over the Kulbehra River, Linga area, Chhindwara district, Central Provinces. *Rec. Geol. Surv. Ind.*, Vol. LXVIII, pt. 3, p. 350 (Flow 3). Analyst M. Raoult.

Grayish black and very fine-grained. Feldspar phenocrysts rare and small amount of primary glass. Glass brownish in tint with numerous microlites. Iron-ores large in size. Augite intersertal. No olivine. Green delessitic palagonite formed at the expense of primary glass.

29. *Basalt* (Normalgabbroid).—Doondea Hill, Hirawari, Central Provinces. *Bull. Geol. Soc. Amer.*, Vol. 33, 1922, p. 774, Table I, No. 12. Analyst H. S. Washington.

Fine-grained, subophitic, holocrystalline basalt. Densely aphanitic and compact without phenocrysts. Black in colour. Composed of labrodorite tables, pale brown augite grains and euhedral magnetite grains.

30. *Dolerite* (Normalgabbroid).—Kateru quarries, near Rajahmundry, Madras. *Bull. Geol. Soc. Amer.*, Vol. 33, 1922, p. 774, Table I, No. 23. Analyst H. S. Washington.

Coarse-grained and brown in colour with minute irregular submiarolitic cavities. Black glass present. Ophitic in texture. Augite grains are intersertal to labradorite tables. Glass is interstitial between feldspars and augite.

31. *Dolerite* (Normalgabbroid).—Bhourameta Hill, Chhindwara, Central Provinces. *Bull. Geol. Soc. Amer.*, Vol. 33, 1922, p. 774, Table I, No. 13. Analyst H. S. Washington.

Medium grained, ophitic, subhyaline greenish black dolerite with yellow glass. Brownish augite is in ophitic to intersertal relationship to labradorite tables. Glass interstitial. Magnetite in small amounts.

32. *Dolerite* (Normalgabbroid).—Igatpuri, Nasik, Bombay Presidency. *Bull. Geol. Soc. Amer.*, Vol. 33, 1922, p. 774, Table I, No. 5. Analyst H. S. Washington.

Coarse-grained, holocrystalline, ophitic dolerite black in colour. Twinned labradorite laths and brownish augite in ophitic relationship. Large phenocrystic individuals of olivine. Magnetite abundant in irregular grains. Apatite needles seen.

33. *Basalt* (Miharaitisch).—Jiran, near Neemuch, Central India. *Bull. Geol. Soc. Amer.*, Vol. 33, 1922, p. 774, Table I, No. 4. Analyst H. S. Washington.

Densely apanitic and compact with subresinous lustre. Conchoidal fracture seen. Small rectangular laths of labradorite and rounded grains of brownish augite are intermingled. Black glass with black dust-like grains of small size. No distinct magnetite or ilmenite seen.

34. *Olivine-Dolerite* (Hornblenditisch).—From Hill near Sonaria and of road east-south-east of Salwa, West Gir Forest, Kathiawar. *Jour. Geol.*, XL, 1932, p. 162, Table I, No. 201 T. Analyst S. K. Chatterjee.

Coarse dolerite with porphyritic and intergranular texture. Phenocrysts of olivine and brownish augite present. Magnetite and ilmenite primary; chlorite is of vermicular habit.

35. *Gabbro* (Normalgabbroid).—From southern end of spur of Nandivela, West Gir Forest, Kathiawar. *Jour. Geol.*, XL, 1932, p. 162, Table I, No. 200 Q. Analyst S. K. Chatterjee.

Composed of plagioclase (An 70 to 60%) brownish pyroxene micropegmatite, magnetite and biotite. Augite altered to actinolite and chlorite with clots of magnetite and iron hydrates. Micropegmatite composed of quartz and orthoclase.

36. *Basalt* (Normal gabbrodioritisch).—Between Race Hill and Sewri, Island of Bombay, *Bull. Geol. Soc. Amer.*, Vol. 33, 1922, p. 774, Table I, No. 6. Analyst H. S. Washington.

Densely aphanitic, deep black, compact rock, with subresinous lustre of trachylyte. Conchoidal fracture seen. Laths of labradorite and augite grains are intermingled. Black glass present. No distinct magnetite or ilmenite seen.

37. *Dolerite* (Normalgabbrodioritisch).—Panandrao, Cutch. *Bull. Geol. Soc. Amer.*, Vol. 33, p. 774, Table I, No. 1. Analyst H. S. Washington.

Coarse, ophitic dolerite greenish black in colour. Composed of labradorite, augite and yellow glass. Glass is interstitial between feldspar and augite.

38. Average of four analyses of traps from Linga area, Central Provinces (si-pyroxenitisch). *Rec. Geol. Surv. Ind.*, Vol. LXVIII, Pt. 3, 1934, p. 350. Analyst M. Raoult.

39. Average of 11 analyses of Deccan traps (including one Rajmahal trap) Normal gabbroid; c gabbroid). *Bull. Geol. Soc. Amer.*, Vol. 33, 1922, p. 774. Analyses by H. S. Washington.

40. *Andesite* (Leukomiharaitisch).—Malabar Hill, Bombay. Malaviya Commemoration Volume, 1932, p. 801. No. 59*b*. Analyst P. R. J. Naidu.

Compact, black rock with sub-conchoidal fracture. Few small phenocrysts of plagioclase (andesine-labradorite) and twinned augite. Groundmass composed of oligoclase-andesine, intersertal augite and glass. Appreciable iron ore in granules. Glass violet brown forming considerable portion of groundmass. Palagonite also seen. Mode as follows: Plagioclase 26·2; Augite 21·6; Iron-ore 9·7; Secondary Minerals 1·1; Glass 41·1.

41. *Andesine Andesite* (Leukomiharaitisch).—Danda, Salsette Island, Bombay. *Quart. Jour. Geol. Min. Met. Soc. Ind.*, Vol. IX, No. 1, 1937, p. 9, App. A, No. 5. Analyst G. P. Contractor.

Compact and dark in colour breaking with sub-conchoidal fracture. Dark-brown glass and lath-shaped feldspar microlites enclose between them subidiomorphic crystals and granules of augite. Delessite found. Phenocrysts are andesine-labradorite. Groundmass microlites are oligoclase-andesine.

42. *Andesite* (Normaldioritisch).—Gokhivre, Bassein. Malaviya Commemoration Volume 1932, p. 801, No. B/3. Analyst P. R. J. Naidu.

Compact and dark. Numerous phenocrysts in a black typically andesitic groundmass. Augite and hypersthene seen. Feldspars corroded by glass. Groundmass with microlites of feldspar showing flow banding around phenocrysts.

43. *Nepheline Syenite* (essexitfoyaitisch).—South part of the west valley; on the path leading to south valley, Girnar Hills, Kathiawar. *Rec. Geol. Surv. Ind.*, Vol. LVIII, pt. 4, 1926, p. 418, No. 5. Analyst M. S. Krishnan.

Holocrystalline coarse; light coloured. Feldspar abundant, orthoclase dominating, albite and oligoclase. Nepheline allotriomorphic and abundant. Slightly bluish sodalite, cancrinite and aegirine-augite present. Muscovite, sphene, apatite and brown iron oxide as accessory minerals. Feldspar and nepheline altered to sericite. Mode: Feldspars 52·2; Nepheline 21·3; Sodalite 15·0; Aegirine 5·5; Magnetite 3·6; Brown iron oxide 1.2, Sphene 1·2.

44. *Trachyte.*—Hill north-west of Kalmapada near Nale Sopara Rly. Station, Bassein. Malaviya Commemoration Volume, 1932, p. 801, No. 40. Analyst P. R. J. Naidu. Rather decomposed; pinkish in colour. Groundmass is felsitic. Feldspars are kaolinized.

45. *Granophyric Trachyte* (Nordmarkitisch).—Kharodi, near Malovni (four miles west of Malad Station) Salsette, Bombay. *Rec. Geol. Surv. Ind.*, Vol. LXII, pt. 3, 1929, p. 373. Analyst M. S. Krishnan.

Light-cream coloured. Fine-grained containing very few dark minerals. Specks of metallic yellow pyrite and yellow-brown limonitic matter. A few large crystals of quartz and feldspar. Holocrystalline and highly feldspathic (orthoclase and some oligoclase) calcite present. Few crystals of quartz and slender needles of apatite. No ferromagnesian minerals, but dirty brown patches represent original pyroxene or amphibole. Grains of pyrite decomposing to limonite.

46. *Granophyric Trachyte* (umptekitisch).—Half a mile north west of Kurla Rly. Station. *Quart. Jour. Geol. Min. Met. Soc. Ind.*, Vol. VII, No. 4, 1935, p. 189. Analyst G. P. Contractor.

Light buff in colour, finely crystalline groundmass, with small crystals of flesh coloured feldspar. Holocrystalline fine-grained matrix without distinct trachytic structure. Orthoclase abundant. Ferromagnesians absent. Some calcite and apatite needles. Quartz in subordinate amount.

47. *Porphyrite* (leukotonalitisch).—From the composite dyke in the nala east of Jamundhonga, Northern slopes of the Satpuras, Central Provinces. *Rec. Geol. Surv. Ind.*, Vol. LXVI, Pt. 2, 1936, p. 341. Analyst Mahadeo Ram.

Pale grey rock with granulitic texture. Lath-shaped plagioclase and micropegmatite are main constituents forming about 90%, latter predominating. Feldspar, oligoclase, altered. Ferromagnesians comprise enstatite-augite and common hornblende, showing tendency to idiomorphism. Palagonite and iron ores present. Accessory minerals are apatite and fibrous zeolites. Nodules of iron pyrites and secondary calcite occur commonly.

48. *Rhyolite Ash* (Tuff) (gibelitisch).—Santa Cruz-Khar, Salsette, Bombay. *Quart. Jour. Geol. Min. Met. Soc. Ind.*, Vol. VII, No. 4, 1935, p. 186. Analyst G. P. Contractor.

Soft white rock with earthy matter. Cryptocrystalline matrix with angular and broken crystals of orthoclase. Fairly large amount of black to brown red hæmatite present (probably due to alteration of hornblende). Apatite needles occasionally found.

49. *Pitchstone* (natronrapakiwitisch).—Lower part of Pavagad Hill. V. S. Debey's thesis for the Ph.D. degree of London University, 1929 (unpublished) Analyst V. S. Dubey.

50. *Augite Orthophyre* (farsunditisch).—From a quarry near Marol village (19° 7′ : 72° 53′), Salsette, Bombay. *Quart. Jour. Geol. Min. Met. Soc. Ind.*, Vol. VII, No. 4, 1935, p. 190. Analyst G. P. Contractor.

Fine-grained, grey, compact rock. Laths of feldspar and greenish dark pyroxene. Quartz and feldspar in graphic intergrowth. Feldspar abundant, presumably orthoclase. Oligoclase also present. Pyroxenes fairly pleochroic, grass green in colour; probably ægirine-augite. Iron-ore present. Skeletal laths of augite embedded in feldspar may be of second generation.

51. *Rhyolite* (leukoquartzdioritisch).—Pavagad Hill, from 2550 ft. V. S. Dubey's thesis for the Ph.D. degree of London University, 1929 (unpublished). Analyst R. K. Saksena.

52. *Rhyolite* (rapakiwitisch).—Near Patanwao (21° 38½′ : 70° 18′), Girnar Hills, Kathiawar. *Rec. Geol. Surv. Ind.*, Vol. LVIII, Pt. 4, 1926, p. 418, No. 6. Analyst M. S. Krishnan.

Commonly a dense black rock; conchoidal fracture and vitreous lustre. Banded rhyolite showing shades of yellow and brown. Partial devitrification has produced minute rods and grains. Bands due to flow-structure. Spherules with radiating fibrous structure seen in abundance. In some portions laths of feldspar (orthoclase) and microlites of ferromagnesian minerals observed.

53. *Felsite* (natronrapakiwitisch).—From one of the intrusions in the Santa Cruz-Khar area. Half a mile south-east of Vakola village (19° 5′ : 72° 51′). *Quart. Jour. Geol. Min. Met. Soc. Ind.*, Vol. VII, No. 4, 1935, p. 187. Analyst G. P. Contractor.

Rock is pinkish in colour; minute crystals of feldspar scattered irregularly. Brown to dark brown bands of hæmatitic matter present. Compact breaking with conchoidal fracture. Quartz and feldspar. Cryptocrystalline. Phenocrysts of feldspar (orthoclase or anorthoclase) present. Groundmass is felsitic as a result of devitrification of the original rhyolitic lava. Grains of black iron-ore scattered in the groundmass. Quartz in the groundmass anhedral.

54. *Vesicular Rhyolite* (natronrapakiwitisch).—ENE of Madh, Summit of hill, 126 ft. Saslette, Bombay. Malaviya Commemoration Volume, 1932, p. 801, Table I, No. 1. Analyst P. R. J. Naidu.

Vesicular and amygdoloidal, showing a horizontal flow-banded arrangement. Light grey or cream coloured. Micro-felsitic. Vesicles low-oriented and filled with yellow mineral, probably chlorite.

55. Granophyric Rhyolite (normalalkaligranitisch).—Half-way between the elevation 126 ft. in Madh and the ferry to the east, Salsette, Bombay, Malaviya Commemoration Volume, 1932, p. 801, Table I, No. 5. Analyst P. R. J. Naidu. Norm as given by the authors.

Porphyritic rhyolite; phenocrysts are euhedral corroded crystals of quartz and feldspar. Some feldspar phenocrysts are sanidine. Brown hæmatitic patches surrounding grains of iron ore. Groundmass micro-felsitic in texture.

EMISSION BANDS OF HALOGENS

Part II. Iodine Bands arising in 1_g ($^3\Pi_{1g}$) and $\Pi_{2,1g}$ States

BY PUTCHA VENKATESWARLU, M.SC.

(*Physics Department, Benares Hindu University*)

Received August 22, 1946

(Communicated by Dr. R. K. Asundi, M.SC., PH.D. (London), F.A.SC.)

INTRODUCTION

IN the previous paper[1] 'Emission Bands of Halogens, Part I', hereinafter called Paper I we have mentioned the existence of groups of diffuse bands in the region 4800 to 2400 A. In Paper I we have dealt with five groups of bands in which the bands have a wavenumber separation of the order of 165 cm.$^{-1}$ They were explained to be due to transitions from a single stable state O_u^+ at 51683 cm.$^{-1}$ to different unstable states dissociating into $^2P_{\frac{1}{2}} + {}^2P_{\frac{1}{2}}$, $^2P_{3/2} + {}^2P_{\frac{1}{2}}$, $^2P_{3/2} + {}^2P_{3/2}$ iodine atoms. In this paper we shall deal with those groups of bands in which the bands have wavenumber separations of the order of 215 cm.$^{-1}$ and 360 cm.$^{-1}$ in the region 4800 to 2687 A.

Experimental details are given in Paper I. Spectra are taken on a 3-prism Steinheil spectrograph, a Hilger medium quartz spectrograph, and E_1 quartz spectrograph. The microphotometric curves of the plates are taken on a Zeiss recording microphotometer.* Plates VIII and IX are the reproductions of the spectrograms and their microphotograms. The wavelengths and wavenumbers of the intensity maxima of all the bands in the region 4800 to 2687 A are given in Table I. The wavelengths of the bands as measured by McLennan[2] and Oldenberg[3] from flourescence experiments and by Curtis and Evans[4], and by Asagoe and Inuzuka[5] from emission experiments are also given. There is fairly good agreement between the values obtained in the present experiments and by previous workers. The intensity values given correspond to the relative values estimated from the bands obtained on process plates taken on E_1 quartz spectrograph and from peaks of microphotometric curves. The bands that arise in the state O_u^+ at 51683 cm.$^{-1}$ and which are discussed in Paper I are also included in Table I. In Table III five groups of bands are given in two sets. The wavenumber separation of the bands in each group is of the order of 215 cm.$^{-1}$ All the

* Thanks to Prof. S. P. Prasad, Science College, Patna, for permission to work in their laboratories, and to Prof. L. M. Chaterjee for help in microphotometric work.

TABLE I

McLennan λ	Oldenberg λ	Curtis & Evans λ	Asagoe & Inuzuka λ	Present experiments		
				Intensity	λ	ν (vac)
	4713		4735·3	0	4747·2	21059
	4660		4659·4	1	4662·1	21444
4608	4596		4585·0	3	4575·6	21849
4550	4541		4524·8	2	4517·7	22129
4505	4489		4477·0	4	4472·1	22354
4452			4437·0	2	4430·6	22564
			4392·6	3	4390·1	22772
			4357·7	3	4356·4	22948
			4320·6	5	4317·8	23153
4290	4290		4282·9	8	4282·2	23346
4250	4253		4246·9	8	4242·5	23564
4210	4217		4211·3	6	4201·8	23793
4170			4158·3	6	4154·4	24064
			4125·3	5	4124·2	24240
4130–4015 (broad band)			4096·2	8	4094·6	24416
			4069·0	7	4067·6	24578
			4040·8	8	4044·6	24717
	4007		4017·8	8	4018·0	24881
			3990·8	3	3991·1	25049
			3953·7	8	3945·6	25338
3925	3925		3922·8	3	3919·4	25507
			3880·3	6	3879·9	25767
3870	3866		3860·8	6	3855·8	25928
			3823·4	3	3821·8	26158
3800	3813		3805·4	4	3798·0	26322
	3765		3773·6	1	3773·2	26495
			3742·9	2	3739·9	26731
3725	3720		3724·7	2	3720·4	26871
	3680		3687·9	2	3686·6	27118
			3674·3	2	3670·1	27239
			3641·7	2	3640·7	27459
3625	3640		3626·4	2	3623·3	27591
			3606·7	2	3600·8	27764
3585	3596		3581·3	2	3578·6	27936
				1	3536·6	28268
3555	3559			7	3515·7	28436
3520	3525			1	3499·8	28565
	3495			1	3479·0	28736
3425	3466		3413·0	10	3416·5 (continuum)	29261
			3333·8	3	3331·7	30006
3315	3311	3306·4	3306·0	4	3306·9	30231
3290	3285	3280·9	3281·9	6	3281·4	30466
3268	3261	3256·9	3257·6	9	3257·4	30691
3245	3237	3233·3	3234·2	10	3233·9	30914
3220	3212	3211·4	3211·1	10	3210·5	31139
3195	3191	3189·8	3190·0	9	3188·6	31353
3175	3169	3171·0	3169·5	3	3168·8	31549
		3141·3	3141·6	3	3142·2	31816
		3123·3	3122·6	9	3122·5	32016
3107		3103·3	3100·1	8	3102·7	32221
3090		3084·8	3084·5	2	3084·6	32410
3065		3062·1	3061·5	5	3061·5	32650
3047		3043·6	3042·9	7	3042·9	32854

TABLE I (*Contd.*)

McLennan λ	Oldenberg λ	Curtis & Evans λ	Asagoe & Inuzuka λ	Present experiments		
				Intensity	λ	ν (vac)
		3023·3	3024·3	3	3024·9	33049
3009		3003·3	3005·6	4	3006·3	33254
2993		2987·2	2987·5	6	2987·1	33468
2960			2966·4	1	2969·7	33664
2946		2954·6	2953·6	5	2952·7	33857
2930		2933·9	2933·9	4	2934·6	34066
2915			2919·2	2	2918·6	34252
2900		2903·1	2904·5	5	2903·4	34432
2883		2875·4	2874·2	5	2874·3	34781
2853		2847·0	2846·2	4	2846·1	35125
2825		2820·9	2821·0	4	2820·1	35449
2799		2793·3	2793·3	4	2792·7	35797
2774		2767·2	2768·0	3	2768·2	36114
2760			2754·6	1	2754·0	36300
2737		2742·0	2744·5	3	2745·1	36418
2727			2731·8	2	2731·2	36603
2715		2711·5	2711·5	4	2712·0	36862
2697		2698·6	2700·4	3	2699·6	37032
2685		2687·2	2687·7	4	2687·5	37198

TABLE II

Bands arising in σ_g, π_u^4, π_g^4, σ_u; O_u^+ *level at* 51683 *with* $\omega = 165{\cdot}1$

Group	ν	Transition
I	24064 24240 24416 24578 24717 24881 25049	$O_u^+ \rightarrow \sigma_g^2, \pi_u^4, \pi_g^2, \sigma_u^2$; $O_g^+(^1\Sigma_g^+)$
II	25336 25507	$O_u^+ \rightarrow \sigma_g^2, \pi_u^4, \pi_g^2, \sigma_u^2$; $O_g^+(^3\Sigma_g^-)$
III	25767 25928	$O_u^+ \rightarrow \sigma_g^2, \pi_u^4, \pi_g^2, \sigma_u^2$; $1_g\,(^3\Sigma_g^-)$
IV	26158 26322	$O_u^+ \rightarrow \sigma_g^2, \pi_u^3, \pi_g^4, \sigma_u$; $1_g\,(^1\Pi_g)$
V	36862 37032 37198	$O_u^+ \rightarrow \sigma_g^2, \pi_u^3, \pi_g^4, \sigma_u$; $O_g^+\,(^3\Pi_{0g})$

bands are diffuse with maximum intensity in the centre. The average width of the bands is of the order of 115 cm.$^{-1}$ The nature of the bands suggests that these bands, like the bands that are discussed in Paper I, are due to transitions from a stable initial state to various unstable states. The fact

TABLE III

Bands arising in $1_g\,(^3\Pi_{1g})$ *state with* $\omega \sim 215$ *cm.*$^{-1}$

Group	ν	Δ_ν	Transition
		FIRST SET	
I	22129 22354 22564 22772	225 210 208	$1_g \rightarrow \sigma_g^2,\ \pi_u^3,\ \pi_g^3,\ \sigma_u^2\ ;\ 1_u\ (^3\Sigma_u^+)$
II	22948 23153 23346 23564 23793	205 193 218 229	$1_g \rightarrow \sigma_g^2,\ \pi_u^3,\ \pi_g^3,\ \sigma_u^2\ ;\ O_u^-(^3\Sigma_u^+)$
		SECOND SET	
III	30006 30231 30466 30691 30914 31139 31353 31549	225 235 225 223 225 214 196	$1_g \rightarrow \sigma_g^2,\ \pi_u^3,\ \pi_g^3,\ \sigma_u^2\ ;\ 1_u^-(^3\Delta_{1u})$
IV	31816 32016 32221 32410	200 205 189	$1_g \rightarrow \sigma_g^2,\ \pi_u^3,\ \pi_g^3,\ \sigma_u^2\ ;\ 2_u\ (^3\Delta_{2u})$
V	32650 32854 33049 33254 33468 33664 33857 34066 34253	204 195 205 214 196 193 209 187	$1_g \rightarrow \sigma_g^2,\ \pi_u^4,\ \pi_g^3,\ \sigma_u^2\ ;\ 1_u\ (^1\Pi_u)$

that the wavenumber separation of the bands in all groups is of the order of 215 cm.$^{-1}$ suggests that these bands are due to transitions from one stable state with a vibrational frequency of 215 cm.$^{-1}$ to different unstable states having flat potential energy curves. The first two groups which are given in the first set are in the visible region and near to each other; and the third, fourth, and fifth groups which are given in second set are in the ultra-violet and near to one another. The wavenumber separation between the first band of the first group and the first band of the third group is 7877 cm.$^{-1}$ which is of the order of the excitation energy in the iodine atom $^2P_{3/2} \rightarrow {}^2P_{\frac{1}{2}}$, *viz.*, (7600 cm.$^{-1}$). Further, flourescence bands which are identical with the

bands of third, fourth and fifth groups can be obtained by excitation with wavelengths between 2100 and 1800 A (48000–55000 cm.$^{-1}$). These facts make it very probable that both the final levels of the first and second groups arise from I ($^2P_{\frac{1}{2}}$) + I ($^2P_{\frac{1}{2}}$) and those of the third, fourth and fifth groups from I ($^2P_{3/2}$) + I ($^2P_{\frac{1}{2}}$). The dissociation limits of the terms that arise from I ($^2P_{3/2}$) + I ($^2P_{\frac{1}{2}}$) and I ($^2P_{\frac{1}{2}}$) + I ($^2P_{\frac{1}{2}}$) are known independently from the visible bands of iodine.[6] These are 20037 cm.$^{-1}$ and (20037 + 7600) = 27637 cm.$^{-1}$ respectively from the ground state of the molecule.

Since all the five groups arise from a common initial level the position of the latter can now be calculated. The calculated value will be necessarily rough for many obvious reasons including that of the diffuse nature of the bands and also because there is at present no means of choosing preferably any one of the many possible repulsive levels as the perfectly flat one. The first set of Table III consists of 9 bands and the second set consists of 31 bands. So we will make use of the bands of the second set to calculate the position of the stable level. The bands of the second set are arranged in three groups which will have, for their lower levels, three repulsive states dissociating into I ($^2P_{\frac{1}{2}}$) + I ($^2P_{3/2}$) atoms at 20037 cm.$^{-1}$ The repulsive states will be nearly flat though they may either have some negligible slope or negligibly shallow minimum. The first bands of the three groups are at 30006, 31816 and 32650 cm.$^{-1}$ Adding 20037 to each of these and taking the mean, we arrive at 51528 cm.$^{-1}$ which therefore represents the approximate position of the initial level.

Having calculated the position of the stable level, the position of the points (lying vertically below the minimum of the stable potential energy curve) on the repulsive curves corresponding to the five groups of bands can be calculated. The points on the repulsive curves corresponding to the first two groups (first set) lie at (51528–22129) = 29399 cm.$^{-1}$ and (51528–22948) = 28580 cm.$^{-1}$ These two repulsive curves, as we have already stated, will dissociate into I ($^2P_{\frac{1}{2}}$) + I ($^2P_{\frac{1}{2}}$) atoms at 27637 cm.$^{-1}$, and as such they will be nearly flat having little slope. The points on the repulsive curves of third, fourth and fifth groups lie at (51528–30006) = 21522 cm.$^{-1}$, (51528–31816) = 19712 cm.$^{-1}$ and (51528–32650) = 18878 cm.$^{-1}$ All these three states will dissociate into I ($^2P_{3/2}$) + I ($^2P_{\frac{1}{2}}$) atoms at 20037 cm.$^{-1}$ and will be nearly flat. The first curve will have a slight slope and the other two will have shallow minima. The fact, that all these five groups of bands are thus explained on the basis of the calculated value of 51528 cm.$^{-1}$, is proof of the approximate correctness of the calculated position of the initial level.

The continuum at 3416 A (29261 cm.$^{-1}$) can also be explained as due to a transition from the stable state at 51528 cm.$^{-1}$ to a repulsive state dissociating into $I(^2P_{3/2}) + I(^2P_{\frac{1}{2}})$. The repulsive curve will be somewhat steep as it gives a genuine continuum. The point on the repulsive curve vertically below the stable state at 51528 cm.$^{-1}$, lies at (51528–29261) = = 22267 cm.$^{-1}$ This continuum was obtained in absorption at high temperatures (1100° C.) by Skorko.[7] The existence of the continuum in absorption at high temperature can be explained as due to transition from an initial repulsive state to the excited stable state ($\omega \sim 215$). This repulsive state is the one obtained by the recombination of $^2P_{3/2} + {}^2P_{\frac{1}{2}}$ iodine atoms which are obtained by the thermal dissociation of the molecules at such a temperature. This view is supported by the fact that at such high temperature, Uchida[8] and others have obtained in emission the visible bands of iodine (well known in absorption) which could be explained only as being brought by thermal luminescence on the supposition that the initial state of the bands, *viz.*, O_u^+ at 15583 cm.$^{-1}$ which is formed by combination of $^2P_{3/2} + {}^2P_{\frac{1}{2}}$ atoms, is reached by thermal excitation.

Before we go further with the theoretical discussion we will give a brief review of the explanations of previous workers. Curtis and Evans[4] have taken the spectrum of iodine vapour excited by high frequency discharge, on the small quartz spectrograph and recorded the wavelength and wavenumbers of the intensity maxima of the bands in the region 3450 →2687 A. They did not come to any definite conclusion about the theoretical explanation of the bands and suggested that work on high dispersion instruments is necessary to decide about the nature of the bands. Asagoe and Inuzuka[5*] have worked on the E_1 quartz spectrograph and took the spectra of iodine vapour excited by transformer, using external electrodes. They recorded the wavelengths of maxima of the diffuse bands between 4800 and 2500 A. They explain that the diffuse bands from 4735 to 3585 A (*i.e.*, from 21112·1 to 27914·9 cm.$^{-1}$) form a single group and are due to transition from a flat potential energy curve arising from $I(^2P_{3/2}) + I(^2P_{\frac{1}{2}})$ atoms, to different vibrational levels of the ground state. But since we now know definitely that the dissociation limit of $I(^2P_{3/2}) + I(^2P_{\frac{1}{2}})$ lies at 20037 cm.$^{-1}$, if this explanation is correct, the bands should not have wavenumbers greater than 20037 cm.$^{-1}$ But all these bands have their wavenumbers between 21112 and 27915 cm.$^{-1}$ and as such the explanation is improbable. Simi-

* The Japanese Journal "Science Reports of the Tokiyo Burnika Daigaku" in which the paper by these two authors has been published, has however come to our notice only recently.

larly they explain that all the bands in the region 29987 cm.$^{-1}$ to 39025 cm.$^{-1}$ form a single group (though named as two systems) and are due to a single transition from a flat potential energy curve arising from $I(^2P_{\frac{1}{2}}) + I(^2P_{\frac{1}{2}})$ atoms to the ground state. As the dissociation limit of $I(^2P_{\frac{1}{2}}) + I(^2P_{\frac{1}{2}})$ lies at 27637 cm.$^{-1}$, this explanation again is untenable. Further their classification of the bands into two groups (21112–27915 cm.$^{-1}$; 29987–39025 cm.$^{-1}$) is not warranted by the general appearance of the bands. An inspection of the spectrograms, taking into consideration the intensities and mutual separations of the bands, shows definitely that the bands form groups with mutual wavenumber separations of the order of 165 cm.$^{-1}$ and 215 cm.$^{-1}$ Such classification into groups is therefore adopted by us. (Lastly these bands, which occur in emission with such great intensity, cannot have an unstable state with a flat potential energy curve as the initial state because such transitions will probably be rare).

Now we will proceed to determine the electronic configuration and electronic terms of the states that give rise to these bands. The stable state at 51528 cm.$^{-1}$ which is the initial state of all the groups of bands in Table III which we are now discussing, has the vibrational frequency of the same order as that of the ground state, and so there will not be much change in the value of ω_e. If this state is to be an *ungerade* state, bands should be obtained in absorption as the transition from the ground state O_g^+ ($^1\Sigma_g^+$) to this state is allowed. The absence of such absorption suggests that the level may be a *gerade* state. Cordes[9] has tentatively explained the iodine absorption bands at 57000 cm.$^{-1}$ as due to a transition from the ground state to $^3\Pi_{1u}$ state at 56933 cm.$^{-1}$. This level cannot be explained as the initial stable level, because it cannot explain the five groups of bands in Table III. The third, fourth, fifth groups can be explained as forming a single group and coming from a transition $^3\Pi_{1u} \rightarrow O_{g2}^+$, O_g^+ being a flat potential energy curve dissociating into $^2P_{\frac{1}{2}} + {}^2P_{\frac{1}{2}}$ atoms at 27637 cm.$^{-1}$ But the occurrence of similar bands in first and second groups cannot be explained as there is no other dissociation level between 27637 cm.$^{-1}$ and 59000 cm.$^{-1}$ Further such an assumption that the stable initial state is $^3\Pi_{1u}$ state at 56933 cm.$^{-1}$ cannot explain the occurrence of the bands of the third, fourth and fifth groups in fluorescence, as the state at 56933 cm.$^{-1}$ cannot be reached directly from the ground state by excitation of wavelengths lying between 2100 and 1850 A. So another level had to be postulated for the stable initial state. If the $^3\Pi_{1u}$ level is at 56933 cm.$^{-1}$ it is natural to expect a $^3\Pi_{1g}$ state below $^3\Pi_{1u}$ and having nearly the same ω_e as that of $^3\Pi_{1u}$. Thus we take the level at 51528 cm.$^{-1}$ as 1_g state according to case (*c*) type coupling, which can be correlated with $^3\Pi_{1g}$ state of case (*a*) or (*b*) type. The electronic configuration of this state is $\sigma_g, \pi_u^4, \pi_g^3, \sigma_u^2$.

We have explained the first two groups as due to transitions from the stable state to the repulsive states that dissociate into $I(^2P_{\frac{1}{2}}) + I(^2P_{\frac{1}{2}})$ atoms. From the combination of these two atomic terms we get the electronic states[11] O_g^+, 1_u and O_u^-. Of these, only the two states 1_u and O_u^- can combine with 1_g. These are the terms that correspond to the repulsive curves which give the first and second groups of bands and are to be correlated with $^3\Sigma_u^+$ of case (*a*) or (*b*) type. The term $^3\Sigma_u^+$ $(1_u, O_u^-)$ can be derived from two types of electronic configuration: $\sigma_g, \pi_u^4, \pi_g^4, \sigma_u$, and $\sigma_g^2, \pi_u^3, \pi_g^3, \sigma_u^2$, the former being higher in energy than the other. As we have already attributed the term $1_u(^3\Sigma_u^+)$ derived from the electronic configuration $\sigma_g, \pi_u^4, \pi_g^4, \sigma_u$ to the final state of Pringsheim-Rosen and Kimura-Miyanishi bands,* we will assign the electronic configuration $\sigma_g^2, \pi_u^3, \pi_g^3, \sigma_u^2$, to the states $^3\Sigma_u^+$ $(1_u, O_u^-)$ that correspond to the two repulsive states dissociating into $^2P_{\frac{1}{2}} + {}^2P_{\frac{1}{2}}$ atoms. So we write the transitions to the first two groups as

First group: $\sigma_g, \pi_u^4, \pi_g^3, \sigma_u^2;\ 1_g(^3\Pi_{1g}) \rightarrow \sigma^2{}_g, \pi_u^3, \pi_g^3, \sigma_u^2;\ 1_u(^2\Sigma_u^+)$.

Second group: $\sigma_g, \pi_u^4, \pi_g^3, \sigma_u^2;\ 1_g(^3\Pi_{1g}) \rightarrow \sigma^2{}_g, \pi_u^3, \pi_g^3, \sigma_u^2;\ O_u^-(^2\Sigma_u^+)$.

We have shown that the repulsive state which is the lower state of the well-known continuum at 3416 A, and the three lower states of the third, fourth and fifth groups dissociate into $^2P_{3/2} + {}^2P_{\frac{1}{2}}$ iodine atoms at 20037 cm.$^{-1}$ A combination of these two terms gives rise to the electronic terms 2_g, 2_u, 1_g, 1_u, 1_g, 1_u, O_g^+, O_g^+, O_g^-, O_u^-[11]$_3$. Of these, the terms that can combine with 1_g are 2_u, 1_u, O_u^-, 1_u, O_u^+. The term O_u^+ corresponds to the stable state which in a transition to the ground state, gives the visible emission bands also known in absorption. Thus we take O_u^- to correspond to the lower state of the continuum, and 1_u, 2_u, 1_u to the lower states of the third, fourth and fifth groups respectively. Now we tentatively correlate these terms with those of the case (*a*) or (*b*) type. From the electronic configuration $\sigma_g^2, \pi_u^3, \pi_g^3, \sigma_u^2$ we get the six states[10] $^1\Sigma_u^+$, $^1\Delta_u$, $^3\Sigma_u^-$, $^3\Sigma_u^+$, $^1\Sigma_u^-$, $^3\Delta_u$. The first three cannot arise from the combination of two ^2P atoms and as such we are not now concerned with them. The other three are among the states that will be possible from a combination of two ^2P atoms.† Of

---

* According to case (*a*) or (*b*) type coupling the probable electronic states that can be derived from the configuration $\sigma_g, \pi_u^4, \pi_g^4, \sigma_u$ are $^1\Sigma_u^+$ and $^3\Sigma_u^+$. The $^1\Sigma_u^+$ of case (*a*) type is to be correlated with O_u^+ of case (*c*) type and $^3\Sigma_u^+$ of case (*a*) is to be correlated with $(O_u^-, 1_u)$ of case (*c*) type. Of these O_u^+ has been assigned to the final state of Cordes bands and 1_u to that of the P—R, K—M bands.[12] These two states will have dissociation products $I^-(^1S_0) + I^+(^3P_2)$.

† Two like atoms in the same ^2P state (J does not matter for this purpose) can give only the following states[11]: $^1\Sigma_g^+$, $^1\Sigma_g^+$, $^1\Sigma_u^-$, $^1\Pi_g$, $^1\Pi_u$, $^1\Delta_g$, $^3\Sigma_u^+$, $^3\Sigma_u^+$, $^3\Sigma_g^-$, $^3\Pi_g$, $^3\Pi_u$ and $^3\Delta_u$.

these $^3\Sigma_u^+$ is correlated already with 1_u and O_u^- of case (*c*) type which correspond to the lower states of the first and second groups respectively. $^1\Sigma_u^-$ is to be correlated with O_u^- of case (*c*) type which gives rise to the continuum at 3416 A. 1_u and 2_u which correspond to the third and fourth groups respectively can be correlated with $^3\Delta_u$ of case (*a*) or (*b*) type. The 1_u term which corresponds to the fifth group will be correlated with the $^1\Pi_u$ of case (*a*) or (*b*) type which comes from the electronic configuration $\sigma_g^2, \pi_u^4, \pi_g^3, \sigma_u$. Thus the various transitions are:

Continuum at 3416 A: $\sigma_g, \pi_u^4, \pi_g^3, \sigma_u^2$; $1_g\,(^3\Pi_{1g}) \rightarrow \sigma_g^2, \pi_u^3, \pi_g^3, \sigma_u^2$; $O_u^-\,(^1\Sigma_u^-)$.

Third group: $\sigma_g, \pi_u^4, \pi_g^3, \sigma_u^2$; $1_g\,(^3\Pi_{1g}) \rightarrow \sigma_g^2, \pi_u^3, \pi_g^3, \sigma_u^2$; $1_u\,(^3\Delta_{1u})$.

Fourth group: $\sigma_g, \pi_u^4, \pi_g^3, \sigma_u^2$; $1_g\,(^3\Pi_{1g}) \rightarrow \sigma_g^2, \pi_u^3, \pi_g^3, \sigma_u^2$; $2_u\,(^3\Delta_{2u})$.

Fifth group: $\sigma_g, \pi_u^4, \pi_g^3, \sigma_u^2$; $1_g\,(^3\Pi_{1g}) \rightarrow \sigma_g^2, \pi_u^4, \pi_g^3, \sigma_u$; $1_u\,(^1\Pi_u)$.

Among the four states O^-, 1_u, 2_u and 1_u, the only two states that can combine with the ground state $O_g^+\,(^1\Sigma_g^+)$ are 1_u and 1_u. So these two transitions can be expected in absorption. But as these two states will have nearly flat potential energy curves dissociating into $^2P_{3/2} + {}^2P_{\frac{1}{2}}$ atoms at 20037 cm.$^{-1}$, the diffuse band absorption expected due to these two transitions will be overlapped by the strong continuum in the visible region.

Now we will turn to the bands given in Table IV which contains two sets of bands. Bands in all these groups have an average wavenumber separation of the order of 360 cm.$^{-1}$ This suggests that all these bands are due to transitions from a single stable state ($\omega \sim 360$ cm.$^{-1}$) to five different unstable states. Further these five states will probably be the same as the five lower states of the five groups of bands of Table III discussed above. This stable state has $\omega > \omega_0$ of the ground state and so its r_e will be less than that of the ground state. By assuming that the lower state of the first group in Table III is the same as that of the first group of Table IV, the position of the stable state which gives rise to all the bands in Table IV will be at about 56000 cm.$^{-1}$ [The first band of the first group of Table IV is at 26495 cm.$^{-1}$, and the point on the repulsive curve vertically below the stable state $1_g(\omega \sim 215)$ is at 29399 cm.$^{-1}$ So the position of the level which we are discussing will be at (26495 + 29399) = 55894 cm.$^{-1}$] The point vertically below this stable state ($\omega \sim 360$) on the repulsive curve that gives rise to the second group is at (56000–26731) = 29269 cm.$^{-1}$ Thus it appears that the two repulsive curves of the first and second groups come near together and this is probably the reason why the bands of the first and second groups overlap each other and the bands appear to be doublets. These two repulsive states are 1_u and O_u^- which dissociate into $I\,(^2P_{\frac{3}{2}}) + I\,(^2P_{\frac{1}{2}})$ at 27637 cm.$^{-1}$

TABLE IV

Bands Arising in $\Pi_{2,\,1g}$ state with $\omega \sim 360\ cm.^{-1}$

Group	v	Δ_v	Transition
		FIRST SET	
I	26495 26871 27234 27591 27936 28268 28568	376 361 357 345 332 300	$\Pi_{2,\,1g} \rightarrow \sigma_g^2,\ \pi u^3,\ \pi g^3,\ \sigma u^2\ ;\ 1u^-(^3\Sigma u^+)$
II	26731 27118 27459 27764 ... 28436 28736	387 341 305 300	$\Pi_{2,\,1g} \rightarrow \sigma_g^2,\ \pi u^3,\ \pi g^3\ \ \sigma u^2\ ;\ 0u^-(^3\Sigma u^+)$
		SECOND SET	
I	34432 34781 35125	349 344 324	$\Pi_{2,\,1g} \rightarrow \sigma_g^2,\ \pi u^3,\ \pi g^3\ \ \sigma u^2\ ;\ 1u\ (^3\Delta_{1u})$
II	35449 35797 36114 36418	348 317 304	$\Pi_{2,\,1g} \rightarrow \sigma_g^2,\ \pi u^3,\ \pi g^3,\ \sigma u^2\ ;\ 2u\ (^3\Delta_{2u})$
III	36300 36603	303	$\Pi_{2,\,1g} \rightarrow \sigma_g^2,\ \pi u^4,\ \pi g^3,\ \sigma u\ ;\ 1u\ (^1\Pi u)$

The three groups of the second set have their lower states 1_u, 2_u, 1_u, which dissociate into $I(^2P_{3/2}) + I(^2P_{\frac{1}{2}})$ atoms at 20037 cm.$^{-1}$ The three points, vertically below the stable potential energy curve on the three repulsive curves lie at (56000–34432) = 21568 cm.$^{-1}$, (56000–35449) 20551 cm.$^{-1}$ and (56000–36300) = 19700 cm.$^{-1}$ It must be mentioned that these bands of the first two groups can also be considered to belong only to one group and to have only one repulsive state instead of two, for the lower state.

Now we have to determine the electronic term and electronic configuration of the stable state at 56000 cm.$^{-1}$ The vibrational frequency of this state is of the order of 360 cm.$^{-1}$ which is greater than that of the ground state. Cordes and Sponer[13] have found in the ultra-violet between 1600 and 2000 A, for each of the molecules ICl, IBr and BrCl, a pair of absorption band systems which can be explained[10] as due to transitions from the ground

state to two vibrational states having frequencies greater than that of the ground states. Similar explanation was given by Cordes[9] to bands obtained by him in absorption of iodine vapour in the vacuum ultra-violet. These states in iodine are explained to be

$\{[\sigma_g^2, \pi^3, \pi^4; \Pi_{u1\frac{1}{2}}]\ \sigma_g^x\}; \Pi_{2,1u}$ at 57794 cm.$^{-1}$ and

$\{[\sigma_g^2, \pi^3, \pi^4; {}^2\Pi_{u\frac{1}{2}}]\ \sigma_g^x\}; \Pi_{1,0_u^+}$ at 62802 cm.$^{-1}$

the Ω components being too close together to be separated under the dispersion used. Here the interaction is between Ω of the core and s of σ_g^x and the coupling is called Ω-s coupling. The external electron is in the 6s orbit whereas the other nine electrons are in 5*p* orbit. Here the distinction between singlets and triplets loses its meaning as Ω and $\wedge$ become good quantum numbers. These states in iodine as obtained by Cordes have a frequency of the order of 260 cm.$^{-1}$ These states mentioned above are *ungerade* states as the external electron is a σ_g electron and the core has an *ungerade* term. If the core has a *gerade* term we get the corresponding *gerade* states $\{[\sigma_g^2, \pi_u^4, \pi_g^3; {}^2\Pi_{g1\frac{1}{2}}]\ \sigma_g^x\}; \Pi_{2,1g}$ and $\{[\sigma_g^2, \pi_u^4, \pi_g^3; {}^2\Pi_{g\frac{1}{2}}]\ \sigma_g^x\}; \Pi_{1,0_g^+}$ which will be expected to lie lower than the corresponding ungerade states. Of these two *gerade* states, the former will be expected to be lower than the latter. We attributed this former state to the stable state at 56,000 cm.$^{-1}$ The components are too close together to be separated under the dispersion used. This state being a *gerade* state cannot be expected to show itself in absorption. The transitions for the five groups in the Table IV can now be written as:—

First Set

First group: $\{[\sigma_g^2, \pi_u^4, \pi_g^3; {}^2\Pi_{g1\frac{1}{2}}]\ \sigma_g^x\}; \Pi_{2,1g} \rightarrow \sigma_g^2, \pi_u^3, \pi_g^3, \sigma_u^2; 1_u ({}^3\Sigma_u^+)$.

Second group: ,, $\rightarrow \sigma_g^2, \pi_u^3, \pi_g^3, \sigma_u^2; 0_u^- ({}^3\Sigma_u^+)$.

Second Set

First group: ,, $\rightarrow \sigma_g^2, \pi_u^3, \pi_g^3, \sigma_u^2; 1_u ({}^3\Delta_{1u})$.

Second group: ,, $\rightarrow \sigma_g^2, \pi_u^3, \pi_g^3, \sigma_u^2; 2_u ({}^3\Delta_{2u})$.

Third group: ,, $\rightarrow \sigma_g^2, \pi_u^4, \pi_g^3, \sigma_u; 1_u ({}^1\Pi_u)$.

Now we proceed to the explanation of the potential energy diagram (Fig. 1). The potential energy curves for the states $0_g^+ ({}^1\Sigma_g^+)$, $0_u^+ ({}^3\Pi_{0_u^+})$ and $1_u ({}^3\Pi_{1u})$ are drawn by using the known constants[14] and using the Morse equation

$$U_y = D_e\ [1 - e^{-\beta (r - r_e)}]^2$$

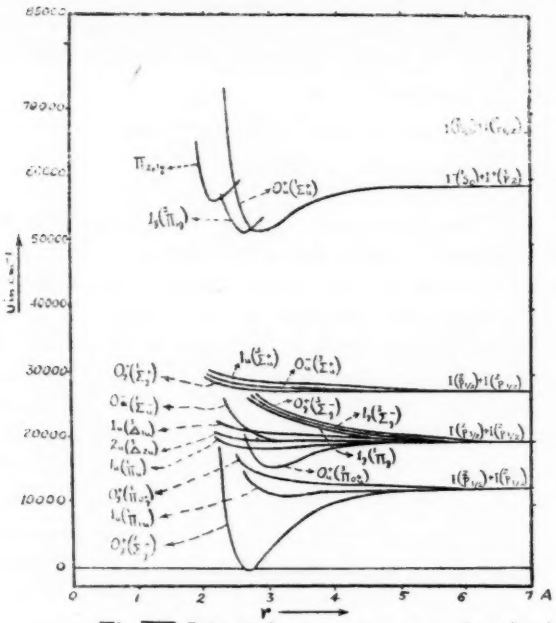

Fig. 1 *Potential energy curves for I_2 molecule*

where $\beta = \sqrt{\frac{2\pi^2 c\mu}{D_e h}}\ \omega_e = 1{\cdot}2176 \times 10^7 \cdot \omega_e \cdot \sqrt{\frac{\mu_A}{D_e}}$

(μ_A = reduced mass of the molecule in atomic weight units and D_e is dissociation energy). For the state O_u^+ at[12] 51683 cm.$^{-1}$ we know $\omega_e = 165{\cdot}1$, $\omega_e x_e = {\cdot}592$ and $D_e \sim 7300$ cm.$^{-1}$ r_e is calculated as follows: We know r_e and ω_e definitely for the ground state and the upper state of the visible descrete bands. The value of $\omega_e r_e^2$ is 1516 and 1160 for the two states respectively and the value of $\omega_e r_e^3$ is 4033 and 3491. The mean value of $\omega_e r_e^2 = 1338$ and that of $\omega_e r_e^3 = 3762$. If we take $\omega_e r_e^2 =$ constant we get r_e for O_u^+ state at 51683 cm.$^{-1}$ as 2·846 and if we take that $\omega_e r_e^3 =$ constant we get the value 2·834. So we take the value of r_e as 2·8 A.* Thus the potential energy curve for O_u^+ state at 51683 cm.$^{-1}$ is drawn by using the above constants. The approximate r_e value for the state with $\omega \sim 215$

* r_e value can be calculated by using Badger's relation $r_e\,(C_{ij}/k_e)^{1/3} + d_{ij}$ when C_{ij} and d_{ij} are constants whose values for iodine molecule are given as $(C_{ij})^{1/3} = {\cdot}49$ and $d_{ij} = 1{\cdot}76$ and K_e is force constant in mego units. The calculated r_e values using this relation for the states O_u^+ and $\Pi_{2,1g}$ are respectively 2·81 and 2·38 Å which agree fairly well with the values obtained by using the empirical relation $\omega e r e^3 = 3762 =$ constant.

is the same as that of the ground state. The approximate r_e value for the state with $\omega \sim 360$ cm.$^{-1}$ is obtained as 2·2 Å using $\omega_e r_e^3 = 3762 =$ constant. The position of these two states are thus marked at 51528 and 56000 cm.$^{-1}$

We know one or two fixed points on every repulsive curve, as we have already calculated the positions of points on the repulsive curves, lying vertically below the stable potential energy curves. Thus marking these points and taking into consideration the nature of the bands to which the different repulsive curves are responsible, the curves for all unstable states discussed in this paper and in the previous paper are drawn.

Fluorescent Spectrum.—The wavelength of the bands obtained in fluorscence by McLennan[2] and Oldenberg[3] are given in the first two columns of Table I. In the region 2680 to 3350 A the agreement between the wavelengths of the bands in fluorescence and those in emission is fairly good. Between 3580 and 3960 A wavelengths of single maxima are recorded instead of doublets obtained in emission. The agreement for wavelengths between 4000 and 4600 A is not satisfactory. If we attribute the discrepancies to the small dispersion of the instruments used in flourescence, the explanation of the flourescent bands becomes simple in the light of the explanation already given to emission bands. In Paper I we have explained the flourescent bands which correspond to the emission bands of Table II, as due to transitions from the state O_u^+ at 51683 cm.$^{-1}$ to different repulsive states, the O_u^+ state having been reached directly by excitation with wavelengths between 2000 and 1800 A. The states $1_g(^3\Pi_{1g})$ and $\Pi_{2,\,1g}$) which are discussed above, can be reached in fluorescence only by indirect excitation, as the ground state is O_g^+ state (*i.e.*, the molecule by absorbing some light quantum will go primarily either to O_u^+ or 1_u state. Then the molecule in the u state will go by further absorption of light quantum to the 1_g ($^3\Pi_{1g}$) and $\Pi_{2,\,1g}$ states). When these two states are reached transitions to various repulsive states discussed above will give fluorescent bands similar to those in emission.

Summary

The wavelengths of the maxima of all the diffuse bands from 4800 to 2680 A are given. The bands occur in different groups which involve frequency differences of the order of 165 cm.$^{-1}$, 215 cm.$^{-1}$ and 360 cm.$^{-1}$ among the component bands. Five groups of bands with frequency difference of 165 cm.$^{-1}$ are explained in Paper I. In this paper five groups with frequency differences of 215 cm.$^{-1}$ and another five groups with frequency differences of 360 cm.$^{-1}$ among the component bands are discussed. It is shown that

they arise in a transition from two initial stable states with frequencies of 215 cm.$^{-1}$ and 360 cm.$^{-1}$ to a common set of five different final states which are all unstable. These final states are identified with just those states which are the only theoretically possible ones. The well-known continuum at 3416 A which occurs in emission and in absorption at high temperature is attributed to the transition $1_g\,(^3\Pi_{1g}) \rightarrow O_u^-\,(^1\Sigma_u^-)$ in the iodine molecule. The mechanism of the fluorescent bands corresponding to the emission bands is also discussed.

The author wishes to express his thanks to Prof. R. K. Asundi for guidance and to Kamalapat Singhania Trust for the award of a scholarship.

References

1. P. Venkateswarlu .. *Proc. Ind. Acad. Sci.*, 1946, **24 A**, 480.
2. J. C. McLennan .. *Proc. Roy. Soc.*, 1913, **88**, 289.
3. O. Oldenberg .. *ZS. f. Phys.*, 1923, **18**, 1 ; 1924, **25**, 136.
4. W. E. Curtis and S. F. Evans .. *Proc. Roy. Soc.*, 1933, **141**, 603.
5. K. Asagoe and Y. Inuzuka .. *Sc. Rep. Tokyo, Burnika, Daigaku*, **2 A**, **84**, 1934.
6. W. G. Brown .. *Phy. Rev.*, 1931, **38**, 709.
7. E. Skorko .. *Nature*, 1933, **131**, 366.
8. Y. Uchida .. *Sci. Papers, Inst. Phy. Chem. Res.* (*Tokyo*), 1936, **30**, 71.
9. H. Cordes .. *ZS. f. Phys.*, 1935, **97**, 603.
10. R. S. Mulliken .. *Phy. Rev.*, 1934, **46**, 549.
11. ———— .. *Rev. Mod. Phys.*, 1932, **4**, 70.
12. P. Venkateswarlu .. "A New Band System of Iodine," *Proc. Ind. Acad. Sci.*, 1946, **24A**, 473.
13. Cordes and Sponer .. *ZS. f. Phys.*, **63**, 334, 1930, **79**, 170, 1932.
14. H. Sponer .. "*Molekül Spektren*," Vol. I.
15. Badger .. *Jour. Chem. Phys.*, 1935, **3**, 710.

Explanation to Plates

PLATE I (*a*) is the spectrogram taken on a 3 prism glass, Steinheil spectrograph. (*b*) is the microphotogram of the spectrum (*a*) taken on a Zeiss microphotometer.

(*c*) is the spectrogram taken on E_1 quarter spectrograph in the region 4500 to 3250 A. (*d*) is the microphotogram of (*c*).

PLATE II (*a*) is also the spectrogram taken on E_1 quartz spectograph in the region 3300 to 2680 A. (*b*) is the microphotogram of (*a*).

Wavelengths of some of the bands are marked in both the plates.

(a)
(b)
(c)
(d)
4018.0
4154.4
4472.1
4356.4
4242.5
4094.6
4018.0
3945.6
3798.0
3773.2
3739.5
3720.4
3578.6
3536.6
3479.0
3416.5
3306.9
3259.4

3257·4
3042·9
2846·1
2792·7
2687·5
(b)
3257·4
3042·9
2846·1
2792·7
2687·5
(a)

EMISSION BANDS OF HALOGENS

Part III. Iodine Bands arising in 1_u ($^3\Sigma_u^+$) and 1_g ($^1\Pi_g$) States

BY PUTCHA VENKATESWARLU, M.Sc.

(Physics Department, Benares Hindu University)

Received October 28, 1946

(Communicated by Dr. R. K. Asundi, M.Sc., Ph.D. (London), F.A.Sc.)

INTRODUCTION

IN pevious papers[1] "Emission Bands of Halogens—Parts I and II" which hereinafter will be called Papers I and II we have explained all the emission bands of iodine between 4800–2685 A including the famous continuum at 3416 A, except three bands at 4747·2, 4662·1 and 4575·2 A. In this paper these bands will be explained. Further the emission bands in the region 2685–2400 A will be discussed.

The three bands (Plate X) at 4747·2 A (21059 cm.$^{-1}$), 4662·1 A (21444 cm.$^{-1}$) and 4575·2 A (21849 cm.$^{-1}$) are very broad and diffuse their overall width being about 332, 239 and 240 cm.$^{-1}$ respectively whereas the width of all other bands in the region 4800–2685 A is of the order of 115 cm.$^{-1}$ The wavenumber separation between first and second bands and second and third bands is 389 and 405 cm.$^{-1}$ respectively. These differences being too big to be regarded as vibrational frequencies for I_2, the bands cannot be explained as forming a single group arising in a single transition.* The bands may probably arise in transitions from a stable state to three different unstable states which will have appreciably steep potential energy curves. In a previous communication,[2] the P-R, K-M (Pringsheim Rosen—Kimura Miyanishi) bands have been explained as arising in a transition from the ground state of the I_2 molecule to an excited state $\sigma_g, \pi_u^4, \pi_g^4, \sigma_g \cdot 1_u$ ($^3\Sigma_u^+$) at 44900 cm.$^{-1}$ which has a frequency of about 90 cm.$^{-1}$ This state 1_u ($^3\Sigma_u^+$) is shown in the potential energy diagram (Fig. 1). In Paper I we have discussed five groups of diffuse bands which arise in the state $\sigma_g, \pi_u^4, \pi_g^4, \sigma_u \cdot 0_u^+$

*There is, however, a state $\{ [\sigma_g^2, \Pi_u^4, \Pi_g^3\ ^2\Pi_{g3/2}]\ \sigma_g^x \}\ \Pi_{2,1g}$ at 56000 cm.$^{-1}$ with $\omega \sim 360$ cm.$^{-1}$ If the above three bands are to be explained as a single group arising in the state $\Pi_{2,1g}$, there should be a repulsive state with a nearly flat potential energy curve at about (56000 — 21059) = 34,941 cm.$^{-1}$ As such a repulsive state is not theoretically possible, and as the mutual wave number separation of these bands, *viz.*, 400 cm.$^{-1}$ is greater than ω of the state $\Pi_{2,1g}$, the three bands cannot be explained as a single group arising in $\Pi_{2,1g}$ state.

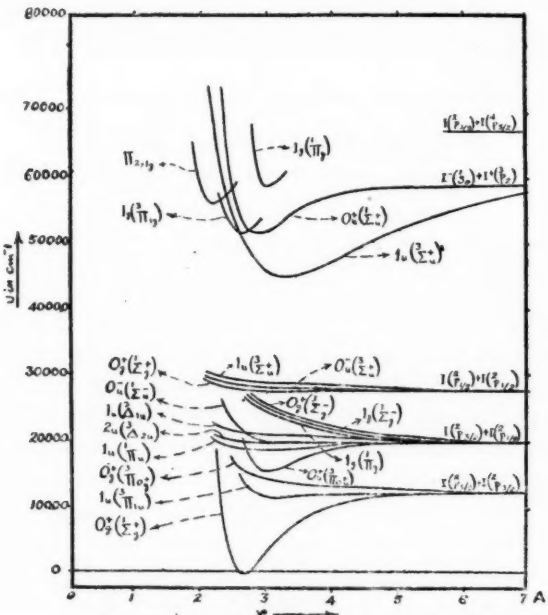

Fig. 1 *Potential energy curves for I_2 molecule*

($^1\Sigma_u^+$), and which have five different unstable states for their final levels. Second, third and fourth of these five groups, are explained as due to transition from the stable state O_u^+ ($^1\Sigma_u^+$) at 51685 cm.$^{-1}$ to the unstable states O_g^+ ($^3\Sigma_g^-$), 1_g ($^3\Sigma_g^+$) and 1_g ($^1\Pi_g$) which dissociate in $^2P_{3/2} + {}^2P_{1/2}$ iodine atoms at 20037 cm.$^{-1}$ All these three states, as shown in the potential energy diagram of Paper II as well as in Fig. 1 of this paper, have appreciably steep potential energy curves which run almost parallel except at their meeting point, and are separated from one another by about 400 cm.$^{-1}$ which is of the same order as the mutual wavenumber separation of the broad bands we are discussing. According to selection rules for case (*c*) type coupling transitions from the state 1_u ($^3\Sigma_u^+$) at 44900 cm.$^{-1}$ to the three unstable states pointed above are allowed and these transitions will explain satisfactorily the three broad bands. The potential energy curves of the unstable states, being appreciably steep, explain the broad and diffuse nature of the bands. The points on the three potential energy curves vertically below the stable state will be at (44900–21059) = 23841, (44900–21444) = 23456 and (44900–21849) = 23051 cm.$^{-1}$ The transitions for the three bands may be written as:

4747·2 A: $\sigma_g, \pi_u^4, \pi_g^4, \sigma_u \cdot 1_u\,(^3\Sigma_u^+) \rightarrow \sigma_g^2, \pi_u^4, \pi_g^2, \sigma_u^2 \cdot O_g^+\,(^3\Sigma_g^-)$

4662·1 A: ,, $\cdot 1_u\,(^3\Sigma_u^+) \rightarrow \sigma_g^2, \pi_u^4, \pi_g^2, \sigma_u^2 \cdot 1_g\,(^3\Sigma_g^-)$

4575·[illegible] A: ,, $\cdot 1_u\,(^3\Sigma_u^+) \rightarrow \sigma_g^2, \pi_u^3, \pi_g^4, \sigma_u \cdot 1_g\,(^1\Pi_g)$

Now we turn to the bands below 2685 A. In the region 2685 to 2400 A we have a number of diffuse bands whose nature seems to be the same as those of the bands in the region 4800–2685 A, except that these bands are weaker and narrower than the others. The experimental details are the same as those described in the previous papers. The wavelengths and wavenumbers of the maxima of the bands between 2685–2448 A are given in Table I. The intensity values correspond to the visually estimated values

TABLE I

Group	Asagoe, Inuzaka $\lambda_{in\ air}$	Present experiments			
		Intensity	$\lambda_{in\ air}$	$\nu_{vac.}$	$\Delta\nu$
I	2672·2	1	2671·1	37427	..
	2662·1	2	2661·1	37567	140
	..	0·5	2652·5	37689	122
	2642·7	2	2642·6	37830	141
	2633·2	2	2633·3	37964	134
	2625·0	0·5	2623·6	38104	140
	2616·8	0·5	2616·6	38206	102
	2608·5	1	2607·5	38339	133
II	2592·7	1	2593·3	38549	..
	2584·0	1	2584·4	38682	133
	2576·1	0·5	2575·9	38810	128
	2569·9	0·5	2569·2	38911	101
	2561·7	1	2562·2	39017	106
		0·5	2555·1	39126	109
		0·5	2548·9	39221	95
		1	2541·6	39333	112
		0·5	2534·1	39450	117
		0·5	2526·7	39565	115
III		0·5	2522·7	39628	..
		1	2516·0	39734	106
		1	2508·6	39851	117
		?	2501·4	39966	115
		1	2494·1	40083	117
		0·5	2487·2	40194	111
		0·5	2481·0	40294	100
		?	2474·1	40407	113
		0·5	2467·9	40508	101
		0·5	2461·8	40608	100
		0·5	2454·9	40723	115
		0·5	2448·8	40824	101

for the bands obtained on a B-20 process Kodak plate. It may be mentioned that Asagoe and Inuzaka[8] have recorded previously the maxima of the

bands only upto 2562 A. These values are also given in the table besides the values obtained in the present experiments. The wavelengths of the bands below 2562 A are, however, being recorded here for the first time.

The bands are arranged into three groups by taking the wavenumber separation into consideration. They have an average wavenumber separation of about 120 cm.$^{-1}$ among the composite bands. So they can be considered as arising in a common initial level with a frequency of about 120 cm.$^{-1}$ and having three different unstable states for their final levels. We have three unstable states 1_u ($^3\Delta_{1u}$), 2_u ($^3\Delta_{2u}$) and 1_u ($^1\Pi_u$) which have nearly flat potential energy curves and which dissociate into $^2P_{3/2} + {}^2P_{1/2}$ iodine atoms at 20037 cm.$^{-1}$ (Paper II). These three states form final levels of three groups of bands between 3307 and 2918 A which arise in 1_g ($^3\Pi_{1g}$) state at 51528 cm.$^{-1}$ and other three groups between 2903 and 2731 A arising in a state $\Pi_{2,1g}$ at 56000 cm.$^{-1}$ Transitions from a stable state to these three unstable states will explain satisfactorily all the three groups of bands in Table I. The first bands of these three groups lie at 37427, 38549 and 39628 cm.$^{-1}$ Adding 20037 to each of these and taking the mean we arrive at 58572 cm.$^{-1}$ which, therefore, represents the approximate position of the initial level. The points on the three repulsive curves below the stable state, lie at (58572–37427) = 21145, (58572–38549) = 20023 and (58572–39628) = 18944 cm.$^{-1}$

It may be mentioned that there are some bands which are very faint overlapping the third group. Probably these form the extension of the bands of the second group. There are also some bands below 2448 A upto 2370 A, *i.e.*, on the short wave side, which are also faint. It appears that these are the extensions of the second and third group of bands, which come from higher vibrational level of the initial state, and which overlap in this region. It is also possible that some of these faint bands (2448–2370 A) may be due to the transitions [*viz.* From O_u^+ ($^1\Sigma_u^+$) at 51683 cm.$^{-1}$ to 1_g ($^3\Pi_{1g}$) dissociating into two $^2P_{3/2}$ atoms and from 1_g ($^3\Pi_{1g}$) at 51528 cm.$^{-1}$ to O_u^- ($^3\Pi_{0_u^-}$), 1_u ($^3\Pi_{1u}$) dissociating into $^2P_{3/2}$ atoms] which are theoretically possible and which may be expected to give bands in this region.

Now we turn to find the electronic configuration and electronic term of the stable state at 58572 cm.$^{-1}$ The only two terms that can combine with all the three terms 1_u ($^3\Delta_{1u}$), 2_u ($^3\Delta_{2u}$) and 1_u ($^1\Pi_u$) are according to case (*c*) type coupling 1_g and 2_g. The state 1_g may be correlated with $^1\Pi_g$ or $^3\Pi_{1g}$ and 2_g may be correlated with $^3\Pi_{2g}$ where $^1\Pi_g$, $^2\Pi_{1g}$ and $^3\Pi_{2g}$ arise from the electronic configuration σ_g, π_u^4, π_g^3, σ_u^2. We have already attributed 1_g ($^3\Pi_{1g}$) [*i.e.*, the term 1_g is correlated with $^3\Pi_{1g}$ or case (*a*) type] to a state at 51528 cm.$^{-1}$

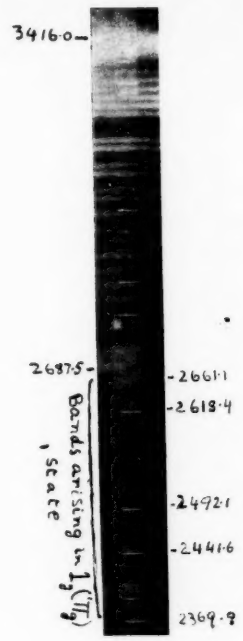
3416·0
2687·5
2661·1
2618·4
2492·1
2441·6
2369·9
Bands arising in $^1\Sigma_g^+(^1\Pi_g)$ state

(b)

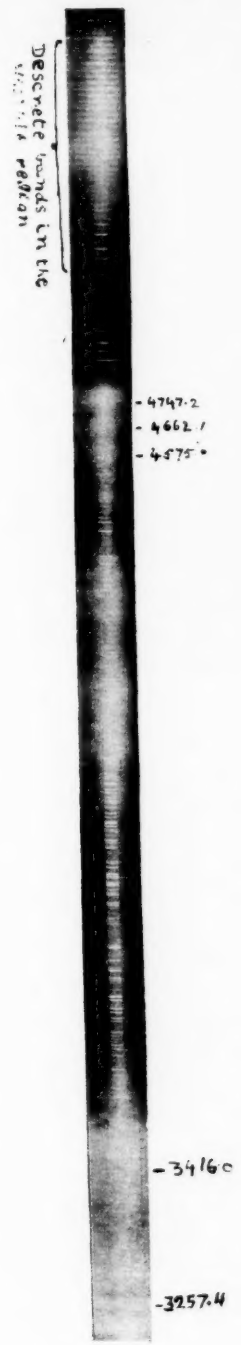
Discrete bands in the
4747·2
4662·1
4575·
3416·0
3257·4

(a)

which has a frequency of about 220 cm.$^{-1}$ Thus the electronic term of the stable state at 58572 cm.$^{-1}$, which we are now considering, will be either $1_g\,(^1\Pi_g)$ or $2_g\,(^3\Pi_{2g})$. But the state $2_g\,(^3\Pi_{2g})$ will be expected to lie below $1_g\,(^3\Pi_{1g})$ state, *i.e.*, below 51528 cm.$^{-1}$ So the state at 58572 cm.$^{-1}$ which has $\omega \sim 120$ cm.$^{-1}$ will have probably the electronic term $1_g\,(^1\Pi_g)$. We can now write the transitions for the three groups of bands as:

I group: $\sigma_g, \pi_u^4, \pi_g^3, \sigma_u^2 \cdot 1_g\,(^1\Pi_g) \rightarrow \sigma_g^2, \pi_u^3, \pi_g^3, \sigma_u^2 \cdot 1_u\,(^3\Delta_{1u})$.

II group: ,, $\cdot 1_g\,(^1\Pi_g) \rightarrow \sigma_g^2, \pi_u^3, \pi_g^3, \sigma_u^2 \cdot 2_u\,(^3\Delta_{2u})$.

III group: ,, $\cdot 1_g\,(^1\Pi_g) \rightarrow \sigma_g^2, \pi_u^4, \pi_g^3, \sigma_u \cdot 1_u\,(^1\Pi_u)$.

The potential energy diagram given in Paper II, is also given in Fig. 1 of this paper with the following addition: The curve for the state $1_u\,(^3\Sigma_u^+)$ at 44900 cm.$^{-1}$ is drawn by using Morse equation with the use of the constants $\omega = 90$ cm.$^{-1}$; $D = (59000\text{–}44900) = 14100$ cm.$^{-1}$ In calculating r_e value we use Badger's relation $r_e = \left(\frac{C_{ij}}{K_e}\right)^{1/3} + d_{ij}$, where k_e is force constant for the state in megadynes per cm., C_{ij} and d_{ij} are constants whose values for the iodine molecule are given by $(C_{ij})^{1/3} = \cdot 49$ and $d_{ij} = 1 \cdot 765$. r_e value obtained is 3·33 A. Similarly r_e for the state $1_g\,(^1\Pi_g)$ at 58572 cm.$^{-1}$ is calculated as 3·02 A. The position of this level is also marked in the figure.

Summary

The three broad bands at 4747·2, 4662·1 and 4575·2 A are explained as due to transitions from a single stable state $1_u\,(^3\Sigma_u^+)$ at 44900 cm.$^{-1}$ to three unstable states $O_g^+\,(^3\Sigma_g)$, $1_g\,(^3\Sigma_g^-)$ and $1_g\,(^1\Pi_g)$ which dissociate into $^2P_{3/2} + {}^2P_{1/2}$ iodine atoms at 20037 cm.$^{-1}$ The bands in the region 2687 to 2400 A form three groups which are explained as arising in a level $1_g\,(^1\Pi_g)$ at 58572 cm.$^{-1}$ and having for their final level the three unstable states $1_u\,(^3\Delta_{1u})$, $2_u\,(^3\Delta_{2u})$ and $1_u\,(^1\Pi_u)$ which dissociate into $^2P_{3/2} + {}^2P_{1/2}$ iodine atoms. The potential energy diagram for iodine molecule is given.

The author wishes to express his sincere thanks to Prof. R. K. Asundi for guidance and to Kamalapat Singhania Trust for the award of a scholarship.

References

1. P. Venkateswarlu .. "Emission Bands of Halogens, Part I and II," *Proc. Ind. Acad. Sci.*, 1946, **24 A**, 480 and this number.
2. ———— .. "Absorption Bands of Iodine in Quartz Ultra-violet," *Ind. Journ. Phys.* (in Press).
3. Asagoe and Inuzuka .. *Sc. Rep. Tokyo, Burnika, Daigaku*, 1934, **2 A**, 84.
4. Badger .. *Journ. Chem. Phys.*, 1935, **3**, 710

EMISSION BANDS OF HALOGENS

Part IV. Diffuse Bands of Bromine

By Putcha Venkateswarlu, M.Sc.
(Physics Department, Benares Hindu University)

Received October 28, 1946
[Communicated by Dr. R. K. Asundi, M.Sc., Ph.D. (London), F.A.Sc.]

Introduction

In a previous communication[1] on the emission bands of bromine, a number of diffuse bands in the region 4200 to 2200 A have been reported. These bands are apparently similar to the diffuse bands of iodine, but are however displaced towards shorter wavelengths as they should be. An explanation of the diffuse bands of iodine, in the region 4800 to 2400 A, is given in a series of papers entitled 'Emission Bands of Halogens, Parts—I, II and III,'[2] which hereinafter will be called Papers I, II and III respectively. It is possible to extend a similar interpretation to diffuse bands of bromine. The present paper deals with this interpretation of bromine bands. General experimental details, and description of the observed emission spectrum from 6700 to 2000 A are given with wavelength data of the maxima of the bands between 4200 and 2000 A, which are interpreted.

Experimental Details

A glass tube 25 cm. in length and 1·5 cm. in diameter, with clear quartz windows attached at the two ends, forms the discharge tube. To one side of the discharge tube, a side tube containing cupric bromide is attached through a stopcock and tubes containing calcium chloride. The side tube is inserted in an improvised small electric furnace. The other side of the discharge tube is connected to an evacuating pump through tubes containing calcium chloride and KOH. The apparatus is first evacuated and the cupric bromide is heated by passing a current of 1 to 1·5 amp. through the electric furnace. The pump is kept running and the discharge tube is excited by high frequency oscillations similar to those used for the excitation of iodine vapour. The flow of the vapour is regulated by adjusting the current through the electric furnace, such that a pure and intense glow is obtained. It was necessary to keep the vapour in flowing condition, to avoid the presence of impurity spectra specially Angstrom bands which make their appearance as soon as the vapour becomes stagnant. The colour of the discharge is pinkish white, similar to that of iodine glow. In the visible

region, the spectrum was photographed on a 3-prism Steinheil spectrograph, and in the region 42000 to 2000 A, a Medium Hilger quartz spectrograph and E_2 and E_3 quartz spectrographs were used. The medium quartz spectrograph has a dispersion of 41 A, 14 A, and 8 A per mm. at 4200, 3000, 2500 A respectively and the dispersion of E_2 spectrograph is 55 A, 22 A and 13 A per mm. at 4200, 3000 and 2500 A respectively. A E_1 quartz spectrograph was also used to photograph the spectrum in the ultraviolet, but the diffuse bands were only broadened and not further resolved. So measurements are made only on the plates taken on E_2 and medium quartz spectrographs. The microphotometric curves on E_2 quartz spectrograms are taken on a Zeiss recording microphotometer. The reproductions of the spectrograms and microphotogram are given in Plate XI.

The spectrum can be divided broadly into two divisions—the first division in the region 6700 to 5000 A consists of bands which are analysed by Uchida and Ota.[3] These bands do not have distinct heads, though they appear degraded towards red. According to Uchida and Ota these bands occur in two systems which arise from two different initial states, having frequencies of 192 and 152 cm.$^{-1}$ to a common final level which is different from the ground level and which has a frequency of about 360 cm.$^{-1}$ Unlike in iodine, therefore, these emission bands do not coincide with the absorption bands. This fact is evident from a juxtaposed spectrum taken for absorption and emission.

The second division in the region 4200 and 2000 A consists of bands which are diffuse. The wavelengths and wavenumbers of the maxima of the bands, which represent the mean values obtained from measurements of five different plates, are given in Table I. The measurements are accurate upto $\pm$ ·5 A below 3000 A and $\pm$ 1 A between 3000–4200 A. The values given in Table I are the same as those published previously[1] except that a band at 3809·2 A is omitted here as its presence is doubtful and a few more extra bands marked* obtained by our experiments with transformer discharge† are included. The intensity values given correspond to the

† The spectrum obtained by exciting flowing bromine vapour with uncondensed transformer discharge is the same as that obtained by high frequency discharge except that a few weak diffuse bands were added below 2190 A. It has been very difficult to eliminate water vapour from the discharge tube, either working with transformer discharge or high frequency discharge, so much so that the intense OH band at 3100 A persisted. However, we were able to get two plates, working with transformer discharge which showed no presence of OH bands. In the region where intense OH band used to persist, is obtained an intense broad band with 4 maxima between 3126 and 3036 A, which undoubtedly belongs to bromine spectrum, as the spectrum obtained is free of impurity spectra. The extra bands obtained with transformer discharge are marked * in Table I.

TABLE I

Intensity	λ	$\nu_{vac.}$	Intensity	λ	$\nu_{vac.}$
4	4224·5	23665	5	2580·6	38739
1	4090·4	24441	5·2	2564·7	38979
1	4021·5	24859	2	2549·3	39215
3	3932·5	25422	6	2526·9	39562
2	3849·7	25969	6	2510·9	39814
2	3739·7	26733	6	2494·2	40081
2	3677·3	27186	7	2478·8	40330
4	3597·8	27787	4	2464·8	40559
10	3549·4	28166	3	2452·6	40761
4	3420·2	29230	2	2444·4	40897
6	3366·8	29693	2	2432·3	41101
10	3336·6	29962	4	2421·1	41291
1	3268·6	30585	?	2406·8	41536
1	3239·2	30863	?	2388·0	41863
4	3126·0*	31981	2	2375·0	42092
4	3094·5*	32306	3	2360·8	42346
4	3064·0*	32628	2	2349·4	42551
3	3036·0*	32929	1	2337·9	42760
1	2980·9	33537	2	2326·3	42979
1	2952·9	33865	2	2313·9	43204
8	2923·8	34192	1	2304·5	43380
10	2900·4	34468	1	2288·0	43693
8	2872·5	34803	1	2261·1	44212
4	2844·2	35149	1	2234·9	44731
5	2814·3	35522	1	2212·7	45180
7	2780·6	35953	1	2196·6	45511
8	2753·6	36305	0·5	2132·4*	46881
7	2732·4	36587	0·5	2109·5*	47390
7	2709·8	36892	0·5	2088·2*	47873
5	2688·7	37182	0·5	2067·3*	48357
4	2654·8	37656	0·5	2048·0*	48812
6	2638·9	37883	0·5	2028·4*	49284
6·2	2623·1	38111	0·5	2010·4*	49725
?	2608·9	38319			

tive values visually estimated for the bands obtained on a process B 20 Kodak plate taken on a medium quartz spectrograph. It may be mentioned that previous workers[4] have recorded in the region 4200–2000 A, only four maxima at 4200, 3600, 3100 and 2880 A instead of so many groups of bands given in Table I.

DISCUSSION

In Table II, bands are arranged in five groups. The average wave-number separation of the component bands in all groups is of the order of 330 cm.$^{-1}$ This suggests that these bands arise in a single state having a frequency of about 330 cm.$^{-1}$ and have five repulsive states for their final levels. The first two groups consist of two bands each which overlap one another and they appear as two continuous broad bands each consisting of two maxima. Thus the repulsive curves of these two states will be steep. The third group consists of four maxima overlapping one another. The

TABLE II

Bands arising in $\sigma_g, \pi_u^4, \pi_g^3, \sigma_u^2, 1_g(^3\Pi_{1g})$ *State at 55534 cm.*$^{-1}$ *with* $\omega \sim 330$ *cm.*$^{-1}$

Group	ν	$\Delta\nu$	Transition
I	27787 28166	379	$1_g(^3\Pi_{1g}) \rightarrow \sigma_g^2, \pi^3_u, \pi^3_g, \sigma^2_u \cdot O_u^-(^3\Sigma^+_u)$
II	29693 29962	269	$1_g(^3\Pi_{1g}) \rightarrow \sigma_g^2, \pi_u^3, \pi_g^3, \sigma_u^2 \cdot O_u^-(^1\Sigma_u^-9)$
III	3198I 32306 32628 32929	325 322 301	$1_g(^3\Pi_{1g}) \rightarrow \sigma_g^2, \pi_u^3, \pi^3_g, \sigma_u^2 \cdot 1_u\ (^3\Delta_{1u})$
IV	33537 33865 34192 34468 34803 35149 35522	328 327 276 335 346 373	$1_g(^3\Pi_{1g}) \rightarrow \sigma_g^2, \pi_u^3, \pi_g^3, \sigma_u^2 \cdot 2_u\ (^3\Delta_{2u})$
V	35953 36305 36587 36892 37182	352 282 305 290	$1_g(^3\Pi_{1g}) \rightarrow \sigma_g^2, \pi_u^4, \pi_g^3, \sigma_u \cdot 1_u\ (^1\Pi_u)$

fourth group consists of seven bands which also overlap. The fifth group consists of five bands which do not overlap to the same extent as those of the other groups. The increasing degree of overlapping of the components from fifth to first group suggests that the steepness of the repulsive curves increases in the same order. The vibrational frequency of the stable state which we are considering is of the same order as that of the ground state ($\omega_e = 324$ cm.$^{-1}$). In the case of iodine there is a state $\sigma_g, \pi_u^4, \pi_g^3, \sigma_u^2 \cdot 1_g(^3\Pi_{1g})$ at 51528 cm.$^{-1}$ which has a vibrational frequency of the same order as that of the ground state of iodine molecule and which gives rise to groups of diffuse bands (Paper II). By taking an analogy with iodine molecule we can attribute the electronic term $\sigma_g, \pi_u^4, \pi_g^3, \sigma_u^2 \cdot 1_g(^3\Pi_{1g})$ to the stable state which gives rise to all groups of Table II. In the spectrum of iodine, we have explained a continuum at 3416 A and three groups of diffuse bands on its short wave side as arising in the state $1_g(^3\Pi_{1g})$ and having respectively for their final levels four repulsive states $\sigma_g^2, \pi_u^3, \pi_g^3, \sigma_u^2 \cdot O_u^-(^1\Sigma_u^-)$, $\sigma_g^2, \pi_u^3, \pi_g^3, \sigma_u^2 \cdot 1_u\ (^3\Delta_{1u})$, $\sigma_g^2, \pi_u^3, \pi_g^3, \sigma_u^2 \cdot 2_u\ (^3\Delta_{2u})$ and $\sigma_g^2, \pi_u^4, \pi_g^3, \sigma_u \cdot 1_u\ (^3\Pi_{1u})$ all of which dissociate into I ($^2P_{3/2}$) + I ($^2P_{\frac{1}{2}}$) atoms (Paper II). In the same way we can explain the four groups of Table II from second to fifth as arising in $\sigma_g, \pi_u^4, \pi_g^3, \sigma_u^2 \cdot 1_g(^3\Pi_{1g})$ state and having for their final levels the

four repulsive states O_u^- ($^1\Sigma_u^-$), 1_u ($^3\Delta_{1u}$), 2_u ($^3\Delta_{2u}$) and 1_u ($^1\Pi_u$). Of these four groups, the last one has bands which do not overlap to such an extent as those of the other groups. So in calculating the position of the level 1_g ($^3\Pi_{1g}$) we take that the final level of the last group (Table II) is nearly flat. The dissociation energy of $^2P_{3/2} + {}^2P_{\frac{1}{2}}$ bromine atoms is 19581 cm.$^{-1}$ * The first band of the last group (Table II) is at 35953 cm.$^{-1}$ So the approximate position of the level 1_g ($^3\Pi_{1g}$) is at 35953 + 19581 = 55534 cm.$^{-1}$ The points on the four repulsive curves of the second, third, fourth and fifth groups, vertically below the state 1_g ($^3\Pi_{1g}$), will be at (55534–29693) = 25841; (55534–31981) = 23553; (55534–33537) = 21997 and 19581 cm.$^{-1}$ respectively. All the states as stated above dissociate into $^2P_{3/2} + {}^2P_{\frac{1}{2}}$ bromine atoms at 19581 cm.$^{-1}$

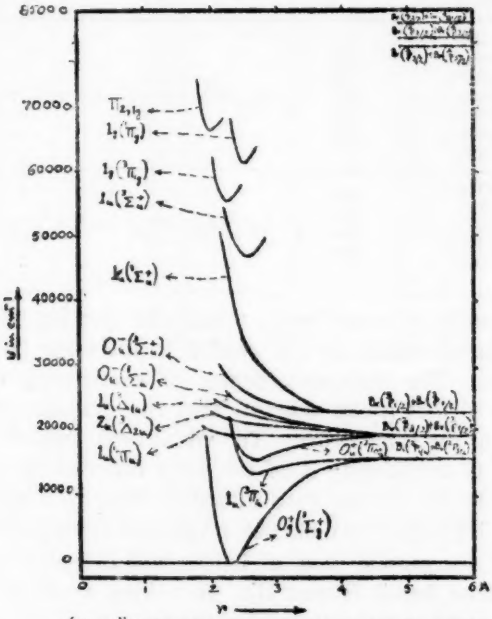

(Fig 1) Potential energy curves for Br_2 molecule

These four repulsive states are shown in the potential energy diagram (Fig. 1) and find support from observations in absorption. In absorption

* The accepted value for the dissociation energy of the ground state of bromine molecule, which dissociates into Br ($^2P_{3/2}$) + Br ($^2P_{3/2}$) is 1·961 volts [5] or 15896 cm.$^{-1}$ The energy difference between Br ($^2P_{1/2}$) − Br ($^2P_{3/2}$) is 3685 cm.$^{-1}$ according to Turner.[6] So the dissociation energy of Br ($^2P_{3/2}$) + Br ($^2P_{1/2}$) is 19581 cm.$^{-1}$ and that of Br ($^2P_{1/2}$) + Br ($^2P_{1/2}$) is 23266 cm.$^{-1}$

we should expect on this basis only two maxima at about 24000 and 20000 cm.$^{-1}$ due to transitions from the ground state O_g^+ ($^1\Sigma_g^+$) to 1_u ($^3\Delta_{1u}$) and 1_u ($^1\Pi_u$) respectively as these transitions are the only allowed ones by selection rules for case (*c*) type. In fact two maxima at about 24100 and 20400 cm.$^{-1}$ are observed by Acton, Aickin and Bayliss[7] which may be identified with the two transitions stated above.

The continuous band with two maxima 27787 and 28166 cm.$^{-1}$ of Group I, which lies on the long wave side of the other four groups of Table II, will have for its final level, a repulsive state which dissociates in two $^2P_{\frac{1}{2}}$ bromine atoms at 23266 cm.$^{-1}$ By a combination of these two atoms we get the terms[8] O_g^+, O_u^- and 1_u of which only O_u^+ and 1_u can combine with 1_g ($^3\Pi_{1g}$) which is the initial state of all bands of Table II. These two states O_r^- and 1_u can be correlated with $^3\Sigma_u^+$ of case (*a*) type which arises from the configuration σ_g^2, π_u^3, π_g^3, σ_u^2 (Paper II). Of these two states, 1_u ($^3\Sigma_u^+$) appears to possess a very steep curve for the following reason: There is continuous absorption[9] in bromine beginning from about 3000 A and extending in the vacuum region.‡ The maximum of this absorption lies at about 2250 A or 44500 cm.$^{-1}$ This extensive absorption can only be explained as due to a transition from the ground state O_g^+ ($^1\Sigma_g^+$) to a steep repulsive state dissociating into two $^2P_{\frac{1}{2}}$ atoms. As the ground state can combine only with the term 1_u of the three possible terms that arise from $^1P_{\frac{1}{2}}$ atoms, the transition for the absorption may be written as σ_g^2, π_u^4, $\pi_g^4 \cdot O_g^+$ ($^1\Sigma_g^+$) $\rightarrow \sigma_g^2$, π_u^3, π_g^3, $\sigma_u^2 \cdot 1_u$ ($^3\Sigma_u^+$). The point on this repulsive curve above the ground state will lie at about 44500 cm.$^{-1}$ as the maximum of absorption lies at about 44500 cm.$^{-1}$; and the repulsive curve will be very steep. A transition from the state 1_g ($^3\Pi_{1g}$) at 55534 cm.$^{-1}$ to the repulsive curve 1_u ($^3\Sigma_u^+$) will be expected to give a continuum in emission in the infra-red with a maximum at about 11000 cm.$^{-1}$ So this state 1_u ($^3\Sigma_u^+$) cannot correspond to the repulsive state of the continuous band of Group I of Table II. So the term O_u^- ($^3\Sigma_u^+$) corresponds to its repulsive state. The point on the repulsive curve O_u^- ($^3\Sigma_u^+$) below the state 1_g ($^3\Pi_{1g}$) will be at about 55534–27787 = 27747 cm.$^{-1}$ The various transitions to all the groups of Table II can now be written as:—

---

‡ According to Cordes and Sponer[9a] the short wave limit of this continuous absorption lies below 1560 A, and its long wave limit, which changes with vapour pressure, reaches 2700 A at about 1·6 atmosphere. Aickin and Bayliss,[9b] working in the quarter ultra-violet region up to 2000 A, report that this continuum begins at about 3000 A, reaches a maximum at about 2250 A and extends to shorter wavelengths.

I Group: $\sigma_g, \pi_u^4, \pi_g^3, \sigma_u^2 \cdot 1_g\,(^3\Pi_{1g}) \rightarrow \sigma_g^2, \pi_u^3, \pi_g^3, \sigma_u^2 \cdot O_u^-\,(^3\Sigma_u^+)$

II Group: ,, $\cdot 1_g\,(^3\Pi_{1g}) \rightarrow$,, $\cdot O_u^-\,(^1\Sigma_u^-)$

III Group: ,, $\cdot 1_g\,(^3\Pi_{1g}) \rightarrow$,, $\cdot 1_u\,(^3\Delta_{1u})$

IV Group: ,, $\cdot 1_g\,(^3\Pi_{1g}) \rightarrow$,, $\cdot 2_u\,(^3\Delta_{2u})$

V Group: ,, $\cdot 1_g\,(^3\Pi_{1g}) \rightarrow \sigma_g^2, \pi_u^4, \pi_g^3, \sigma_u \cdot 1_u\,(^1\Pi_u)$

Table III consists of bands which are arranged in four groups. The average wavenumber separation of the component bands of all these groups

TABLE III

Bands arising in $\sigma_g, \pi_u^4, \pi_g^3, \sigma_u^2 \cdot 1_g\,(^1\Pi_g)$ *at* 61444 *cm.*$^{-1}$ *with* $\omega \sim 220$ *cm.*$^{-1}$

Group	ν	$\Delta\nu$	Transition
I	37656	227	$1_g\,(^1\Pi_g) \rightarrow \sigma_g^2, \pi_u^2, \pi_g^3, \sigma_u^2 \cdot O_u^-\,(^1\Sigma^-_u)$
	37883	228	
	38111	208	
	38319		
II	38739	240	$1_g\,(^1\Pi_g) \rightarrow \sigma_g^2, \pi_u^3, \pi_g^3, \sigma_u^2 \cdot 1_u\,(^3\Delta_{1u})$
	38979	236	
	39215		
III	39562	252	$1_g\,(^1\Pi_g) \rightarrow \sigma_g^2, \pi_u^3, \pi_g^3, \sigma_u^2 \cdot 2_u\,(^3\Delta_{2u})$
	39814	267	
	40081	249	
	40330	229	
	40559	202	
	40761	136	
	40897	204	
	41101	190	
	41291	245	
	41536		
IV	41863	229	$1_g\,(^1\Pi_g) \rightarrow \sigma_g^2, \pi_u^4, \pi^3 g, \sigma_u \cdot 1_u\,(^1\Pi_u)$
	42092	254	
	42346	205	
	42551	209	
	42760	219	
	42979	225	
	43204	176	
	43380		

is of the order of 220 cm.$^{-1}$ This suggests that these bands arise in a common initial level with vibrational frequency of 220 cm.$^{-1}$ and have four repulsive states for their final levels. In iodine molecule we have a state $\sigma_g, \pi_u^4, \pi_g^3, \sigma_u^2 \cdot 1_g\,(^1\Pi_g)$ at 58572 cm.$^{-1}$ which has a frequency of about 120 cm.$^{-1}$ and which gives rise to three groups of bands (Paper III). We can attribute $\sigma_g, \pi_u^4, \pi_g^3, \sigma_u^2 \cdot 1_g\,(^1\Pi_g)$ to the state which gives rise to the four groups of Table III. Then the four groups can satisfactorily be explained to have respectively for their final levels the four repulsive states $O_u^-\,(^1\Sigma_u^-)$, $1_u\,(^3\Delta_{1u})$,

2_u ($^3\Delta_{2u}$) and 1_u ($^1\Pi_u$) which as we have discussed above dissociate into $^2P_{3/2} + {}^2P_{\frac{1}{2}}$ bromine atoms at 19581 cm.$^{-1}$ and are the final levels of the second, third, fourth and fifth groups of Table II. To calculate the position of the state 1_g ($^1\Pi_g$) we take the repulsive curve of the last group of Table II to be nearly flat, dissociating into $^2P_{3/2} + {}^2P_{\frac{1}{2}}$ atoms at 19581 cm.$^{-1}$ The first band of this group lies at 41863 cm.$^{-1}$ So the approximate position of the state 1_g ($^1\Pi_g$) can be calculated to be 41863 + 19581 = 61444 cm.$^{-1}$ The points on the repulsive curves, lying vertically below the 1_g ($^1\Pi_g$) state, will lie at (61444 − 37656) = 23788; (61444 − 38739) = 22705; (61444 − 39562) = 21882 and (61444 − 41863) = 19581 cm.$^{-1}$ These points will, therefore, be points on the repulsive curves at $r = r_e$, where r_e corresponds to the state 1_g ($^1\Pi_g$) with $\omega \sim 220$ cm.$^{-1}$

The broad band at 29230 cm.$^{-1}$, whose overall width is 260 cm.$^{-1}$ as compared to 130 cm.$^{-1}$ of all the bands of Table III, can be explained as to a transition from the state 1_g ($^1\Pi_g$) to the repulsive state 1_u ($^3\Sigma_u^+$) which dissociates into $^2P_{\frac{1}{2}} + {}^2P_{\frac{1}{2}}$ bromine atoms at 23266 cm.$^{-1}$ The point on the repulsive curve at $r = r_e$ of 1_g ($^1\Pi_g$) will be at 61444 − 29230 = 32214 cm.$^{-1}$ This repulsive state as discussed above, is steep and forms the final level of the continuous absorption of bromine in the extreme ultra-violet and vacuum region. [Transition from the state 1_g ($^1\Pi_g$) to the repulsive state O_u^- ($^3\Sigma_u^+$) should be possible. But the maximum due to this, as can be seen from potential energy diagram (Fig. 1), lies at about 35000 cm.$^{-1}$ which is probably overlapped by the bands of Group IV of Table II and so is not separately observed. The abnormally high intensity of the Group IV bands is a further evidence.]

The transitions to the bands arising in the state 1_g ($^1\Pi_g$) can thus be expressed as:

I Group: $\sigma_g, \pi_u^4, \pi_g^3, \sigma_u^2 \cdot 1_g\,(^1\Pi_g) \rightarrow \sigma_g^2, \pi_u^3, \pi_g^3, \sigma_g^2 \cdot O_u^-\,(^1\Sigma_u^-)$

II Group: ,, $\cdot 1_g\,(^1\Pi_g) \rightarrow$,, $\cdot 1_u\,(^3\Delta_{1u})$

III Group: ,, $\cdot 1_g\,(^1\Pi_g) \rightarrow$,, $\cdot 2_u\,(^3\Delta_{2u})$

IV Group: ,, $\cdot 1_g\,(^1\Pi_g) \rightarrow \sigma_g^2, \pi_u^4, \pi_g^3, \sigma_u \cdot 1_u\,(^1\Pi_u)$

Band at 29230 cm.$^{-1}$,, $\cdot 1_g\,(^1\Pi_g) \rightarrow \sigma_g^2, \pi_u^3, \pi_g^3, \sigma_u^2 \cdot 1_u\,(^3\Sigma_u^+)$

Now we turn to the bands given in Table IV. These bands are weak. They are arranged in two groups. The wavenumber separation of the component bands is of the order of 480 cm.$^{-1}$ So it appears that all these arise in a state which has a frequency of 480 cm.$^{-1}$ which is higher than that of the ground state ($\omega_e = 324$ cm.$^{-1}$). In iodine we have a state $\{[\sigma_g^2, \pi_u^4, \pi_g^3, {}^2\Pi_{g3/2}]\, \sigma_p^x\}\, \Pi_{2,1g}$ at about 56000 cm.$^{-1}$, which has a frequency of about

TABLE IV

Bands arising in $\{(\sigma_g^2, \pi_u^4, \pi_g^3, \cdot^2\Pi_{g3/2})\ \sigma_g^x\}\ \Pi_{2,1g}$ *at 66500 cm.*$^{-1}$ *with* $\omega \sim 480$ *cm.*$^{-1}$

Group	ν	$\Delta\nu$	Transition
I	43693		$\Pi_{2,1g} \rightarrow \sigma_g^2, \pi_u^3, \pi_g^3, \sigma^2 u, 2_u\ (^3\Delta_{2u})$
	44212	519	
	44731	419	
	45180	449	
	45511	331	
II	46881		$\Pi_{2,1g} \rightarrow \sigma_g^2, \pi_u^4, \pi_g^3, \sigma_u, 1_u\ (^1\Pi_u)$
	47390	509	
	47873	483	
	48357	484	
	48812	455	
	49284	472	
	49725	441	

360 cm.$^{-1}$ while the frequency of the ground state is 214 cm.$^{-1}$, and which gives rise to groups of bands. By analogy with iodine we can take that the $\Pi_{2,1g}$ corresponds to the state with a frequency of 480 cm.$^{-1}$ in bromine molecule. Then the two groups of Table IV may be explained as arising in $\Pi_{2,1g}$ state and having for their final levels $2_u\ (^3\Delta_{2u})$ and $1_u\ (^1\Pi_u)$ which are also the final levels of the second and third groups of Table III. The first band of the second group lies at 46881 cm.$^{-1}$ and so the approximate position of the level $\Pi_{2,1g}$ is at 46881 + 19581 = 66462 ~ 66500 cm.$^{-1}$ The points on the repulsive curves at $r = r_e$ for $\Pi_{2,1g}$, will lie roughly at about (66500 − 43693) = 22807 and (66500 − 46881) = 19619 cm.$^{-1}$ The transitions may be expressed as:

I Group: $\{[\sigma_g^2, \pi_u^4, \pi_g^3, {}^2\Pi_{g3/2}]\ \sigma_u^x\}\ \Pi_{2,1g} \rightarrow \sigma_g^2, \pi_u^3, \pi_g^3, \sigma_u^2 \cdot 2_u\ (^3\Delta_{2u})$

II Group: ,, $\Pi_{2,1g} \rightarrow \sigma_g^2, \pi_u^4, \pi_g^3, \sigma_u \cdot 1_u\ (^1\Pi_u)$

In Table V there are nine bands. These bands are broad and diffuse and their mutual wavenumber separations are in general so great and are so irregular that these bands cannot be explained as forming a single group arising due to a single transition. They can only be explained as arising in a single state and having different repulsive states for their final levels. In iodine molecule we have a state $\sigma_g, \pi_u^4, \pi_g^4, \cdot 1_u\ (^3\Sigma_u^+)$ at about 44900 cm.$^{-1}$ which has a frequency of about 90 cm.$^{-1}$ and which forms the upper level of the discrete absorption bands of iodine in the ultra-violet region. We can attribute $1_u\ (^3\Sigma_u^+)$ to the initial state of the nine bands of Table V. Now we have to find out the probable electronic terms of the repulsive states of the bands. From a combination of two $^2P_{\frac{1}{2}}$ atoms we get O_g^+, 1_u, O_u^- of

TABLE V

Bands arising in $\sigma_g, \pi_u^4, \pi_g^4, \sigma_u \cdot 1_u(^3\Sigma_u^+)$ *at about* 47000 *cm.*$^{-1}$

ν	$\Delta\nu$	Transition
23665	776	$1_u\ (^3\Sigma_u^+) \rightarrow \sigma_g^2, \pi_u^4, \pi_g^2, \sigma_u \cdot O_g^+(^1\Sigma_g^+)$
24441	418	" → " $O_g^+(^3\Sigma_g^-)$
24859	563	" → " $1_g\ (^3\Sigma_g^-)$
25422	547	" → " $2_g\ (^1\Delta_g)$
25969	764	" → $\sigma_g^2, \pi_u^3, \pi_g^4, \sigma_u \cdot 1_g\ (^1\Pi_g)$
26733	453	" → " O_g^-
27186	3399	" → " O_g^+ } $(^3\Pi_g)$
30585	278	" → " 1_g
30863		" → " 2_g

which only O_g^+ can combine with $1_u(^3\Sigma_u^+)$. This O_g^+ can be correlated with $^1\Sigma_g^+$ of case (*a*) type which arises from the configuration $\sigma_g^2, \pi_u^4, \pi_g^2, \sigma_u^2$ (Paper I). So we will attribute $O_g^+(^1\Sigma_g^+)$ to the repulsive state of the band at 23665 cm.$^{-1}$ The *gerade* terms which arise from $^2P_{3/2} + {}^2P_{\frac{1}{2}}$ atoms are O_g^+, 1_g, 2_g, 1_g and O_g^-[8] all of which can combine with the state $1_u(^3\Sigma_u^+)$. O_g^+ and 1_g are to be correlated as in the case of iodine, with $^3\Sigma_g^-$ of case (*a*) type, and 2_g with $^1\Delta_g$ where $^3\Sigma_g^-$ and $^1\Delta_g$ arise from the configuration $\sigma_g^2, \pi_u^4, \pi_g^2, \sigma_u^2$. 1_g is to be correlated with $^1\Pi_g$ and O_g^- with $^3\Pi_{0-g}$ where $^1\Pi_g$ and $^3\Pi_{0-g}$ arise from the configuration $\sigma_g^2, \pi_u^3, \pi_g^4, \sigma_u$. These five states $O_g^+(^3\Sigma_g^-)$, $1_g(^3\Sigma_g^-)$, $2_g(^1\Delta_g)$, $1_g(^1\Pi_g)$ and $O_g^-(^3\Pi_{0-g})$ may be attributed respectively to the repulsive states of second to sixth bands. The *gerade* states that can be derived from two $^2P_{3/2}$ atoms are O_g^+, O_g^+, 1_g and 2_g. Of these one O_g^+ corresponds to the ground state of the bromine molecule. The other three, which can combine with $1_u(^3\Sigma_u^+)$, can be attributed to the seventh, eighth and ninth bands of Table V. These three states are to be correlated with $^3\Pi_g$ of case (*a*) type which arise from the configuration $\sigma_g^2, \pi_u^3, \pi_g^4, \sigma_u$. Thus we have attributed to the repulsive states of the nine bands of Table V just those nine electronic terms which are theoretically possible.

The first band (Table V) lies at 23665 cm.$^{-1}$ and it has for its final level a repulsive curve which dissociates into two Br ($^2P_{\frac{1}{2}}$) atoms at 23266 cm.$^{-1}$ The rough value for the position of the level $1_u(^3\Sigma_u^+)$, which is the initial state of all the bands of Table V, can be estimated to be about 23665 + 23266 = 46931 ~ 47000 cm.$^{-1}$ [The points on the nine repulsive curves below the state $1_u(^3\Sigma_u^+)$ will lie approximately at about 23335, 22559, 22141, 21578, 21031, 20267, 19814, 16415 and 16137 cm.$^{-1}$] The repulsive curves are shown separately in the potential energy diagram (Fig. 2).

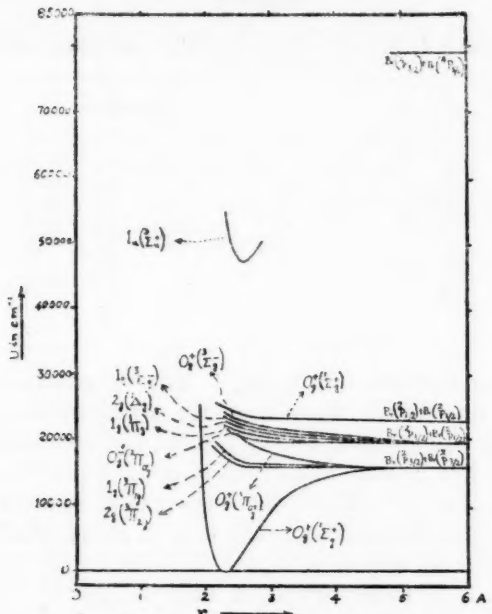

(Fig. 2) Potential energy curves for Br_2 molecule

As the position of the level $1_u\,(^2\Sigma_u^+)$ is at about 47000 cm.$^{-1}$, we should expect banded absorption in the extreme ultra-violet similar to Kimura, Miyanishi bands in iodine.[10] In fact Aickin and Bayliss[9] have indicated the presence of a weak band system, accompanying the continuous absorption in the ultra-violet. As can be seen from the potential energy diagram (Fig. 1), the repulsive curve $\sigma_g^2, \pi_u^3, \pi_g^3, \sigma_u^2 \cdot 1_u\,(^3\Sigma_u^+)$ and the stable curve $1_u\,(^3\Sigma_u^+)$ of the configuration $\sigma_g, \pi_u^4, \pi_g^4, \sigma_u$ run close together. So it is likely that the band absorption will be overlapped by the strong continuous absorption so as not to be observed easily.

Now we proceed to the explanation of the potential energy diagrams. The potential energy curves for the states $O_g^+\,(^1\Sigma_g^+)$, $O_u^+\,(^3\Pi_{0+u})$ and $1_u\,(^3\Pi_{1u})$ are drawn by using Morse equation. The constants used for these three states are taken from Darbyshire's paper.[10] The approximate r_e values for the $\Pi_{2,1g}$ state whose $\omega \sim 480$ cm.$^{-1}$ and $1_g\,(^1\Pi_g)$ state whose $\omega = 220$ are calculated as $r = 2{\cdot}0$ A and $r_e = 2{\cdot}55$ A by using Badger's[11] relation $r_e = \left(\frac{C_{ij}}{k_e}\right)^{\frac{1}{3}} + d_{ij}$, where k_e is force constant for the state in megadynes per cm. and C_{ij} and d_{ij} are constants whose values for bromine molecule are

given by $(C_{ij})^{1/3} = \cdot 505$ and $d_{ij} = 1 \cdot 48$. The r_e value for the state $1_g(^3\Pi_{1g})$ will be approximately the same as that of the ground state, as the vibrational frequencies of the two states are approximately equal. So knowing the r_e values the states $1_g(^3\Pi_{1g})$, $1_g(^1\Pi_g)$ and $\Pi_{2,1g}$ are marked at 55534, 61444 and 66500 cm.$^{-1}$ respectively. The position of the level $1_u(^3\Sigma_u^+)$ at 47000 cm.$^{-1}$ is also indicated approximately.

The curves for all unstable states are drawn as in the case of iodine, since we have already calculated the positions of one or more points on every repulsive curve lying vertically below the stable potential energy curves. The curves for the unstable *gerade* states are shown separately in Fig. 2, for the sake of clarity.

Summary

A large number of new diffuse bands in the emission spectrum of bromine are recorded. The wavelengths of all the diffuse bands of bromine in the region 4200–2000 A are given together with the experimental details. The bands occur in different sets of groups which involve frequency differences of the order of 330, 220 and 480 cm.$^{-1}$ among the component bands. These are explained, as in the case of iodine, as arising in three initial states $1_g(^3\Pi_{1g})$, $1_g(^1\Pi_g)$ and $\Pi_{2,1g}$ with frequencies of about 330, 220 and 480 cm.$^{-1}$ The final states of all these bands will be repulsive, and they are attributed to just these states which are theoretically possible. Besides these bands, there are nine broad bands whose mutual vibrational frequencies are so irregular that they cannot be considered as belonging to a single group arising in a single transtion. These bands are explained as arising in a state $1_u(^3\Sigma_u^+)$ and having for their final levels nine repulsive states which are identified with just the theoretically possible ones. The approximate position of these four states $1_g(^3\Pi_{1g})$, $1_g(^1\Pi_g)$, $\Pi_{2,1g}$ and $1_u(^3\Sigma_u^+)$ are at 55534, 61444, 66500 and 47000 cm.$^{-1}$, whereas for iodine they are at 51583, 58572, 56000 and 44900 cm.$^{-1}$

The author wishes to express his sincere thanks to Prof. R. K. Asundi for guidance and to Kamalapat Singhania Trust for the award of a scholarship.

References

1. P. Venkateswarlu .. *Current Science*, 1946, **15**, 123.
2. ———— .. "Emission Bands of Halogens, Parts I, II and III." *Proc. Ind. Acad. Sci.*, 1946, **24 A**, 480 and this number.
3. Uchida and Ota .. *Jap. Jour. Phys.* (Tokyo), 1928, **5**, 59.
4. Strutt and Fowler .. *Proc. Roy. Soc.* (London), 1911, **86 A**, 105.
   Ludlam and West .. *Ibid.*, Edinburgh, 1923–24, **44**, 185.

5. Sponer .. *Molekul Spektren*, Vol. I (Berlin), 1935.
6. Turner .. *Phys. Rev.*, 1926, **27**, 397.
7. Acton, Aickin and Bayliss .. *Jour. Chem. Phys.*, 1936, **4**, 474.
Mulliken .. *Ibid.*, 1936, **4**, 620.
———— .. *Phys. Rev.*, 1940, **57**, 500.
8. ———— .. *Rev. Mod. Phys.*, 1932, **4**, 70.
9. (*a*) Cordes and Sponer .. *Zs. f. Phys.*, 1930, **63**, 334.
(*b*) Aickin and Bayliss .. *Trans. Farad. Soc.*, 1938, **34**, 1371.
0. Darbyshire .. *Proc. Roy. Soc.*, 1937, **159 A**, 93,
Badger .. *Journ. Chem. Phys.*, 1935, **3**, 710.

Explanation to Plate

(*a*) Spectrum (*a*) is taken on Medium quartz spectrograph using a 'Kodak superpanchropress P–1200,' plate.

(*b*) Spectrum (*b*) is taken on E_2 quartz spectrograph using a 'Kodak B–20 Process regular' plate.

(*c*) Spectra (*c*) (1) & (2) are taken on a E_3 quartz spectrograph 'Kodak B–20 Process regular' plates are used.

(*d*) Tnis shows the microphotometric curve of the spectrum taken on the E_2 quartz spectrograph. Magnification 1·5.

Wavelengths of some of the bands are marked on the plate.

-5782·3
-4224·5
-3932·5
-3336·6
-2753·6
-2564·7
-2478·8
-3549·4
-2900·4
-2709·8
-2623·1
-2564·7
-2478·8
-2360·8
-2313·9
2900·4
2709·8
2623·1
2421·1
2360·8
-3549·4
-3336·6
-2900·4
-2753·6
-2623·1
-2564·7
-2478·8
-2421·1
-2360·8
-2313·8
O-H Bd

FINITE LONGITUDINAL VIBRATIONS

By B. R. Seth, F.A.Sc.

(From the Department of Mathematics, Hindu College, Delhi)

Received December 10, 1946

It is known that, if we neglect terms of the second order, the differential equation satisfied by the displacement ξ in the case of longitudinal vibrations of strings and rods is

$$\frac{\partial^2 \xi}{\partial t^2} = c^2 \frac{\partial^2 \xi}{\partial x^2}. \tag{1}$$

It is also known that, assuming Hooke's law holds good for large values of ξ, this equation is not merely an approximation, but is accurate for large values of ξ. But Hooke's law does not hold good for large values of ξ. In such a case the theory of Finite Strain gives the relation between the tension T and the ordinary stretch s as[1]

$$T = \tfrac{1}{2} E \left[1 - \frac{1}{(1+s)^2} \right], \tag{2}$$

E being Young's modulus. It will be therefore of interest to determine what form the differential equation satisfied by ξ takes for finite values of ξ. It is found that in such cases the equation is exactly the same as the general equation for long waves in a uniform canal with vertical sides.

Let A be a fixed point of the string AB when unstretched and placed in a straight line. Let PQ be any element of the unstretched string, P'Q' the same element at the time t. Let $AP = x$, $AP' = x'$. Let T and $T + dT$ be the tensions at P' and Q', and let m be the mass of a unit length of the unstretched string. The equation of motion then is

$$m \frac{\partial^2 x'}{\partial t^2} = \frac{\partial T}{\partial x}. \tag{3}$$

As $s = \dfrac{\partial}{\partial x}(x' - x)$,

$$T = \tfrac{1}{2} E \left[1 - \left(\frac{\partial x'}{\partial x} \right)^{-2} \right], \quad \frac{\partial T}{\partial x} = E \frac{\partial^2 x'}{\partial x^2} \left(\frac{\partial x'}{\partial x} \right)^{-3} \tag{4}$$

(3) now takes the form

$$\frac{\partial^2 x'}{\partial t^2} = \frac{E}{m} \cdot \frac{\partial^2 x'}{\partial x^2} \left(\frac{\partial x'}{\partial x} \right)^{-3}. \tag{5}$$

If the unstretched state of the string be chosen as the standard of reference, we can put $x' = x + \xi$, and we get

$$\frac{\partial^2 \xi}{\partial t^2} = \frac{E}{m} \frac{\frac{\partial^2 \xi}{\partial x^2}}{\left(1 + \frac{\partial \xi}{\partial x}\right)^3}, \tag{6}$$

which is of the same form as the general equation for long waves.[2]

Proceeding, as is usual in such cases, we find that the complete integral of (5) is[3]

$$x' = \alpha x + \beta t + c_1, \tag{7}$$

where the arbitrary constants α and β are connected by the relation

$$\beta = \pm 2c(1 - \alpha^{-\frac{1}{2}}), \quad c^2 = E/m.$$

The general integral is

$$\left.\begin{aligned} x' &= \alpha x \mp 2c(1 - \alpha^{-\frac{1}{2}})\, t + \phi(\alpha) \\ o &= x \mp c\alpha^{-3/2}\, t + \phi'(\alpha) \end{aligned}\right\} \tag{8}$$

Putting $u = \partial x'/\partial t$, we get

$$u = 2c(\alpha^{-\frac{1}{2}} - 1), \tag{9}$$

and

$$x' - t(\tfrac{3}{2}u + c) = \phi(\alpha) - \alpha\phi'(\alpha), \tag{10}$$

ϕ being an arbitrary function.

From (10) we get

$$u = f[x' - t(\tfrac{3}{2}u + c)], \tag{11}$$

f being an arbitrary function. Thus, in such cases, as is well known, waves cannot be propagated without change of form.

Summary

The theory of Finite Strain gives the interesting result that the differential equation for finite longitudinal vibrations of strings and rods is the same as the general equation for long waves.

References

1. Seth, B. R. .. *Phil. Trans. Roy. Soc.*, 1935, **234**, 231.
2. Lamb, H. .. *Hydrodynamics*, 5th ed., 1930, 241.
3. ———— .. *Loc. cit.*, 458.

CHEMICAL EXAMINATION OF *ARTEMISIA SCOPARIA* WALDST. AND KIT.

Isolation of an Essential Oil and Laactone

By Dharam Bal Parihar and Sikhibhushan Dutt
(Department of Chemistry, Delhi University)

Received October 14, 1946

Artemisia scoparia or *Blur* or Dona as it is known in Punjabi and Las Bela in Hindi and Urdu is an annual scandent herb belonging to the genus of Artemisia and the natural order of Compositeæ. It is found wild in the lower reaches of the Western Himalayas, the Simla Hills, Eastern and Northern Punjab and the upper Gangetic plains. It is the only species of Artemisia that grows in the plains in India. The botanical identification of the plant was done both in the Forest Research Institute, Dehra Dun and the Government Botanical Gardens, Calcutta.

Artemisia scoparia is a faintly aromatic plant that often grows to a height of 5 feet. In large specimens the stems have a tendency to become woody in character. The flowering heads and the seeds are the most highly aromatic parts of the plant and contain the greatest concentration of the active principles namely the lactone and the essential oil. The plant has got interesting medicinal properties. In the Punjab the smoke from the smouldering dried plant is considered to be very efficacious for burns, and the infusion of the green plant is often given as a purgative. The leaves of the plant made into a paste with water are sometimes used as poultice in ear affections. A decoction of the flowering heads is considered an excellent mouthwash in all tooth troubles.

Although a number of varieties of Artemisia growing all over the world have been worked for their constituents, yet no work seems to have been done on the chemical examination of *Artemisia scoparia* growing in India. Hence in view of the medicinal importance of the plant and its definitely aromatic nature, the present work was undertaken to find out its constituents by systematic chemical examination.

As the result of the examination two important compounds were isolated from the plant, one a crystalline lactone with the molecular formula $C_{16}H_{30}O_5$ and the other a pleasant smelling essential oil. The detailed study of the essential oil has been reserved for a separate communication, while in the

present one the lactone has been studied in detail and a number of important derivatives of the same have been prepared.

Experimental

4·54 Kilos of the air-dried and mixed flowering heads and seeds of the plant were extracted with hot petroleum ether (B.P. 40°–60° C.) under reflux in lots of 1 kilo at a time. The extracts were filtered hot and the solvent distilled off on a water-bath. The syrupy concentrate, which had a deep green colour was allowed to stand for twenty-four hours when a thick magma of colourless crystals separated. These were filtered off and washed with a little petroleum ether. The mother-liquor and the washings on further concentration gave two more crops of the same crystalline substance with identical melting point. The ultimate mother-liquor freed from petroleum ether had an oily consistency and a pleasant smell, and was found to contain an essential oil. This was recovered by steam distillation. The oil had the following physical and chemical constants:—

Refractive Index at 23° C.	= 1·5220
Specific Gravity at 23° C.	= 0·9497
Saponification value	= 77·28
Acid Value	= 6·3
Rotation	= nil.
Saponification value after acetylation ..	= 163·2

The various crops of the crystalline matter mentioned above were mixed together and recrystallised from boiling alcohol with the addition of animal charcoal, when the substance was obtained in colourless glistening prisms melting sharp at 146° C., and the melting point did not rise any further on repetition of the above process. In this way 42 gms. of the crystalline substance was obtained from 4·5 Kilos of the raw material, thus giving an yield of 0·92 per cent. on the dried stuff. The substance has been named "Scoparin". It possesses the nature of a lactone and has a characteristic pleasant odour. The substance as well as all its derivatives have extraordinary power of crystallisation.

Scoparin is sparingly soluble in methyl alcohol, acetone, carbon disulphide, ethyl acetate, ether and petroleum ether in the cold but dissolves readily on heating. It is slightly soluble in cold alcohol, and acetic acid, and easily soluble in chloroform benzene and pyridine. It is insoluble in hot or cold water. It is also insoluble in cold concentrated sulphuric acid but dissolves on warming to a colourless solution. Addition of water precipitates the original compound in practically unchanged condition.

Scoparin is insoluble in concentrated hydrochloric acid either in the cold or in the hot. When treated with aqueous or alcoholic caustic potash, it dissolves with an intense yellow coloration, which is characteristic of many unsaturated lactones. It does not give any colouration with alcoholic or aqueous ferric chloride. Scoparin contains no nitrogen and does not reduce Fehling's solution, but Tollen's reagent is reduced in the cold showing thereby the presence of an α: β-unsaturation in the molecule. It slowly decolourises bromine in chloroform. It has got no action on alkaline sodium nitroprusside. From the solution of the substance in aqueous or alcoholic caustic soda or potash, acid precipitates the original substance. (Found: C = 66·21, 65·57, 65·48 per cent.; H = 6·73, 6·84, 6·67 per cent.; M.W., Cryscopic in Phenol, = 294·2, 285·9, 291·1; $C_{16}H_{20}O_5$ requires C = 65·75, H = 6·85 per cent.; M.W. = 292.)

Repeated attempts to acetylate and benzoylate Scoparin under different conditions were unsuccessful, thus indicating the absence of hydroxyl group in the molecule. Determination of methoxyl groups according to Zeises' method gave evidence of two such groups in the molecule. (Found: OCH_3 = 23·06, 22·21; $C_{14}H_{14}O_3$ $(OCH_3)_2$ requires OCH_3 = 21·23 per cent.)

Preparation of the lead salt.—Scoparin was dissolved in hot alcohol and to it was added hot alcoholic solution of lead acetate (2%). The mixture was refluxed for a few minutes on the water-bath; on cooling a crystalline precipitate came down. This was filtered, washed with alcohol and water, and recrystallised from alcohol in the form of sharp elongated needles, M.P. 178°C. (Found: Pb = 26·21, $C_{15}H_{19}O_3$. $COO\frac{Pb}{2}$ requires Pb = 26·2 per cent.).

Scoparin dibromide.—Scoparin (2 gms.) dissolved in benzene (20 c.c.) was treated with an excess of bromine dissolved in the same solvent. The mixture was allowed to stand at the ordinary temperature overnight and then warmed on the water-bath for about half an hour. The excess of bromine and benzene were distilled off and the residual liquid washed with a mixture of aqueous potassium iodide and sodium thiosulphate and finally with water. The product was then dissolved in a small quantity of hot benzene and allowed to crystallise spontaneously. The Scoparin dibromide crystallised in orange-red needles, M.P. 109°C. It is insoluble in water, methyl alcohol, ether and petroleum ether, but is soluble in benzene, alcohol and chloroform. (Found: Br = 35·6, $C_{16}H_{20}O_5$. Br_2 requires Br = 35·4 per cent.)

Scoparin monoxime.—To a solution of 0·5 gm. of scoparin in 20 c.c. alcohol, were added one gm. of hydroxylamine hydrochloride and 0·5 gms.

of sodium acetate. The mixture was refluxed for about half an hour on the water-bath. Hot water was then added to the boiling liquid so that a slight turbidity appeared. On cooling, the oxime crystallised out in fine crystals. It was recrystallised from alcohol in very small cubes melting at 85° C. It is soluble in alcohol, acetone, and chloroform, but is insoluble in water, ether and petrol-ether. (Found: N = 4·71; $C_{16}H_{20}O_4$ = NOH requires N = 4·5 per cent.).

Scoparin semicarbazone.—To 0·5 gm. of scoparin dissolved in 20 c.c. alcohol were added 1 gm. of semicarbazide-hydrochloride and 0·5 gm. sodium acetate, and the mixture refluxed for about half an hour on a water-bath. Addition of hot water to the liquid precipitated the semi-carbazone in crystalline form. This was filtered, washed, dried and recrystallised from alcohol in thick prismatic needles melting at 162° C. It is soluble in chloroform alcohol and acetone, but insoluble in water. (Found: N = 12·61, 12·43; $C_{17}H_{23}N_3O_5$ requires N = 12·03 per cent.)

Scoparin phenylhydrazone.—To a solution of 0·5 gm. of scoparin in 10 c.c. of hot glacial acetic acid was added a solution of 1 c.c. of phenyl hydrazine in 2 c.c. glacial acetic acid. The mixture was warmed on the water-bath for about twenty minutes and then diluted with hot water until a slight turbidity was produced. On cooling the phenylhydrazone came down as a crystalline precipitate which was recrystallised from alcohol in pale yellow thin needles melting at 72–73° C. It is soluble in chloroform, ethyl acetate and carbon tetrachloride in the cold, but is insoluble in cold or hot water, ether and petroleum-ether. In methyl or ethyl alcohol it is slightly soluble. (Found: N = 7·28; $C_{16}H_{20}O_4$ = N.NHC$_6$H$_5$ requires N = 7·3 per cent.)

Scoparin 2:4-*Dinitrophenylhydrazone.*—This was prepared from scoparin and 2:4-dinitrophenylhydrazine dissolved in methyl alcohol in a similar way to the above. It was recrystallised from methyl alcohol in yellow glistening plates melting at 132° C. It is soluble in alcohol, chloroform, ethyl acetate and benzene, but insoluble in water. (Found: N = 11·91, $C_{22}H_{24}O_8N_4$ requires N = 11·9 per cent.)

Fusion with sodium hydroxide.—2 gm. of the compound was gradually added to a molten mixture of 10 gm. of caustic soda and 1 c.c. of water in a nickel crucible maintained at 150° C. Much frothing took place during the reaction. The mass was finally heated at 280° C. for half an hour. The cold melt was dissolved in water and neutralised with hydrochloric acid. A pale yellow precipitate came down which was filtered, washed and dried. It was then crystallised from alcohol in small colourless needles, which shrink

at 60° C. and melt at 68° C. The compound was found to be insoluble in cold or hot aqueous caustic soda and no yellow colouration was produced as was the case with the original compound. On strongly heating, it volatilised partially emanating a peculiar odour. It did not give any colouration with $FeCl_3$. The compound is insoluble in water, ether and petroleum-ether, but is soluble in alcohol, ethyl acetate and chloroform. The substance was found to be ketonic in nature and its dinitrophenylhydrazone prepared in the usual way, crystallised in long yellow glistening needles melting at 93° C. This is soluble in hot alcohol, but insoluble in cold methyl alcohol and water. It dissolves easily in benzene, acetone and chloroform. (Found: N = 17·52; $C_{27}H_{30}O_{10}N_8$ requires N = 17·89 per cent.)

From the results of the analysis it appears that the compound formed is a diketone with the formula $C_{15}H_{22}O_4$.

Reduction of scoparin with tannous chloride.—2 gm. of scoparin dissolved in 50 c.c. of alcohol were treated with 1 gm. of stannous chloride and 1 c.c. of concentrated hydrochloric acid, and the mixture was refluxed on the water-bath for half an hour. It was then poured into water and the resultant crystalline precipitate filtered, washed with water and dried. It was recrystallised from alcohol in fine silky needles melting at 84–85° C. It is insoluble in methyl alcohol, water, ethyl acetate, ether and petrol-ether but dissolves easily in hot alcohol and chloroform. It does not add on bromine, has no action on ammoniacal silver nitrate and does not react with 2:4-dinitrophenylhydrazine. The compound is insoluble in aqueous caustic soda and no yellow colouration is produced by this reagent as in the case of scoparin. From the reactions of the reduced product, it appears to be a saturated secondary alcohol. With acetic anhydride it formed a monoacetyl derivative.

Oxidation of the reduced product with chromic acid.—One gm. of the above reduced product dissolved in 10 c.c. glacial acetic acid was treated with 1 gm. of chromium trioxide dissolved in 5 c.c. of the same solvent. The mixture was refluxed on a sand-bath for about half an hour. It was then poured in cold water. The resultant crystalline precipitate was filtered and thoroughly washed with acidulated water. It was recrystallised from alcohol in colourless needles melting at 101° C. The compound does not add on bromine, and does not give any reaction of an acid. It is soluble in methyl and ethyl alcohols and benzene, but is quite insoluble in water. This compound behaves like a mono-ketone and with 2:4-dinitrophenylhydrazine gave a hydrazone crystallising in yellow glistening plates and needles from

methyl alcohol melting at 114°C. (Found: N = 11·84; $C_{22}H_{30}O_6N_4$ requires N = 11·81 per cent.)

The compound therefore appears to be a mono-ketone with the molecular formula $C_{16}H_{22}O_4$.

Further work on this subject is in progress.

Summary and Conclusion

1. From the flowering heads and seeds of *Artemisia scoparia*, which is the only species of *Artemisia* growing in the plains of India, a lactone and an essential oil have been obtained in yields of 0·92 and 0·75 per cent. respectively.

2. The lactone, which has been named "Scoparin", has been found to have the molecular formula $C_{16}H_{20}O_5$. It contains an $\alpha:\beta$-unsaturation, one ketonic group and two methoxyl groups.

3. A number of derivatives of the lactone have been prepared and analysed.

LUMINESCENCE IN THE SOLID STATE: BORIC ACID AS BASE

Part III. Azo-Dyes from *o*-Hydroxy-Carbonyl Compounds as Activators

By K. Neelakantam, S. Narayanan and M. V. Sitaraman
(Andhra University, Waltair, and Presidency College, Madras)

Received January 20, 1947

Out of nearly fifteen hundred dyes listed in the Colour Index only about eighty-five are classified as fluorescent in the dissolved state, the solvent being water, alcohol, xylene or tetralin. It is remarkable that not even a single azo-dye is to be found in the list. Recent work, however, has shown that many of the "non-fluorescent" dyes of the Index are quite as strongly fluorescent as the "fluorescent" dyes, when in a state of solid solution in solvents like gelatine, sugar, etc., or when adsorbed on wool. Under certain conditions they are even phosphorescent. Among azo-dyes also, there are several which fluoresce when dyed on silk, cotton or other textile fibres or when adsorbed on activated alumina.[1] It is well known that the phosphorescence of many compounds is specially strong when dissolved in solid anhydrous boric acid.[2,3,4] A variety of organic compounds have been utilised as activators of phosphorescence, with this base but among the dyes only those of the fluorescein series and a few others have been used so far and no systematic study of any group of dyes has been attempted by previous workers. The authors of the present paper have, therefore, taken up the study of the azo-dyes derived from *o*-hydroxy-carbonyl compounds[5] in this connection.

Experimental

Procedure.—The procedure adopted for the preparation of activated boric acid melts and their examination under filtered U.V. light was identical with that already described in Part I.[3] Aqueous or alcoholic solutions of the dye-stuffs were employed. In all cases 1 gram of boric acid was used and with each dye, the amounts used were in the ratio of 100 : 10 : 1, the maximum amount of dye used being 1·0 mg. The results obtained with different concentrations of the activator in this ratio are reported in columns A, B and C respectively in the table. The figures in brackets indicate the period of after-glow in seconds. The intensities of phosphorescence in all cases were very weak.

No.	Azo-dye	Luminescence (U.V. Excitation)					
		A		B		C	
		Fluorescence	Phosphorescence	Fluorescence	Phosphorescence	Fluorescence	Phosphorescence
1	Benzene-azo-*salicylic acid* ..	Orange-red	Nil	Yellow	(5) Pale blue	Cream	(10) Blue
2	*o*-Hydroxy-benzene-azo- ,, ..	Yellow	(6) Pale blue	Pale yellow	(8) Do	Pale blue	(7) Pale blue
3	*p*-Hydroxy-benzene-azo- ,, ..	Blue violet	(8) Blue	Pale blue	(9) Do	Do	(8) Do
4	*p*-Sulpho-benzene-azo- ,, ..	Brownish yellow	Nil	Pale yellow	(6) Light blue	Very pale yellow	(6) Do
5	*p*-Chlor-benzene-azo- ,, ..	Bright orange-yellow	Nil	Yellow	(4) Do	Pale yellow	(8) Blue
6	*p*-Nitro-benzene-azo- ,, ..	Yellowish brown	Nil	Yellow	(6) Pale blue	Pale blue	(8) Pale blue
7	*m*- do do do ..	Nil	Nil	Pale yellow	Nil	Blue violet	(5) Do
8	*m*-Tolyl-azo-acid ..	Orange-yellow	Nil	Yellow	(6) Pale blue	Pale green	(9) Do
9	α-Naphthyl-azo- ,, ..	Pale orange	(6) Light blue	Pale yellow	(10) Do	Pale blue	(10) Do
10	β- do do do ..	Orange red	(4) Pale blue	Light orange	(6) Light blue	Do.	(7) Do
11	Benzene-azo-1-hydroxy-2-naphthoic acid	Orange-yellow	(6) Light blue	Light yellow	(9) Pale blue	Blue	(10) Do
12	Benzene-azo-2-hydroxy-3 naphthoic acid	Dark red	Nil	Rose red	(6) Do	Pale red	(8) Do
13	Benzene-azo-resacetophenone (A)	Brownish yellow	Nil	Pale yellow	(6) Do	Pale blue	(11) Do
	Do (B)	Yellow	Nil	Do	(8) Pale blue	Do	(8) Do
14	Chrysamine G ..	Pink	(4) Very pale pink	Pink	(6) Very pale pink	Very pale pink	(6) Do
15	Cotton yellow G. I. ..	Bluish violet	(6) Very pale blue	Nil	(9) Very pale blue	Nil	(10) Very pale blue
	Do R. ..	Flesh colored	(10) Do	Very pale pink	(14) Do	Nil	(15) Do
16	Diamine brown M ..	Fiery red	(3) Do	Flesh coloured	(7) Do	Nil	(7) Do
17	Diamine Green B ..	Nil	(12) Green	Nil	(7) Green	Nil	(7) Green
18	Diamond black F ..	Nil	(9) Greenish yellow	Nil	(11) Greenish yellow	Nil	(16) Greenish yellow
19							
20	Diamond Green G ..	Orange	(4) Pale blue	Orange yellow	(9) Pale blue	Light yellow	(9) Pale blue

Discussion

None of the dyes used in the above investigation fluoresce in aqueous or alcoholic solutions. As shown in a previous investigation[3] some of them fluoresce, though weakly, when dissolved in concentrated sulphuric acid and examined under U.V. light. On the addition of boric acid to this solution, intensification of fluorescence occurred in several cases. From the data presented in the table, it is clear that all the dyes fluoresce under U.V. excitation, when dissolved in anhydrous boric acid. The phosphorescence, however, is very weak in intensity in all cases. The period of after-glow is of the same order of magnitude as with the simple salicylic acid or resacetophenone molecule but the intensities are definitely weaker. It is well known that the azo group is markedly bathofluoric although it does not destroy the ability to fluoresce completely. From the present study it is clear that the azo-dyes are poor activators of phosphorescence, although they fluoresce when dissolved in anhydrous boric acid. The azo-group is, therefore, on the whole a poor luminophore.

References

1. Pringsheim and Vogel .. *Luminescence of Liquids and Solids and its Practical Applications*, 1943, 73.
2. Neelakantam & Sitaraman .. *Proc. Ind. Acad. Sci.*, 1945, **21 A**, 45, 272.
3. ———— .. *Ibid.*, 1946, **23 A**, 16.
4. G. N. Lewis *et al.* .. *J. Am. Chem. Soc.*, 1941, **63**, 3005.

HYSTERESIS IN SORPTION

XI. Permanence of Sorption-Desorption Hysteresis

By T. Krishnappa,* K. Subba Rao‡ and B. Sanjiva Rao,§ F.A.Sc.
(*Department of Chemistry, Central College, Bangalore, S. India*)

Received January 6, 1947

Introduction

Van Bemmelen[25] was the first to notice the phenomenon of hysteresis in sorption. Later, other workers like Zigmondy,[29] Anderson,[3] Coolidge,[4] Winnings and Williams,[28] Shiels,[21] McGavack and Patrick,[8] Urquhart,[24] Sheppard and Newsome,[20] McBain and Ferguson[7] studied this effect. But for a long time the reality of the effect remained uncertain. By careful experiments on charcoal, Allmand and collaborators[1,2] showed that the hysteresis effect was real. Working with hydrous oxides Lambert and co-workers also proved the reality of the phenomenon. Recently, Rao, K. S.[9] has established, by extensive investigations on various porous adsorbents that the hysteresis effect is remarkably permanent and can be reproduced any number of times. Besides establishing the permanence and reproducibility of the effect, intersting phenomena such as drift[10, 11] and disappearance[12, 13, 14, 22] of the hysteresis loop have been discovered. A new method of study of hysteresis called "scanning" of the loop has been developed.

Weiser and collaborators[26, 27] have recently reported that if hydrous oxide gels are prepared by mixing boiling solutions of the two reactants, the hysteresis effect with reference to water vapour is completely eliminated. Such elimination has been reported with silica gel in particular.

Several explanations have been offered from time to time for the hysteresis effect. After making a critical study of these in a recent review,[18] Rao concludes that the cavity concept affords the only general explanation of the hysteresis and all other related phenomena.[6, 23]

In accordance with the cavity concept, a rigid porous adsorbent like silica gel should always show a permanent hysteresis effect. Complete elimination of the hysteresis effect without a marked fall in the sorptive capacity is improbable. Weiser's observations however are in contradiction

* Mysore Government Scholar, University of Sheffield, Sheffield.
‡ Senior Research Fellow of the National Institute of Sciences of India.
§ Principal and Professor of Chemistry, Central College, Bangalore.

to this view. Therefore a careful study of sorption and desorption has been made in this laboratory on gels of silica, alumina and titania, prepared by mixing the boiling hot solutions of the reactants in accordance with the procedure adopted by Weiser and collaborators (*loc. cit.*).

Experimental

Composition of sodium silicate

On analysis, the sodium oxide and silicon dioxide ratio was found to be 1·02 in the meta silicate and 0·52 in the water glass used.

Silica gels

Silica gel A (*precipitated at* 25° *C.*).—80 c.c. of sodium silicate solution (containing 0·13 gm. of silicon dioxide per c.c.) were added slowly to 100 c.c. of acetic acid solution containing 30 c.c. of glacial acetic acid, the mixture being stirred vigorously by an electrical stirrer. The mixture was kept overnight, then mixed with water, filtered and washed free from acid. The washed gel was dried in air for some hours at room temperature (25° C.). Gels were prepared both from sodium metasilicate and water glass.

Silica gel B (*precipitated at* 100° *C.*).—The sodium silicate solution was first boiled for six hours under reflux. Boiling hot solutions of the silicate and acetic acid were then mixed, the concentrations and quantities of solutions being the same as in the above experiment. Gels were prepared from both metasilicate and water glass by the above procedure.

Silica gel C (*Gel B treated with boiling water*).—A portion of the washed silica gel B was refluxed in boiling water for 96 hours. After this treatment the gel was washed and dried in air.

Silica gel D (*gel B heated in water at* 120° *C.*).—Another portion of washed silica gel B was suspended in water and heated to 120° C. in an autoclave for 3 hours. The gel was washed and dried in air.

Titania gels

Gel A.—50 gm. of titanium tetrachloride were dropped into concentrated hydrochloric acid. The mixture was diluted so that the resulting solution was 0·5 N with respect to titanium tetrachloride and 0·2 N with respect to hydrochloric acid. 0·7 N ammonium hydroxide was added at room temperature (25° C.) in a thin stream to the titanium tetrachloride solution, the liquid being vigorously stirred. Two per cent. excess of ammonium hydroxide was added. The precipitate was filtered off, washed and dried in air.

Gel B.—The titania gel was prepared in the same way as indicated above but the precipitation was conducted in boiling hot solutions.

Alumina gels

Gel A.—To 0·5 N solution of aluminium sulphate, excess of 0·5 N ammonium hydroxide was added at room temperature (25° C.) in a thin stream while stirring the former. The mixture was filtered, washed free from sulphate and dried in air.

Gel B.—The alumina gel was prepared in the same way but by precipitation in boiling hot solutions.

Sorption and desorption of water vapour

The quartz fibre spring technique[9] was employed in the investigations. Distilled water kept in the bulb of the sorption apparatus was rendered air free by evaporating a portion of the water in vacuum obtained by the Cenco Hyvac pump.

The air-dried gel was placed in the bucket and the spring was introduced into the sorption tube. The system was then evacuated at 30° C. for 5 or 6 hours at a pressure of 10^{-3} mm.

After degassing the gel, sufficient amount of water vapour from the bulb was introduced into the sorption tube and the stopcock was closed. The gel was allowed to attain equilibrium with water vapour. The equilibrium pressure of the system and the stretch of the spring were measured. More water was introduced and measurements were continued until the saturation pressure was reached. Desorption was then carried out by removing sufficient amount of water vapour with the aid of the Hyvac pump. After the attainment of equilibrium, the pressure and stretch were measured. The desorption was continued until zero pressure was reached. For the attainment of equilibrium, the appropriate time required was about 6 hours for silica gel, 4 hours for titania and 3 days for alumina. In actual practice however, 10 hours were allowed for silica gel, 6 hours for titania and 4 days for alumina. A series of sorptions and desorptions of water vapour at 30° C. on the various gels gave permanent hysteresis loops (Figs. 1 to 10).

Residual water

In each system, at the end of the experiment when the gel was at the zero point after desorption, it was removed for the estimation of the residual water. The water content of the gel was determined by igniting to constant weight in a platinum crucible. The residual water in each gel is indicated in the corresponding graph.

Discussion

Hysteresis in sorption has been explained on the basis of the cavity concept. In any rigid porous system, there are open pores as also the capillaries with constricted ends. The latter types of capillaries—the cavities, are responsible for the hysteresis effect. Existence of only one type, *i.e.*, either the cavity or the open pore in a porous system is highly improbable in a random distribution. Silica gel prepared by us in close conformity with the procedure adopted by Weiser, Milligan Holes and Simpson has in

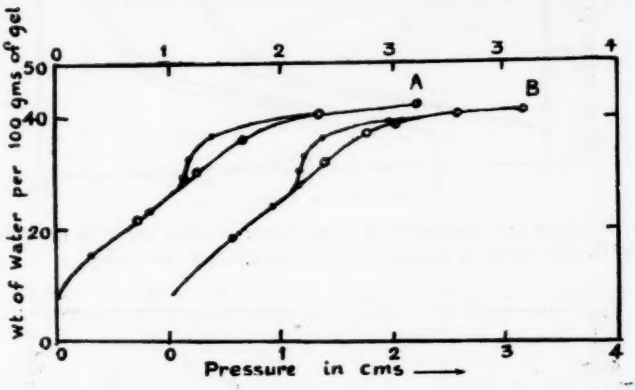

Fig. 1. Sorption and desorption of water vapour on silica gel from metasilicate precipitated at 25° C. (A. 2nd cycle, B. 3rd cycle).

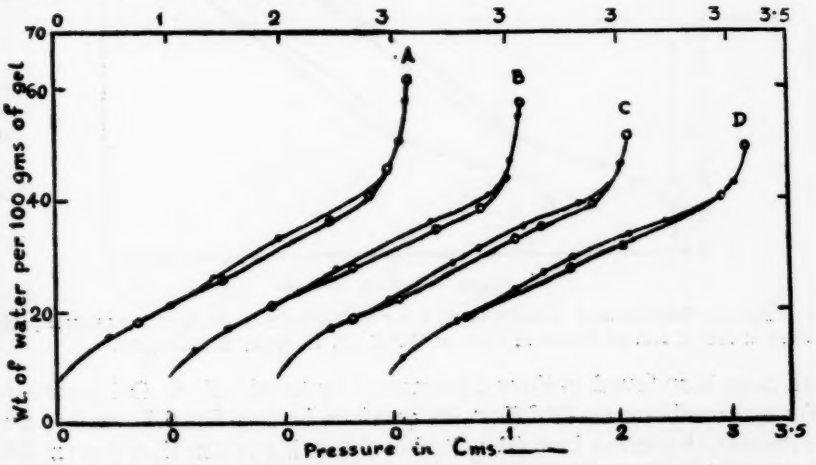

Fig. 2. Sorption and desorption of water vapour on silica gel from metasilicate precipitated at 100° C. (A. 1st cycle, B. 2nd cycle, C. 3rd cycle, D. 4th cycle).

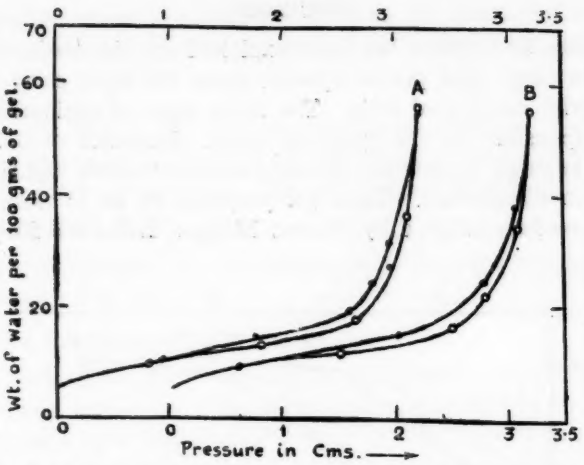

FIG. 3. Sorption and desorption of water vapour on silica gel from metasilicate precipitated at 100° C. and heated in boiling water (A. 1st cycle, B. 3rd cycle).

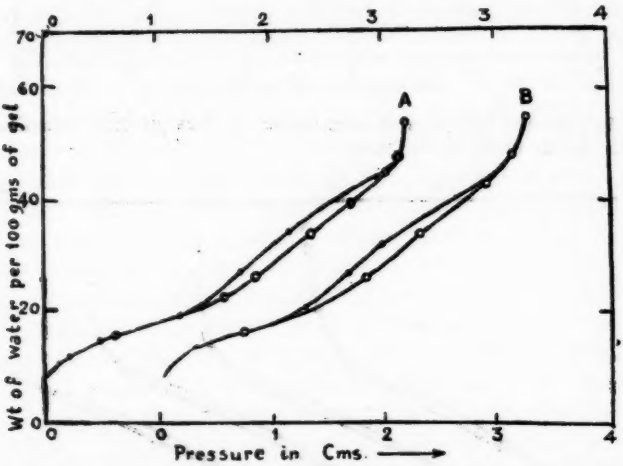

FIG. 4. Sorption and desorption of water vapour on silica gel from metasilicate precipitated at 100° C and gel heated in water at 120° C. (A. 1st cycle, B. 2nd cycle).

all cases been found to show a permanent hysteresis effect. Gel precipitated from metasilicate at 100° C., with previous boiling for 6 hours has given permanent hysteresis loop (Fig. 2), though smaller in size than that exhibited by the gel precipitated at 25° C. (Fig. 1). A sample of air-dried gel, precipitated at 100° C., was boiled in water under reflux for 96 hours. The gel

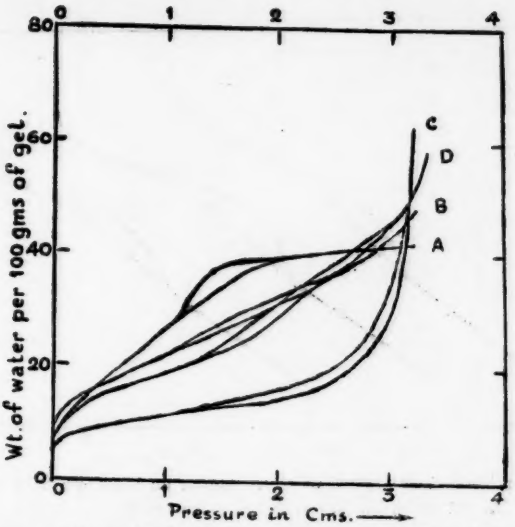

FIG. 5. Sorption and desorption of water vapour on silica gel from metasilicate and heated in boiling water and heated in water at 120° C.

A. Gel precipitated at 25° C.
B. " " 100°C.
C. " " "
D. " " "

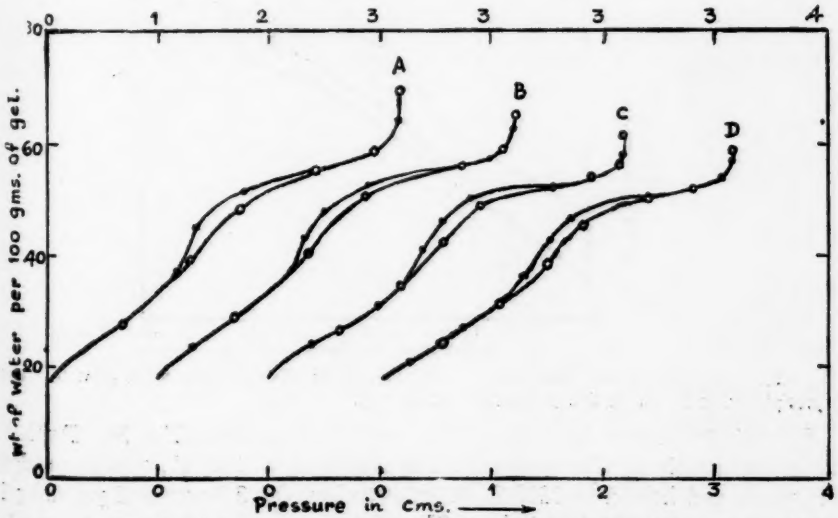

FIG. 6. Sorption and desorption of water vapour on silica gel from water glass precipitated at 25° C. (A. 1st cycle, B. 2nd cycle, C. 3rd cycle, D. 4th cycle).

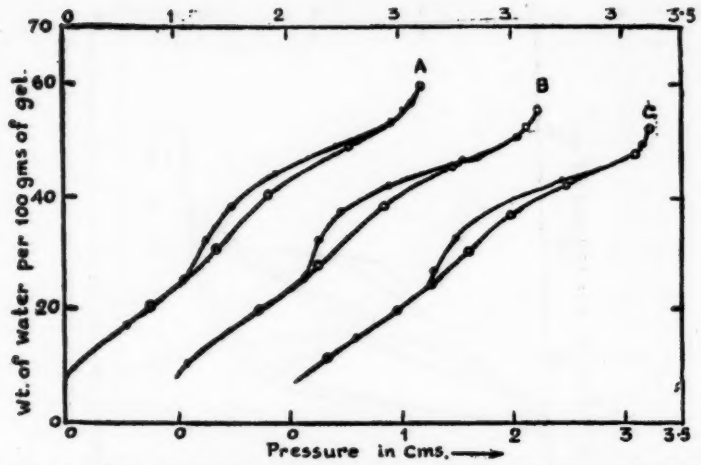

FIG. 7. Sorption and desorption of water vapour on silica gel from water glass precipitated at 100° C. (A. 1st cycle, B. 3rd cycle, C. 11th cycle).

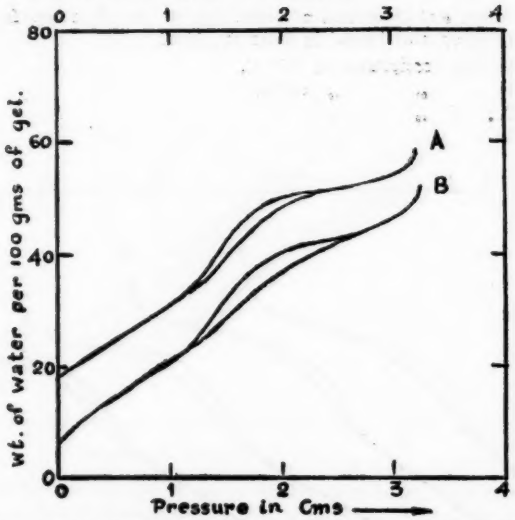

FIG. 8. Sorption and desorption of water vapour on silica gel from water glass (A. Gel precipitated at 25° C. B. Gel precipitated at 100° C).

after this treatment showed a permanent hysteresis loop (Fig. 3). Further, another sample of the air-dried gel precipitated at 100° C., was suspended in water and heated to 120° C., in an autoclave for 3 hours and yet the gel gave a permanent hysteresis loop (Fig. 4).

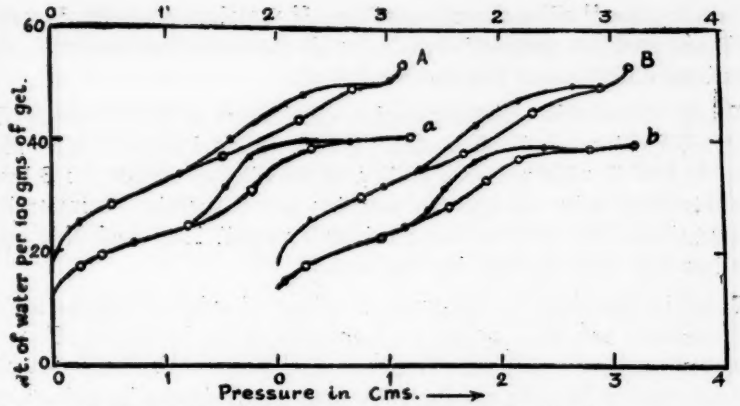

FIG. 9. Sorption and desorption of water vapour on Titania gel
Gel precipitated at 25° C (A. 1st cycle. B. 2nd cycle)
„ „ at 100° C. (*a*. 1st cycle, *b*. 2nd cycle).

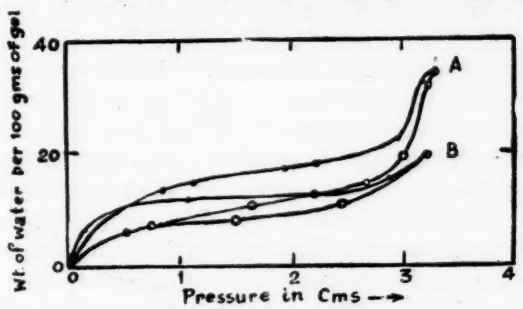

FIG. 10. Sorption and desorption of water vapour on alumina gel
A. Gel precipitated at 25° C. (1st cycle).
B. „ „ 100° C. (1st cycle).

Similarly, gels precipitated from water glass at 25° C., and 100° C. (with previous boiling of the water glass solution under reflux) have shown permanent hysteresis loops (Figs. 6 and 7). These loops have been studied up to the eleventh cycle of sorption and desorption.

Sorption studies with gels of titania and alumina precipitated at 25° C. and 100° C. have also shown permanent hysteresis loops (Figs. 9 and 10). In none of the systems studied above, is complete elimination of the hysteresis loop noticeable. Though in their paper, Weiser and collaborators conclude, that aging the sol, at the boiling point before coagulation to gel, even eliminates the sorption-desorption hysteresis with water, a careful scrutiny of the hysteresis loops obtained by them (with gels of hydrous oxides of silica

from water glass,[26] silica from metasilicate,[26] tantalum pentoxide,[27] stannic oxide[27] and titanium dioxide[27] reveals that in none of these systems is there a complete elimination of the hysteresis loop.

The only system in which a complete elimination of the hysteresis effect is reported by Weiser and collaborators is with silica gel prepared from metasilicate at 100° C. with previous boiling of the silicate solution for 3 hours. But in this case, only one cycle of sorption and desorption seems to have been studied and even in this instance, there is a small loop and this apparently has not been noticed by the authors.

There is therefore no adequate experimental evidence supporting the view that there can be a complete elimination of the hysteresis effect. In the light of the cavity concept, a complete elimination of the hysteresis effect is in fact, improbable in a rigid porous adsorbent. It may be pointed out that though Weiser and co-workers have obtained gels with very small hysteresis loops, the gels show no marked diminution in sorptive capacity. Decrease in the hysteresis effect must in our opinion, be accompanied by a corresponding reduction in sorptive capacity. It is only in systems of elastic gels with solvating liquids like rice-water,[12, 13] dhal-water,[12] gum arabic-water,[14] gelatin-water,[22] casein-water,[22] and egg albumin-water[22] that complete elimination or disappearance of the hysteresis loop, without a diminution in the sorptive capacity is possible. In a rigid porous gel however, hysteresis in sorption is a rule rather than an exception. If in a rigid gel there is a rule rather than an exception. If in a rigid gel there is complete elimination of the hysteresis effect, the total sorptive capacity being unaffected, it is a case of the absence of superheating[19] of liquid in cavities and no such instance is known of the elimination of superheating by altering the mode of preparation of the gel.

In the several systems studied, it is noticed that with an increase in the temperature of precipitation of the silicic acid, there are changes in the total sorptive capacity, the size, shape and position of the hysteresis loops. But there is no strict correlation between these changes and the temperature of precipitation.

The gels of the hydrous oxides of silica from water glass (Fig. 8), silica from sodium metasilicate (Fig. 5), titania (Fig. 9) and alumina (Fig. 10) precipitated at 100° C., sorb less water (particularly at pressures below saturation) than the corresponding gels precipitated at 25° C. Sorption and desorption curves obtained by Weiser and co-workers for gels of silica from water glass,[26] silica from sodium metasilicate,[26] stannic oxide[27] and titania[27] indicate a similar decrease in sorptive capacity by raising the temperature

of precipitation from 0° C. to 100° C. Tantalum pentoxide[27] however, is an exception and shows an increase in the amount of water sorbed by raising the temperature of precipitation from 0° C. to 100° C. Barring this exceptional behaviour of tantalum pentoxide, the temperature of precipitation has a noticeable effect on the capillary space in the precipitated gels. A rise in the temperature of precipitation affects the nature and the extent of the capillary space. Thus the sorptive capacity of the gels generally decreases with an increase in the temperature of precipitation. In a few cases however, though the sorptive capacity at lower relative vapour pressures has decreased, the sorptive capacity of gel at saturation pressure has actually increased. This indicates that wider capillaries have been formed in the gel at higher temperatures of precipitation.

In addition to lowering the sorptive capacity of gels, the temperature of precipitation has a marked influence in several cases, on the size, shape and position of the hysteresis loop. The loop of silica gel precipitated from metasilicate at 100° C. with previous boiling differs markedly in shape from that of gel precipitated at 25° C. (Fig. 5). The hysteresis loop of the gel heated in water to 120° C. differs in the same way from that of the gel at 25°C. With gel boiled in water for 96 hours, there is a similar change in the shape of the hysteresis loop and the change is very prominent. The positions of the hysteresis loops of the gels indicate, that the cavities in gel precipitated at 25° C. are concentrated in a fairly narrow range of capillary radius, whereas those of other gels are distributed over a wide range (Fig. 5). The hysteresis loop of silica gel precipitated from water glass at 100° C., though slightly bigger, is practically of the same shape as that of gel precipitated at 25° C. (Fig. 8). With titania and alumina the loops of gels precipitated at 100° C. are nearly the same in shape and size as those of gels precipitated at 25° C. (Figs. 9, 10).

With reference to the hysteresis loops obtained by Weiser and collaborators, it may be pointed out that the hysteresis loops of silica gels precipitated at 0° C., 25° C. and 60° C. from water glass are practically of the same size but that of the gel precipitated at 100° C. is negligibly small.[26] Gel precipitated at 25° C. from metasilicate shows a slightly bigger hysteresis loop than gel precipitated at 0° C. and the loop becomes smaller for gel formed at 100° C.[26] Tantalum pentoxide shows a slight decrease in the area of the hysteresis loop as the temperature of precipitation of the gel rises from 0° C. to 100° C.[27] Titanium dioxide gel also shows a similar change.[27] Stannic oxide gel however, forms an exception.[27] The loop of stannic oxide gel precipitated at 100° C. is nearly the same as, or slightly bigger than that

of gel precipitated at 0° C. The positions of the loops are markedly different and indicate that the cavities in the gel precipitated at 100° C. are wider than those in the gel precipitated at 0° C.

It may be pointed out, that there is no strict correlation between the temperature of precipitation of the gel and the size, shape and position of the hysteresis loop. In most of the systems studied, there is however, a general tendency for the area of the hysteresis loop to diminish with an increase in the temperature of precipitation of the gel, indicating a corresponding diminution in the total cavity volume.

In conclusion, it may be stated that there is no evidence of any complete elimination of the hysteresis loop. Higher temperature of precipitation renders a hydrous oxide gel less porous and there is a corresponding diminution in the number of cavities which are responsible for the hysteresis phenomenon.

Summary

The effect of variation of the temperature of precipitation of gels of hydrous oxides of silica, titania and alumina on the hysteresis effect in the sorption of water vapour has been studied at 30° C. Gels have been obtained by precipitating the hydrous oxides at 25° C. and 100° C. with previous boiling of the silicate solution.

In all the systems studied, permanent hysteresis loops have been obtained. With increase in the temperature of precipitation, there has been a diminution in the sorptive capacity of gels for water at different partial pressures and in most of the systems the hysteresis loop suffers a diminution in size with a change in the shape and position of the loop. But in none of these systems, is any complete elimination of the loop noticeable. Gels precipitated at 100° C. are less porous than the gels precipitated at 25° C. and appear to have fewer cavities that are responsible for the phenomenon of hysteresis.

References

1. Allmand, Hand and Manning .. *J. Phys. Chem.*, 1929, **33**, 1694.
2. ——— and Chaplin .. *Proc. Roy. Soc.* (Lond.), 1930, **A 129**, 264.
3. Anderson, J. S. .. *Z. Physik. Chem.*, 1914, **88**, 264.
4. Coolidge .. *J. Amer. Chem. Soc.*, 1927, **49**, 708.
5. Lambert and Foster .. *Proc. Roy. Soc.* (Lond.), 1932, **A 136**, 363.
6. McBain .. *J. Amer. Chem. Soc.*, 1935, **57**, 699.
7. ——— and Ferguson .. *J. Phys. Chem.*, 1927, **31**, 564.
8. McGavack and Patrick .. *J. Amer. Chem. Soc.*, 1920, **42**, 946
9. Rao, K. S. .. *J. Phys. Chem.*, 1941, **45**, 500.
10. ——————— .. *Ibid.*, 1941, **45**, 522.

11.	Rao, K. S.	..	*Curr. Sci.*, 1939, **8**, 546.
12.	———	..	*J. Phys. Chem.*, 1941, **45**, 531.
13.	———	..	*Curr. Sci.*, 1939, **8**, 256.
14.	———	..	*Ibid.*, 1940, **9**, 19.
15.	———	..	*Ibid.*, 1939, **8**, 468.
16.	———	..	*Proc. Ind. Acad. Sci.*, 1942, **6**, 298.
17.	———	..	*Ibid.*, 1942, **6**, 302.
18.	———	..	*J. Mys. Uni.*, 1943, **4**, 1.
19.	———	..	*Curr. Sci.*, 1940, **9**, 68.
20.	Sheppard and Newsome	..	*J. Phys. Chem.*, 1929, **33**, 1817.
21.	Shiels	..	*Ibid.*, 1929, **33**, 1167.
22.	Subba Rao, G. N., Rao, K. S., and Rao, B. S.	..	Hysteresis in Sorption XV, *Proc. Ind. Acad. Sci.*, 1947, **25**, 190.
23.	Taylor, H. S.	..	*A Treatise on Physical Chemistry*, Macmillan & Co., London, 1931, **2**, 1661.
24.	Urquhart	..	*J. Textile Inst.*, 1929, **20 T**, 125.
25.	Van Bemmelan	..	*Die Absorption. Theodor, Stainkopff, Dresden*, 1910.
26.	Weiser, Milligan and Holes	..	*J. Phys. Chem.*, 1942, **46**, 586.
27.	——— and Simpson	..	*Ibid*, 1942, **46**, 1051.
28.	Winnings and Williams	..	*Ibid.*, 1931, **35**, 2915.
29.	Zsigmondy	..	*Z. Anorg. Chem.*, 1911, **71**, 356.

HYSTERESIS IN SORPTION

XII. Influence of the Temperature of Activation of Silica Gel on the Hysteresis Effect

By T. Krishnappa,* K. Subba Rao‡ and B. Sanjiva Rao,§ F.A.Sc.
(Department of Chemistry, Central College, Bangalore, S. India)

Received January 6, 1947

Introduction

It has been shown in a previous paper[3] that the porosity of gels of hydrous oxides depends upon the mode of preparation of the gel. Gels are activated by heating them to a suitable temperature in a current of dry air. The effect of the temperature of activation of silica gel on the hysteresis phenomenon was studied using water vapour as adsorbate.

Experimental

Silica gel.—Silica gel was precipitated at 25° C. from water glass by adding acetic acid as described in the previous paper.[3]

Activation of the gel.—The gel precipitated at 25° C. and air dried was activated by heating to different temperatures in a current of dry air. The following activation temperatures were employed, 35° C., 70° C., 140° C., 300° C., 500° C., 750° C. and 1000° C. A hot water-bath was employed for activation at 35° C. and 70° C. and an electric furnace was used to obtain the other temperatures. A mercury thermometer was used in measurement of temperatures up to 500° C. and a thermo-couple was used for higher temperatures.

Sorption and desorption of water vapour.—Sorption and desorption measurements were carried out by employing the quartz fibre spring technique.[1, 2] Equilibrium was attained within 4 hours but 6 hours where actually allowed before each measurement. For the completion of each cycle of sorption and desorption, 6 to 7 days were required. At the end of each cycle the gel was found to retain some water. This bound water in each case is given in Table I.

Discussion

All the gels activated at different temperatures, gave permanent and reproducible hysteresis loops (Figs. 1 to 7). When the temperature of

* Mysore Government Scholar, University of Sheffield, Sheffield.
‡ Senior Research Fellow of the National Institute of Sciences of India.
§ Principal and Professor of Chemistry, Central College.

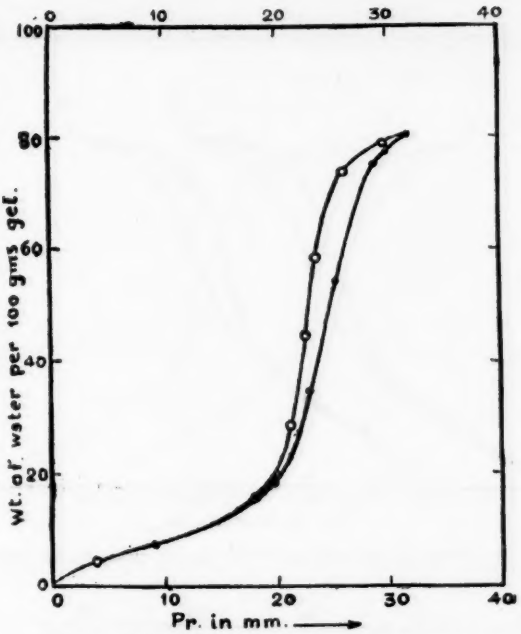

FIG. 1. Silica gel activated at 35° C. (3rd cycle)

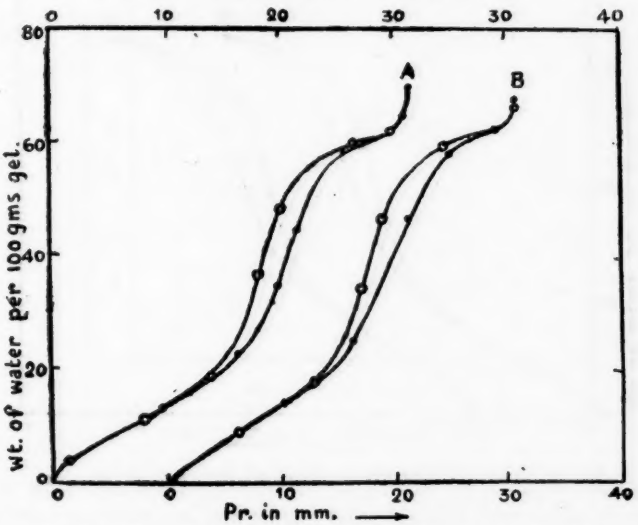

FIG. 2. Silica gel activated at 70° C. (A 2nd cycle, B 3rd cycle)

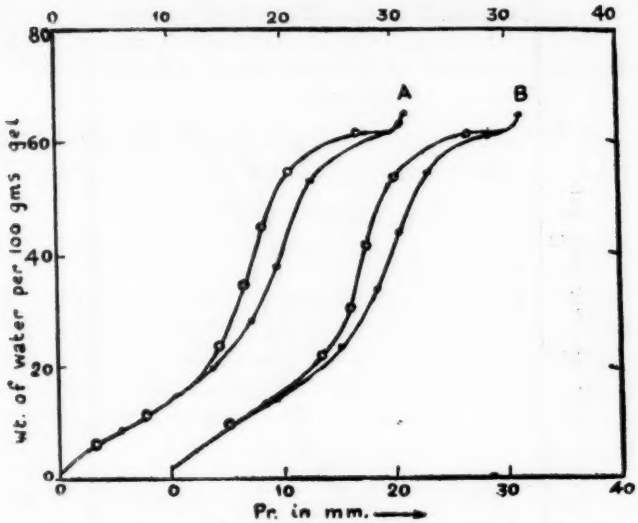

FIG. 3. Silica gel activated at 140° C. (A 1st cycle, B 2nd cycle)

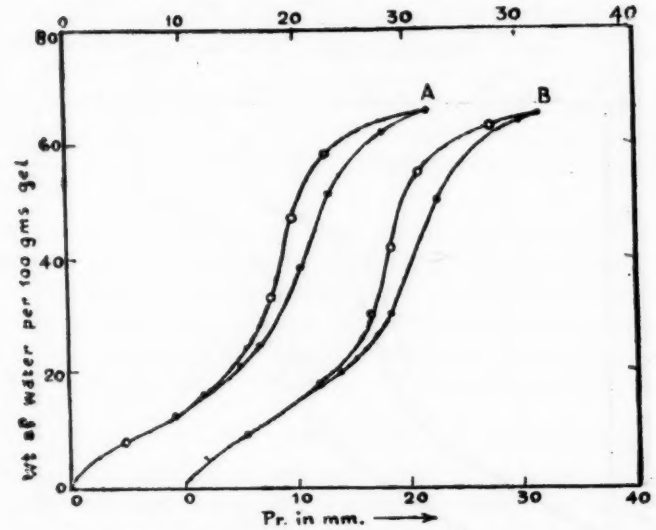

FIG. 4. Silica gel activated at 300° C. (A 2nd cycle, B 3rd cycle)

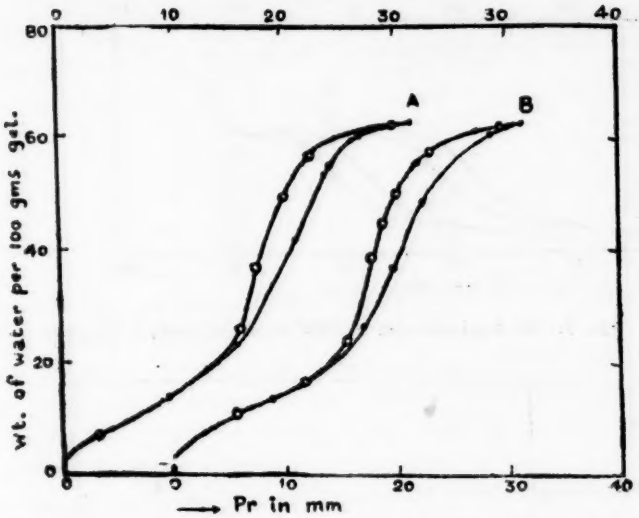

FIG. 5. Silica gel activated at 500° C. (A 3rd cycle, B 5th cycle)

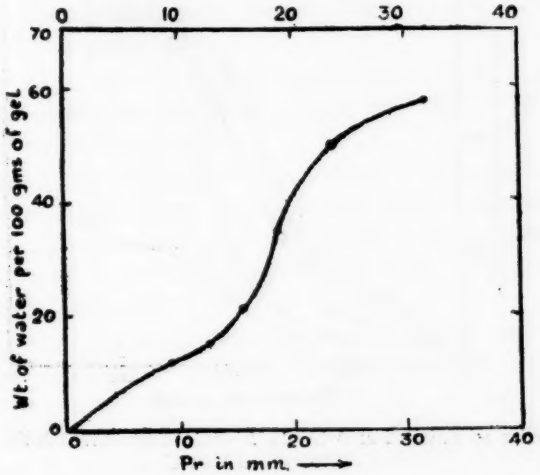

FIG. 6. Silica gel activated at 750° C.

activation of the gel is raised from 35° C. to 140° C., there is a decrease in the total sorptive capacity of the gel for water at the saturation pressure, indicating a corresponding decrease in the total capillary volume (Fig. 8). There

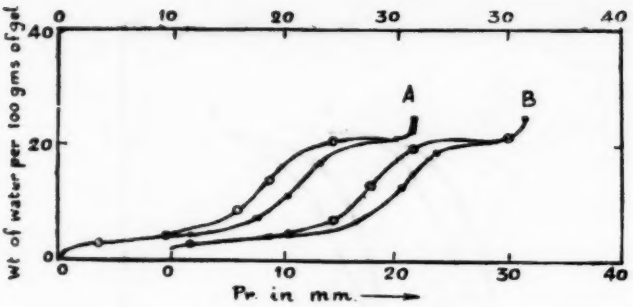

FIG. 7. Silica gel activated at 1000° C. (A 3rd cycle, B 4th cycle)

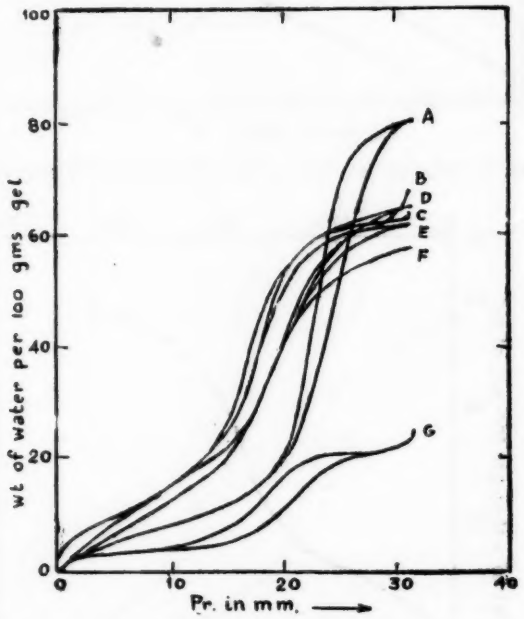

FIG. 8. Silica gel activated at A 35° C., B 70° C., C 140° C., D 300° C., E 500° C. F 750° C., G 1000° C.

is also a small decrease in the area of the loop which indicates a corresponding decrease in the total cavity volume of the gel.

From 140° C. to 500° C., the total sorptive capacities of the gels remain practically the same and the hysteresis loops are nearly coincident. These

TABLE I

Activation temperature	Bound water per 100 gm. of gel	Residual water per 100 gm. of gel	Sorptive capacity for water at saturation pressure per 100 gm. of gel
°C.			
35	0·05	..	84·2
70	0·93	6·90	68·1
140	0·90	6·13	63·1
300	0·93	6·87	63·8
500	2·23	6·56	63·0
750	2·97	..	58·2
1000	1·90	0·09	23·6

facts indicate that the total capillary volume and also the cavity volume in each gel remain practically unaltered.

Above 500° C., a rise in the temperature of activation has a marked influence. There is a decrease in the sorptive capacity and the area of the loop indicating a decrease in the total capillary volume and in the cavity space.

The above interesting changes lead to the following conclusions. Rise in the temperature of activation from 35° C. to 140° C. brings about a contraction of the gel and collapse of some of the capillaries resulting in a diminution of the total capillary volume. There is also a small decrease in the residual water of the gel.

From 140° C. to 500° C., the residual water in the gel is practically the same. The gel suffers no structural change as indicated by the unaltered character of the hysteresis loops.

Above 500° C., an increase in the activation temperature has a profound influence on the gel structure. The residual water is lost, the gel shrinks and there is a marked collapse of the capillaries. The total capillary volume in the gel activated at 1000° C. decreases nearly to a third of the capillary volume of the gel activated at 500° C.

For producing the maximum capillary volume in silica gel, a high temperature of activation is harmful. In this connection it may be pointed out that by measuring the sorptive capacity for carbon tetrachloride at saturation pressure, employing the dynamic method of measurement of sorption, Rao, K. S., and Rao, B. S.[4] have reported that for gels of alumina and ferric oxide, there is an optimum temperature of activation.

SUMMARY

The effect of the activation temperature of silica gel on the hysteresis effect has been studied. Sorption and desorption of water vapour at 30° C.

have been conducted on gels activated at 35° C., 70° C., 140° C., 300° C., 500° C. and 1000° C.

All the gels gave permanent and reproducible hysteresis loops. A marked variation however, was noticed in the total sorptive capacity and the area of the loop.

The results indicate that from 35° C. to 140° C., there is a decrease in the capillary space in the gel but from 140° C. to 500° C., the capillary space remains practically unaltered. Whereas, above 500° C., the gel suffers structural change, the capillaries collapse and there is a marked decrease in the total capillary volume.

References

1. McBain .. *J. Amer. Chem.*, 1935, **57**, 699.
2. Rao, K. S. .. *J. Phys. Chem.*, 1941, **45**, 500–31.
3. ———— .. "Hysteresis in Sorption —XI", *Proc. Ind. Acad. Sci.*, 1947, **25**, 162.
4. ——— and Rao, B. S. .. *Proc. Ind. Acad. Sci.*, 1936, **4**, 562.

HYSTERESIS IN SORPTION

XIII. Mode of Preparation of Silica Gel and Its Influence on Hysteresis

By T. Krishnappa,* K. Subba Rao‡ and B. Sanjiva Rao,§ F.A.Sc.
(*Department of Chemistry, Central College, Bangalore, S. India*)

Received January 6, 1947

Introduction

A survey of the literature on sorption indicates that the sorptive capacity of an adsorbent is greatly influenced by the method of its preparation. Silica gel whose sorptive capacity has been extensively studied can be prepared in several ways. Glassy silica gel[3] is prepared by allowing to set to a jelly, a silicic acid sol obtained by the interaction of sodium silicate and hydrochloric acid. Chalky silica gel has been obtained by Holmes, Sullivan and Metcalf[1] by precipitating the gel from a solution of sodium silicate by ferric chloride solution. "Wet heat treatment"[1] has been found to lessen the shrinkage of the gel on drying and has yielded a product of greater porosity. Bartell and Fu[2] have obtained a sample of chalky gel by adding a saturated solution of nickel nitrate to a mixture of sodium silicate and hydrochloric acid before the latter sets to a jelly.

In a study of the hysteresis effect in sorption, Rao, K. S. has found that gels obtained by precipitation (titania,[4] alumina,[5] and ferric oxide[6]) gave hysteresis loops markedly different from that of glassy silica gel[7] prepared from silicic acid jelly. The mode of preparation of an adsorbent therefore, seems to influence the hysteresis by its effect on the size and shape of cavities. To confirm this view, hysteresis was studied with silica gels prepared by different methods.

Experimental

Preparation of silica gel by precipitation

Silica gel A (transparent variety).—0·3 litre of 0·5 N sodium silicate solution was slowly dropped into 3 litres of 0·5 N ammonium chloride solution, the latter being mechanically stirred vigorously. A gelatinous precipitate was slowly formed. The precipitate was filtered over a cloth filter and washed free of chloride. The precipitate was next dried in an

* Mysore Government Scholar, University of Sheffield, Sheffield.
‡ Senior Research Fellow of the National Institute of Sciences of India.
§ Principal and Professor of Chemistry, Central College.

electric oven at 120° C. for about 24 hours. The resulting product was hard, transparent and glassy.

Silica gel B (opaque variety).—Ten volumes of 0·8 N ammonium chloride were mixed with one volume of 0·8 N sodium silicate in the way already indicated. A gelatinous precipitate was quickly formed. This was filtered, washed and dried as above. The dried gel was hard and opaque.

Activation of gels

The gels were activated by heating to 450° C., in a current of dry air for 4 hours in an electric furnace.

Residual water in gels

The residual water in the activated gel was determined by igniting to constant weight over a Fisher burner, a known weight of the gel in a platinum crucible. Gel A contained 5·2% residual water and gel B contained 5·57%.

Sorption and desorption

A series of sorptions and desorptions of water vapour at 30° C. on the gels was conducted. The time required for completing three cycles of sorptions and desorptions with silica gel A was 3 months and for 4 cycles with gel B was 4 months. At the end of the first desorption, the amounts of water held irreversibly in gels A and B were 1·9% and 3·5% respectively. At saturation pressure, gel A took 85·8 gm. of water per 100 gm. of activated gel, whereas gel B took 131·4 gm. The results obtained are graphically represented in Figs. 1 and 2. The hysteresis loops of the two samples of

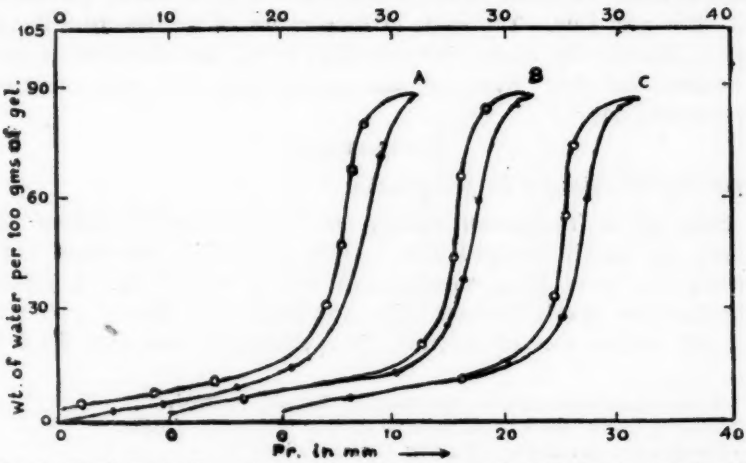

FIG. 1. Precipitated silica gel (Glassy)—water (A 1st cycle, B 2nd cycle, C 3rd cycle)

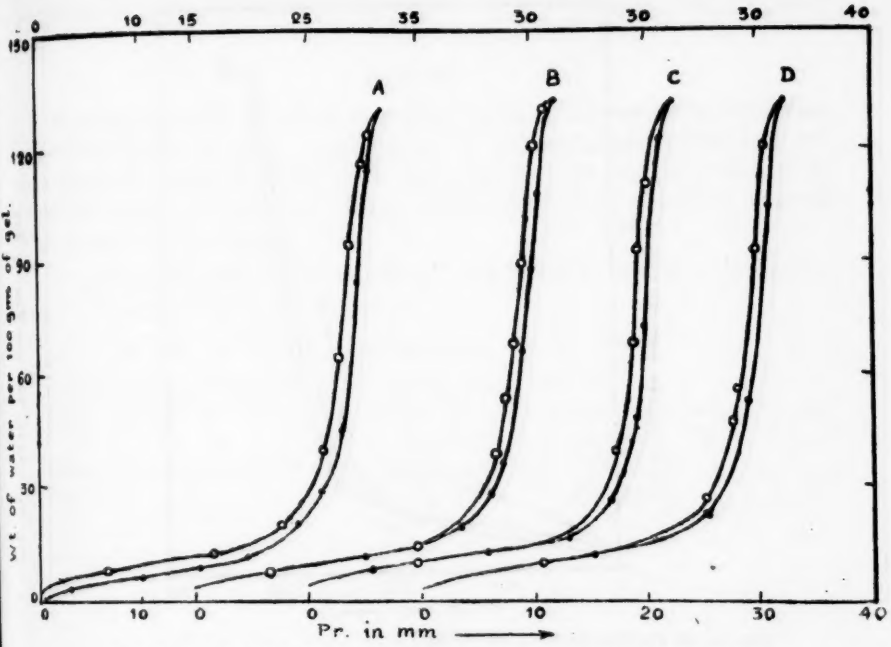

FIG. 2. Precipitated silica gel (Opaque)—water (A 1st cycle, B 2nd cycle, C 4th cycle, D 5th cycle)

precipitated gels A and B together with the hysteresis loop (reproduced from Rao, K. S., *J. Phys. Chem.*, 1941, **45**, 513) of glassy silica gel obtained from silica jelly are shown in Fig. 3.

DISCUSSION

The two samples of precipitated silica gel have shown a permanent and reproducible hysteresis effect for water vapour. At low relative humidities, the two gels take up water to about the same extent. At saturation pressure, however, there is a marked difference in the sorptive capacities of the two gels. Gel A takes 85·8 gm. of water per 100 gm., whereas gel B takes 131·4 gm. In both cases, for high values of humidity the sorption and desorption curves rise steeply and are almost perpendicular to the pressure axis. This indicates that the major part of the capillary volume in both the gels is concentrated in a narrow region of capillary radius.

A study of Fig. 3 reveals that in gel B the cavities and their necks are wider than those in gel A. The loops of the two samples of precipitated

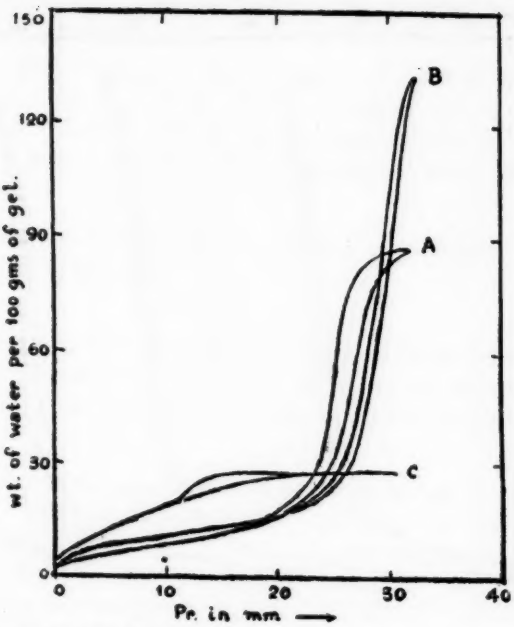

FIG. 3. A Precipitated silica gel (Glassy)
B " " (Opaque)
C Set silica gel glassy (Reproduced from Rao, K. S. *Jour. Phys. Chem.*, 513, 45, 1941)

silica gels A and B are similar in shape to those of gels of titania, alumina and ferric oxide (*loc. cit.*) which were obtained by precipitation.

The hysteresis loop of silica gel C obtained from silicic acid jelly presented in a previous paper[7] is reproduced in Fig. 3 for comparison. Up to 60% humidity this gel retains more water than the precipitated gels. But beyond this value, its capacity for water remains practically the same, while the precipitated gels show a marked increase in sorptive capacity at higher pressures. At the saturation pressure, the adsorbent C got from the jelly retains only 28% water, whereas the precipitated gel B retains 131·4% water. The shapes of the hysteresis loops given by the two gels are quite different. At about 60% humidity, the hysteresis loop of gel C terminates, while those of the precipitated gels just commence. The relative positions of the loops indicate that in gel C the cavities and their necks are very much smaller than those in the precipitated gels. The foregoing results indicate prominently how the mode of preparation of the adsorbent has a profound influence

on the nature of the capillaries as revealed by the form of the hysteresis loop.

Summary

By employing the quartz fibre spring technique, the hysteresis in sorption has been studied, of water vapour at 30° C. on precipitated silicic acid gel. A comparative study has been made with regard to the shape and size of the hysteresis loops of precipitated silica gel with that of the adsorbent obtained from silicic jelly.

The mode of preparation of the gel was found to greatly influence the shape and size of the hysteresis loop.

References

1. Holmes, Sullivan and Metcalf .. *Ind. Eng. Chem.*, 1925, **17**, 280.
2. Bartell and Fu .. *Colloid Symposium Annual.* Edited by H. B. Weiser, John Wiley and Sons, 1930, 7, 135.
3. McGavack and Patrick .. *J. Amer. Chem. Soc.*, 1920, **42**, 946.
4. Rao, K. S. .. *J. Phys. Chem.*, 1941, **45**, 500.
5. ——— .. *Current Science*, 1940, **9**, 68.
6. ——— .. *J. Phys. Chem.*, 1941, **45**, 522.
7. ——— .. *Ibid.*, 1941, **45**, 513.

HYSTERESIS IN SORPTION

XIV. Influence of the Temperature of Activation of Titania Gel on the Hysteresis Effect

By R. S. Subramanya,* K. Subba Rao‡ and B. Sanjiva Rao,§ F.A.Sc.
(*Department of Chemistry, Central College, Bangalore, S. India*)

Received January 6, 1947

Introduction

The influence of the temperature of activation of silica gel on the hysteresis effect in the sorption of water has been indicated in a previous paper.[1] With progressive increase in the temperature of activation, the gel exhibited changes in capillary volume over certain ranges of temperature. A similar study of the effect of activation temperature of titania gel on the hysteresis effect exhibited by the gel in regard to sorption of water, is presented in this paper.

Experimental

Preparation of titania gel

The gel was prepared by the method described in an earlier paper.[1]

Activation of titania gel

The gel was activated by heating it in a current of dry air at the following temperatures, 30° C., 97° C., 214° C., 400° C., 600° C., and 1,000° C. For heating the gel at 30° C. and 97° C., a water-bath was used. For activation at higher temperatures an electric furnace was employed. Temperatures above 400° C. were measured with a suitable thermocouple.

Sorption and desorption of water vapour on the activated gel

The quartz fibre spring technique[2] was employed in the investigations. The activated gel was introduced into the glass bucket attached to the spring and was degassed at 10^{-3} mm. pressure for five hours. Sorption and desorption of water vapour on the activated gel were studied at 30° C. The results are shown in Fig. 1. The hysteresis loop obtained in the second cycle of sorption and desorption in each case has been indicated.

---

* Lecturer in Chemistry, intermediate College, Mysore.
‡ Senior Research Fellow of the National Institute of Sciences of India.
§ Principal and Professor of Chemistry, Central College.

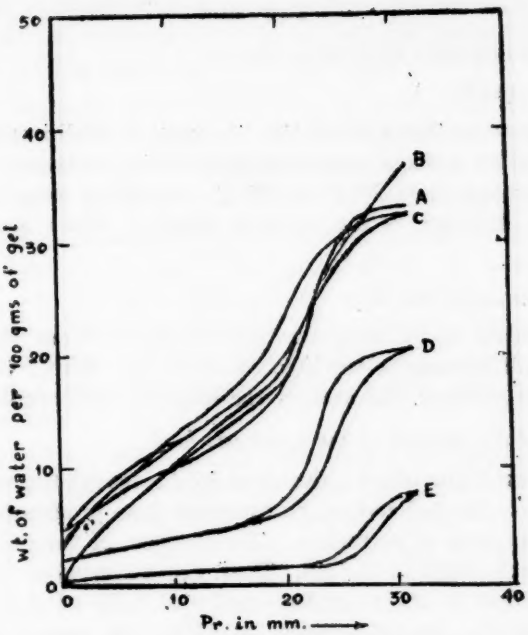

FIG. 1. Sorption of water on titania gel activated at A 30° C., B 97° C., C 214° C., D 400° C, E 600° C.

At the end of the first desorption in each gel, some amount of the water was retained by the gel irreversibly. This bound water has been indicated in Table I. The residual water in the activated gel was determined by igniting to constant weight in a platinum crucible, a known weight of the gel. The residual water thus determined in each activated gel and also the sorptive capacity as determined by the total amount of water taken at saturation pressure have been indicated in Table I.

TABLE I

Activation temperature in °C.	Bound water per 100 gms. of activated gel	Residual water per 100 gms. of activated gel	Sorptive capacity at saturation pressure per 100 gms. of cultivated gel
30	..	15·1	33·16
97	3·6	14·6	36·90
214	3·3	11·6	32·90
400	1·5	7·3	20·50
600	0·5	1·6	8·00
1000	0·0	0·0	0·00

Discussion

The following facts are noteworthy:—

1. *Sorptive capacity*

Examination of Table I and Fig. 1 reveals a small increase in sorptive capacity of gel for water at saturation pressure by an increase in the temperature of activation from 30° C. to 97° C. At higher temperatures there is a progressive decrease in the sorptive capacity which drops to zero at 1000° C.

2. *Area of the hysteresis loop*

With increase in the temperature of activation from 30° C. to 97° C., there is a small increase in the area of the loop. With a further increase in temperature however, the area of the loop becomes smaller.

3. *Position of the tail-end of the hysteresis loop*

With the exception of gel activated at 30° C., the relative vapour pressure corresponding to the tail end of the hysteresis loop progressively increases with the temperature of activation. The position of the tail end indicates the smallest neck radius in the gel. Thus, gels activated at 214° C., 400° C. and 600° C, have in them smallest necks of radii of 4 Å, 14·5 Å and 29·5 Å respectively. In gel activated at 97° C., the loop starts from zero relative vapour pressure and this indicates that the necks of cavities in this gel are extremely small and are of molecular dimension.

4. *Bound water and residual water*

The percentage of bound water and of residual water progressively decreases with an increase in the activation temperature.

The foregoing observations lead to the following conclusions:—

The decrease in sorptive capacity of the gel for water vapour at saturation pressure indicates a decrease in total capillary volume. With an increase in the temperature of activation from 30° C. to 97° C., the total capillary space in the gel slightly increases. Above 97° C., it progressively diminishes and at 1000° C., the capillary space is completely lost.

That the hysteresis effect is due to cavities with constricted ends has already been established.[2] The area of the hysteresis loop being a measure of the total cavity volume, the relative magnitudes of the loops indicate that the total cavity volume is higher in gel activated at 97° C. than in gel activated at 30° C. Above 97° C., the loop progressively diminishes in size indicating a diminution in total cavity volume.

Barring gel activated at 30° C., the smallest neck radius in the different gels increases in the temperature of activation, *i.e.*, as the temperature is increased, the smallest cavity necks are destroyed.

The bound water is attributed to the finest crevices in the activated gel retaining a portion of sorbed water irreversibly. The decrease in bound water with an increase in the temperature of activation (Table I) indicates that fine crevices of molecuclar dimensions are decreasing.

It follows from these observations that an increase in the temperature of activation from 30° C. to 97° C. brings about an increase in total capillary space and in total cavity volume. Above 97° C., the gel suffers structural change. There is progressive decrease in the total capillary space and in the total cavity volume. The smallest cavity necks collapse. At 1000° C., there is entire breakdown of the structure with complete loss of the capillary space.

It is obvious from these results that there is an optimum temperature of activation (presumably between 97° C. and 214° C.) in the case of titania for getting gel of maximum sorptive capacity. Existence of an optimum temperature of activation has been reported for gels of silica, alumina and ferric oxide.[3]

Summary

The effect of variation of activation temperature on the hysteresis effect has been studied for titania gel. Sorption and desorption of water vapour at 30° C. on titania gels activated at 30° C., 97° C., 214° C., 400° C., 600° C. and 1000° C. have been measured.

At different temperatures of activation, permanent and reproducible hysteresis loops have been obtained. There is however, a marked variation in the total sorptive capacity, the area of the hysteresis loops and the relative vapour pressures corresponding to the tail end of the hysteresis loops.

The results indicate that with an increase in the temperature of activation from 30° C. to 97° C., there is a small increase in the total capillary space and in the total cavity volume. Above 97° C., the gel suffers a structural change with a diminution in capillary space and in cavity volume. There is also a collapse of the smaller cavity necks. At 1000° C., there is a breakdown of the gel structure and a complete collapse of the capillary space.

References

1. Krishnappa, T., Rao, K. S., and Rao, B. S. .. "Hysteresis in Sorption—XII," *Proc. Ind. Acad. Sci.*, 1947, **25**, 174.
2. Rao, K. S. .. *J. Phys. Chem.*, 1941, **45**, 500.
3. —— and Rao, B. S. .. *Proc. Ind. Acad. Sci.*, 1936, **4**, 562.

VERY HIGH FREQUENCY SOUND VELOCITIES IN ACETONE WATER MIXTURES

By B. Ramachandra Rao

(*From the Department of Physics, Andhra University, Waltair*)

Received October 18, 1946

(Communicated by Prof. S. Bhagavantam, F.A.SC.)

1. Introduction

In a communication to *Nature*[1] it has just been reported that very high frequency sound waves (up to 100 Mc. per sec.) have been communicated to water and the diffraction pattern obtained in this laboratory by the usual arrangement. In the present investigation, the variation of sound velocity at such high frequencies with composition in the binary mixtures of acetone and water has been studied. Parthasarathy,[2] and Smith and Ewing[3] have done some work in this direction. Parthasarathy studied mixtures of non-electrolytes among themselves and concluded that the sound velocity varies almost linearly with concentration. Smith and Ewing on the other hand reported that in mixtures of acetic acid and water the sound velocity attains a maximum at 30% concentration and then decreases rapidly. Acetone and water are taken in the present investigation as both have a low absorption coefficient enabling high frequency waves to be communicated into the mixtures. Further, acetone is one of the few non-electrolytes which dissolve completely in water and enable sound velocities at all concentrations to be determined.

2. Experimental Details

A very high frequency and high power oscillator is constructed using a Taylor T55 valve which works with its maximum output of 60 watts even up to 120 Mc. A specially built power pack gives the plate supply of 1100 volts. Amphenol parts are used for all the mountings and R. F. chokes to avoid dielectric losses. A flat copper strip is used as the inductance of the tank circuit and the ends of the strip are incorporated in the condenser assembly thus reducing the contact resistance. Improved stability and efficiency of the oscillator are thus achieved. Also a specially designed holder made with amphenol parts is used for mounting the crystal. A tourmaline crystal prepared in this laboratory with a thickness of 5·2 mm. and of a fundamental of about 0·72 Mc. per sec. is made to oscillate up to its 90th harmonic. Stationary waves are set up in a column of the liquid mixture to be studied and the Debye Sears pattern is used in the usual manner for determining the velocity of sound waves. It is found that the temperature

of the liquids exposed to these high frequency sound waves increases considerably in a very short time. Hence fringe widths are measured with a good travelling microscope in as short a time as possible to avoid temperature variations. Much heat is liberated when acetone and water are mixed together and hence the mixture is cooled down to the laboratory temperature before observations are taken. All observations are made at the same temperature avoiding changes in sound velocity due to temperature variation. Also for each mixture, the density is determined by the usual laboratory methods. The frequency of the oscillator is maintained constant throughout and is measured by beating it with a standard Phillips heterodyne wavemeter using an audio amplifier for hearing the beat note. Mixtures of definite composition are obtained by mixing known volumes of water and acetone, and from these values the weight percentages of acetone in water are calculated.

3. Results

Table I gives the velocities in mixtures of acetone and water together with percentages by weight of acetone. Density values experimentally determined and the adiabatic compressibilities calculated therefrom are also given. In Fig. 1 are given the curves for the variation of sound velocity,

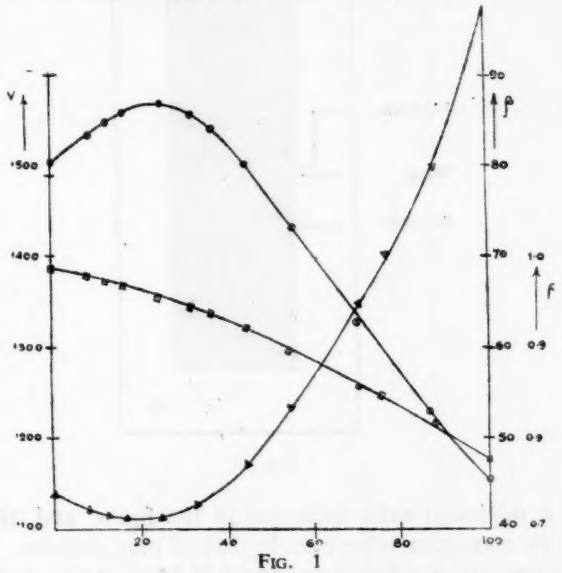

Fig. 1

I. ○ Sound Velocity in Metres/Sec. ——→ Percentage of Acetone by weight.
II. △ Adiabatic Compressibility in Cm.²/Dyne.
III. □ Density in Gm./cc.

density and adiabatic compressibility with concentration of acetone. The sound velocity in water is found to increase first with addition of acetone gradually until it reaches a maximum value of 1583 meters/sec. at a concentration of 24% by weight of acetone and then it is found to decrease rapidly with further increase of concentration of acetone. The density variation curve on the other hand shows slight concavity towards the concentration axis. The adiabatic compressibility however attains a minimum at a concentration of 22% by weight of acetone. In order to show this peculiar feature of the variation of the sound velocity of the mixture, the diffraction patterns due to pure water, pure acetone and the particular mixture giving maximum velocity are photographed on the same plate and shown in Fig. 2. As acetone is added to water the fringe width is found to

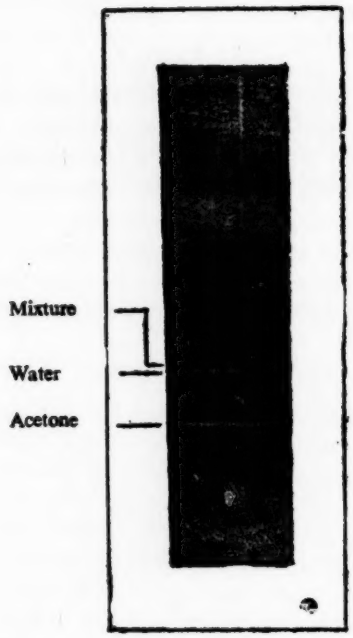

FIG. 2

decrease to a minimum value indicated in the figure and then it rapidly increases to its maximum value namely that of pure acetone. All the velocities are determined at a frequency of 64·36 Mc. per sec. in this investigation, the temperature being 30·6° C.

TABLE I. *Acetone-water mixture*

Composition % by weight of acetone	0	8·16	12·37	16·66	25·53	31·97	36·67	44·37	54·55	70·58	76·19	87·80	100
Fringe widths in cms.	2·502	2·450	2·426	2·414	2·400	2·418	2·440	2·502	2·631	2·850	2·931	3·084	3·284
Ultrasonic velocities in meters per sec.	1517	1547	1563	1571	1581	1569	1554	1517	1440	1331	1294	1229	1154
Densities ..	·9951	·9841	·9803	·9715	·9612	·9508	·9421	·9218	·9008	·8612	·8493	·8167	·7761
Adiabatic compressibilities in $cm.^2$/dyne $\times 10^{12}$	43·69	42·46	41·78	41·71	41·61	42·73	43·96	47·13	53·53	65·54	70·30	80·04	96·74

4. Discussion of Results

The variations of sound velocity observed in mixtures of acetone and water by the author are analogous to the variations in viscosity and heats of solution in the same mixture. It is found from the values given in the International Critical Tables that viscosity and heats of solution of the mixtures exhibit a similar maximum at a concentration of about 30% by weight of acetone. Sambasiva Rao[4] studied the influence of acetone on the intensities of the Raman bands of water and concluded that the variations are of the same order as that of weak and strong electrolytes. But acetone being a non-electrolyte cannot dissociate into free ions. That there is no appreciable hydrate formation in aqueous solutions of non-electrolytes has been shown by Jones and his collaborators.[5] By assuming that acetone changes the water equilibrium due to variations in the proportions of single (H_2O), double $(H_2O)_2$ and triple $(H_2O)_3$ molecules, a possible explanation may be given. Acetone dissolved in water probably splits up the triple molecule $(H_2O)_3$ into single or double molecules such that the consequent increase in velocity of water is higher than the decrease due to the presence of acetone and hence there will be an increase in velocity of sound waves in the mixture for the first few concentrations. When most of the polymerized molecules are dissociated so that no more dissociation can take place, the velocity falls down rapidly as more and more of acetone is added. Only acetone among all non-electrolytes gives rise to such anomalous effect presumably because acetone is capable of dissociating more numbers of triple $(H_2O)_3$ molecules with the result that the velocity increases.

5. Summary

Sound velocities are determined in mixtures of acetone and water at a frequency of 64·36 Mc. per sec. for different concentrations. Results show an anomalous increase in velocity of water with addition of acetone reaching a maximum of 1583 m/sec. at a composition of 24% by weight of acetone. A possible explanation is given on the assumption that acetone induces the breaking up of polymerized water molecules into simpler ones.

References

1. Bhagavantam and Ramachandra Rao .. *Nature*, 1946, **158**, 484.
2. Parthasarthy, S. .. *Proc. Ind. Acad. Sci.*, (A), 1936, **3**, 297.
3. Smith, A. W., and Ewing, L. M. .. *Jour. Chem. Phys.*, 1931, **7**, 632.
4. Sambasiva Rao, C. .. *Phil. Mag.*, 1935, **10**, 587.
5. *Carnegie Institution of Washington Publication*, 1907, No. 60.

TORSIONAL OSCILLATIONS IN QUARTZ PLATES

By S. Ramachandra Rao

(From the Department of Physics, Andhra University, Waltair)

Received October 18, 1946

(Communicated by Prof. S. Bhagavantam, F.A.SC.)

1. Introduction

In view of the recent developments in this laboratory of experimental methods for the determination of the elastic constants of crystals by ultrasonic methods, a detailed investigation of the nature of oscillations in quartz plates with special reference to shear modes is taken up in the present investigation. From Christoffel's equation[1] for the propagation of sound in anisotropic media, it will be seen that in any crystal plate, like quartz, of a particular orientation there are three distinct velocities of propagation usually corresponding to the three natural fundamental frequencies of that plate. Atanasoff and Hart,[2] by taking suitably oriented plates and applying electric fields in various directions could obtain experimentally many different modes in quartz plates. They determined the elastic constants for all of them and identified some of them as shear modes. Later, Parthasarathy and his collaborators,[3] studying the oscillations of X-cut quartz plates, by the method of diffraction of light by ultrasonic waves, found certain additional frequencies which could not be explained either as the odd or the even overtones of the longitudinal fundamental. They interpreted these as half odd overtones of the same longitudinal fundamental. Then Bhagavantam and Suryanarayana[4] suggested that shear modes could also be obtained by the same diffraction method and they actually found that an asymmetry of electric field in the crystal plate produces shear modes and even overtones with considerable strength. In this laboratory other workers have subsequently transmitted shear modes even through non-crystalline plates by suitable methods.[5]

In this paper, various methods favourable for producing shear modes in quartz plates and communicating them to a liquid to get the diffraction patterns are investigated. Methods of obtaining various types of asymmetry of field by different kinds of silvering on the surfaces of the crystal plate and of introducing varying degrees of error in the orientation of the X-cut quartz plates with a view to produce and detect shear modes form the main work.

2. Experimental Details

A good specimen of quartz with well developed faces is taken and the plates required are prepared in this laboratory by the author. Constant thickness gadgets are utilised to get plates of uniform thickness with an accuracy of ·01 mm. Parallel plates with the required orientation, especially of such a low order error as 1°, 2°, 3°, etc., could be easily and accurately secured by means of inclined gadgets designed for the purpose. A suitable Hartley shuntfed oscillator with a sufficiently high power is constructed and used to excite crystal plates piezo-electrically. The bottom electrode is an annular ring while the top one is a small brass disc. The usual diffraction method of Debye and Sears[6] is employed to detect the resonance positions. The frequencies are measured with a Phillips heterodyne wave-meter and a receiver. The liquid used for producing stationary ultrasonic waves is carbon tetrachloride.

3. Results

(*a*) *Fully silvered X-cut plate*

Table I

Thickness of plate = 1·02 mm.

Frequency F Mcs.	No. of orders	Intensity	Order of harmonic N	F/N
2·860	10	V, B	1	2·860
5·735	2	1B, 1F	2	2·867
8·680	3	B	3	2·893
11·380	1	F	4	2·845
14·340	1	B	5	2·868

Mean Fundamental = 2·865 Mcs. V. B = Very bright ; B = bright ; F = faint.

From Table I it will be seen that in an X-cut fully silvered quartz plate, only one set of frequencies corresponding to the longitudinal mode is obtained. Both even and odd overtones are observed but the intensity as well as the number of orders of the even overtones are found to be less than the next higher odd overtones. The relative strengths of the even and odd overtones in such a case will be clear from Fig. 1 in Plate XII. Attempts to find shear modes in this case or the so-called half-odd overtones have not met with any success.

(*b*) *Effect of different kinds of silvering*

Many types of desilvering are tried on X-cut plates, of which three different ones are shown in Fig. 4. These are found to give distinct and

different results. All the rest studied fall in one or other of these groups and hence they are not described here.

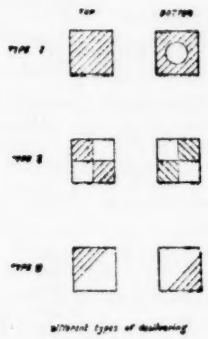

FIG. 4

TABLE II

Plate No.	Thickness mm.	Types of silvering	Mean fundamental frequency Mcs			Elastic constant $\times 10^{-10}$ dynes/cm.^{2}		
			Long.	Shear I	Shear II	Long.	Shear I	Shear II
I	2·02	Full	1·436	..	..	89·13	..	..
,,	,,	Type I	1·432	1·280	..	88·63	70·82	..
,,	,,	Type II	1·436	..	·750	89·50	..	24·32
,,	,,	Type III	1·423	1·274	·842	87·54	70·73	30·65
II	2·04	Full	1·407	..	..	87·22	..	..
,,	,,	Type III	1·413	1·264	·817	87·98	70·86	29·45

The intensity of a particular mode, which occurs in different types of desilvering, is fairly constant in all the types. The general intensity of shear modes is considerably high for desilvered crystals. Moreover, desilvering of any type increases the strength of the even overtones of the longitudinal mode while the intensity of odd ones is reduced slightly. With desilvering of type I, besides the longitudinal frequencies with a fundamental of 1·436 Mcs., another set having an entirely different fundamental namely 1·20 Mcs. is observed. Both even and odd overtones of this mode up to the 7th are obtained. With type II desilvering also, only one shear mode, with its overtones up to the 12th, has made its appearance but this is different from the previous one and has a fundamental of ·750 Mcs. With type III desilvering, the longitudinal mode with its even and odd overtones upto the 8th, and the two torsions with their overtones upto the 7th for torsion I in Table II and upto the 10th for torsion II in Table II are obtained. In all the above cases, the resonance positions of the torsion modes are very sharp.

occurring as flashes at higher overtones. Their intensity is always less than that of the corresponding longitudinal ones.

(*c*) *Effects of errors in orientation*:—

TABLE III

Direction*	Orientation	Thickness mm.	Third overtone of the shear modes present		Fundamental frequencies of modes obtained Mcs.			Elastic Constants $\times 10^{-10}$ dynes/cm.^{2}		
			No. of orders	Intensity Shear II	Long.	Shear I	Shear II	Long.	Shear I	Shear II
X–Y	1°	1·180	1	V. F	2·495	..	1·320	91·07	..	25·77
,,	2°	1·250	1	F	2·334	..	1·336	90·86	..	29·77
,,	3°	1·290	2	M	2·264	..	1·425	90·36	..	35·80
,,	4°	1·300	2	B	2·250	1·980	1·401	90·61	70·18	35·13
,,	5°	1·170	3	B	2·524	2·189	1·572	92·08	70·04	35·84
,,	10°	1·100	4	V. B Shear I	2·631	2·131	1·518	100·3	65·77	33·40
X–Z	1°	1·205	2	M	2·438	2·138	1·455	90·65	69·72	31·99
,,	3°	1·280	3	B	2·299	1·988	1·379	91·70	68·61	33·01
,,	5°	1·215	5	V. B	2·455	2·058	1·511	94·23	65·16	35·70
,,	10°	1·115	..	..	2·778	2·139	..	101·60	60·23	..

Notation for intensities: V. F. = very faint; F = faint; M = medium; B = bright; V. B = very bright.

* (X–Y) denotes all plates obtained by rotating the plate normal about the Z-axis so that the X-cut plate as a whole tends towards Y-cut plate.

(X–Z) denotes all plates obtained by rotating the plate normal about the Y-axis.

In the first series of plates, the normals are inclined to the X-axis slightly, *i.e.*, 1°, 2°, 3°, etc., due to rotation about Z-axis. It will be seen from Table III that in these cases even at 1° inclination one torsion begins to appear, though with a low intensity. The resonance of shear modes is sharp but their intensity is low. As the inclination is increased to 2° and 3° the intensity as well as the number of orders of the shear mode go on increasing. By the time an error of 4° is reached, the second shear mode also begins to appear with almost the same intensity as the first one. At 5° the strength of the two torsions becomes so great that they are almost equal in intensity to the corresponding longitudinal mode. This effect is reproduced in Fig. 2 of Plate XII. At 10°, the intensity of shear modes quite excels that of the longitudinal mode. The gradual increase, in intensity and in the number of orders, with increasing error in orientation is shown in Fig. 3 of Plate XII where the third overtone corresponding to shear II of Table III at different angles is photographed under similar conditions. The slight difference of the thickness of the plates does not affect the intensity of the modes.

A second series of plates where the plate normals are rotated about the Y-axis are also studied. The results are given in Table III. It will be seen that even at 1°, the two shear modes appear. The intensity of the shear mode with smaller fundamental, decreases as the orientation is increased till finally at 10° it vanishes. The intensity of the other shear mode increases rapidly with orientation so that even at 5° it excels that of the corresponding longitudinal mode in strength.

All the above plates with errors of orientation are fully silvered before using.

4. Discussion of Results

The occurrence of even overtones in a correctly X-cut crystal even when properly silvered is a well-known phenomenon. This may be due to the asymmetry of the electric field inside the crystal plate caused by imperfections like twinning, etc. Bergmann also notices their presence if strong and unsymmetric electric fields are applied. But they are less intense because their presence is not natural and only due to some defect. When the crystal plate is desilvered, a non-uniformity of field is artificially set up within the crystal and the occurrence of even overtones is facilitated. Hence their shooting up in intensity under such circumstances stands explained. But now the area over which the electric field becomes effective is small and the general intensity is reduced. We further notice in this investigation that under certain circumstances, the effect of an asymmetric field is also to produce shear modes since the inclined lines of force between the electrodes can be resolved into components in the two perpendicular directions in the plane of the crystal plate. The appearance of the two different shear modes in the two types of desilvering may be explained as follows: In one type the component in a particular direction may be strong enough to produce one torsion, while in the second the component in the second direction might have attained sufficient strength to produce the second shear and suppress the first. The interesting result is that efforts to get the two torsions simultaneously have become successful with desilvering of type III. Both are produced here showing that components of field necessary for both are sufficiently strong. The constants obtained from experimental frequencies are in good agreement with theoretically calculated ones. Instead of the plate normal being exactly along X-axis, if it is slightly inclined either towards Y-axis or Z-axis, as is the case with all the oriented plates worked above, a component of the electric field will be set up in Y or Z directions or in both depending on the orientation. There is at once every possibility of the shear modes being produced as a consequence. It is observed that even an inclination of 1° to the strictly X-cut plate, either towards (X-Y)

direction or towards (X-Z) direction, is sufficient to produce such modes as has been shown in this investigation. In larger orientations, the power of shear vibrations is very great because the electric field deviates much from the X-direction, so that the strength of longitudinal mode becomes less and less. Thus, the explanation that such frequencies are due to half-odd overtones becomes *prima facie* unacceptable.

It remains to be explained how these shear vibrations are being communicated to the liquid. This point has been dealt with in the earlier publications from this laboratory already cited and is presumably due to coupling effects by which every torsional mode also produces a corresponding longitudinal distortion of the crystal plate, however small it may be in amplitude. But as this is only an indirect method, the intensity of the diffraction pattern will not be as strong as for direct longitudinal vibrations. Elastic constants obtained from plates with 1° inclination are without much error, but as the orientation is increased the modes become more and more complicated and the error in the constants is increased as may be expected. The purpose of this investigation is however not to determine the exact values of elastic moduli. They are mainly utilized to identify different modes.

5. Summary

Various methods of producing torsions and their overtones in quartz plates and communicating them to a liquid are investigated. The effects of different types of desilvering and of producing slight errors in orientation are systematically studied. Three types of desilvering are found to give different results showing a possibility of producing either of the two torsions or both in any one instance in addition to the usual longitudinal mode. Even an inclination of 1° to the ideal X-cut towards either the Y or the Z directions is found to be enough to produce torsions. It is also found that as the inclination is increased, the strength of the torsions is also increased both in intensity and in the number of overtones present. One characteristic nature of torsions observed is their sharpness of resonance, occurring as flashes at higher overtones. In a properly silvered and correctly X-cut plate, both even and odd overtones of the longitudinal frequency only are observed, the intensity of even ones being less than the odd ones. Torsions and their overtones are absent in such a case.

References

1. Love .. *Mathematical Theory of Elasticity*, 1927.
2. Atanasoff and Hart .. *Phy. Rev.*, 1941, **59**, 85.
3. Parthasarathy and others .. *Jour. Sci. and Ind. Research*, 1944, **2**, 295.
4. Bhagavantam and Suryanarayana .. *Proc. Ind. Acad. Sci.*, 1945, **21**, 19.
5. ——— and Ramachandra Rao .. 1946, **23**, 254.
6. Debye and Sears .. *Proc. Nat. Acad. Sci.*, 1932, **18**, 409.

FIG. 1

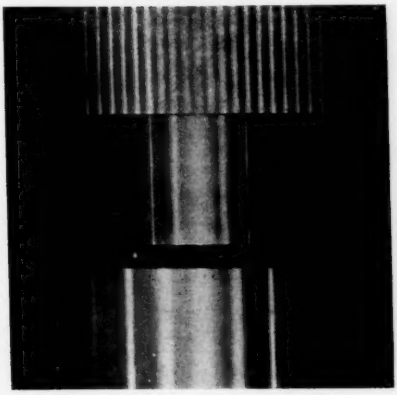

FIG. 2

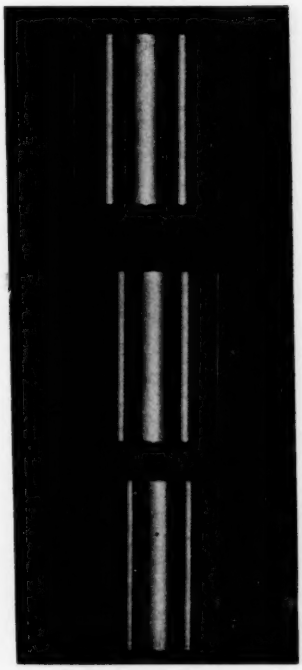

5° Inclination

FIG. 3

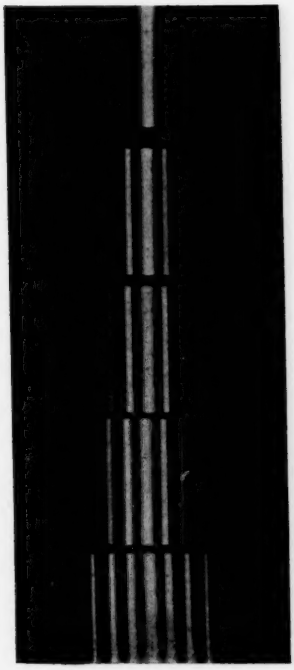

Third Overtone of Shear II

COPY OF MICR

THE MAGNETIC PROPERTIES OF IRON-PYRITES

By S. Ramaseshan

(From the Department of Physics, Indian Institute of Science, Bangalore)

Received January 20, 1947

(Communicated by Sir C. V. Raman, Kt., F.R.S., N.L.)

1. Introduction

The magnetic susceptibility of iron-pyrites (FeS_2) has been determined by various workers and widely different results have been reported. Recent studies on this substance by Sigamony (1944) have shown that the mass susceptibility values range from $0{\cdot}2 \times 10^{-6}$ to 190×10^{-6}, although a majority of the crystals tend to have values near about the lower limit. It was, therefore, thought that the study of the magnetic properties of a large number of crystals and an attempt to correlate the magnetic properties with other physical properties would be of considerable interest.

From the large stock of crystals in the possession of Sir C. V. Raman, 105 perfect crystals were selected. All the crystals, excepting one which was a twin, were approximately cubic in form having a bright metallic lustre. The crystals were all tin-white in colour.

2. Variation of Susceptibility with Specimen

An approximate determination of the susceptibility of each of the 105 crystals was made by observing the deflection produced in a Curie balance. The values of the mass susceptibility varied from $0{\cdot}2 \times 10^{-6}$ to 300×10^{-6}. Of the 105 crystals, 95 had values between $0{\cdot}2 \times 10^{-6}$ to $0{\cdot}7 \times 10^{-6}$, seven between $2{\cdot}5 \times 10^{-6}$ to 40×10^{-6} and three between 100×10^{-6} to 300×10^{-6}. Of these, 16 crystals having no flaws or imperfections were selected and accurate determinations of the mass susceptibility were made. For crystals having low susceptibilities Rabi's null method was used with a dilute solution of $MnCl_2$ as the bath. The crystal was suspended in the non-homogeneous field from one arm of a Curie balance of low torsional constant. Any deviation from the null point when the field was put on, could be very sensitively detected by a lamp and scale arrangement. It was found that in all cases the susceptibility was higher at a lower field. The crystals were usually saturated for fields above 5000 gauss, and the baths were adjusted for exact balance for fields greater than this. The value of mass susceptibility of crystals 3, 40, 105 and 17 were found by comparison with very strong

solutions of manganous chloride. The value for crystal No. 17 is only approximate. The susceptibility values of the 16 crystals are given in Table I.

TABLE I

Crystal No.	5	9	6	1	2	7
$\chi \times 10^6$	0·206	0·219	0·236	0·247	0·312	0·333
Crystal No.	4	8	16	18	33	35
$\chi \times 10^6$	0·356	0·391	0·492	0·503	0·530	0·627
Crystal No.	3	40	105	17		
$\chi \times 10^6$	2·43	28·9	187	280		

The field dependence of susceptibility of 7 crystals were determined and the results are given in Table II.

TABLE II

Crystal No.	$\chi \times 10^6$ 2900 gauss	$\chi \times 10^6$ 3700 gauss	$\chi \times 10^6$ 4500 gauss	$\chi \times 10^6$ 5400 gauss
5	0·224	0·210	0·206	0·206
6	0·263	0·244	0·236	0·236
7	0·351	0·340	0·334	0·333
35	0·671	0·639	0·628	0·627
3	..	2·97	2·50	2·43
40	..	34·5	29·8	28·9
17	..	365	289	..

The dependence of susceptibility on temperature was investigated for two crystals having low susceptibility values. The usual Curie balance method was employed. A heater with its coils non-inductively wound was used. The temperature was measured to an accuracy of one degree with a copper constantan thermocouple. It was found that if crystals were heated above 200° C. and cooled, the susceptibility values before and after heating differed slightly. The susceptibility of crystals increased from $0{\cdot}206 \times 10^{-6}$ to $0{\cdot}215 \times 10^{-6}$. This increase was absent when crystals were heated to 170° C. Table III gives the variation of mass susceptibility with temperature at different field strengths.

TABLE III

Crystal No.	Temperature	Susceptibility $\chi \times 10^6$		
		2900 gauss	3700 gauss	4500 gauss
1	25°	0·267	0·255	0·247
	65°	0·252	0·251	0·237
	92°	0·250	0·236	0·220
	122°	0·247	0·230	0·218
	163°	0·245	0·228	0·218
2	26°	0·339	0·326	0·312
	61°	0·329	0·319	0·302
	87°	0·323	0·312	0·295
	115°	0·317	0·307	0·290
	144°	0·315	0·305	0·285

All the 10 crystals having higher susceptibilities were tested for remanent magnetism. The periods of oscillation in the earth's magnetic field before and after the crystals were magnetised in a strong magnetic field (17000 gauss) were determined. The periods were the same within 0·005% indicating that there was practically no remanent magnetism. The crystals having high susceptibility (No. 17 and No. 105) were found to be slightly anisotropic.

3. CHEMICAL ANALYSIS

An estimation of the sulphur content of some typical crystals was made by chemical analysis. The method adopted is the one advocated by Hillebrand (1929). FeS_2 is oxidised by a solution of bromine in CCl_4 and HNO_3 to $FeSO_4$. The sulphur is precipitated out as B SO_4 and weighed. An accuracy of 0·5% could only be achieved. Table IV gives the sulphur content of some of the crystals.

TABLE IV

Crystal No.	Sulphur%			$\chi \times 10^6$
	Determination I	Determination II	Mean	
2	53·57	53·40	53·48	0·312
5	53·42	53·37	53·40	0·206
7	53·62	53·38	53·50	0·332
66	53·42	53·22	53·32	20·0

The results indicate that there are some stochiometric variations in sulphur content but the evidence is not conclusive owing to the inaccuracies

in the determination. It must be mentioned here that there was some insoluble component (most probably silica) in each of the crystals, the amount of this component being never more than 0·4%.

4. Specific Gravity Determination

As the chemical analysis was not very conclusive, a systematic determination of the specific gravity was undertaken. Each crystal was suspended from the arm of a chemical balance by means of a very fine quartz fibre. The weight of the crystal in air and in distilled water (25° C.) were determined from which the specific gravity was calculated. Table V and Fig. 1 give the specific gravity and magnetic susceptibility of 12 typical crystals. It is estimated that the error in the specific gravity determination could not be more than 2 or 3 units in the 3rd place of decimal. The letter (A) indicates the values of susceptibility that have been determined only approximately.

Table V

Crystal No.	Specific Gravity	$\chi \times 10^6$
1	5·001	0·247
4	4·997	0·356
10	4·995	0·230
8	4·990	0·391
3	4·992	2·43
103	4·980	7 (A)
91	4·973	15·0 (A)
66	4·982	20·0 (A)
40	4·970	28·9
45	4·943	139 (A)
105	4·930	187
17	4·919	289

5. Discussion of Results

The density of pure FeS_2 has been observed (1912, 1932) to be between 5·00 and 5·02 which is higher than the values of density of the different crystals used in this investigation. It will be noticed from Table V that the magnetic susceptibility is higher for crystals having lower densities. This precludes the possibility of the paramagnetic susceptibility arising out of iron as impurity; for in that case the density should increase with susceptibility. The lower values of the density could only be due to the absence of atoms of iron or sulphur or both from the lattice of iron-pyrites. The magnetic data, however, seem to favour the idea that the number of atoms of sulphur absent from the structure is more than twice the number of atoms of iron absent. In such a case the Fe: S ratio would be greater than 1:2.

In this connection the work of Juza and Blitz (1932) is of great interest. These workers have prepared a series of compounds of the formula FeS_n, n having values between 1 and 2, by heating pure iron pyrites under different

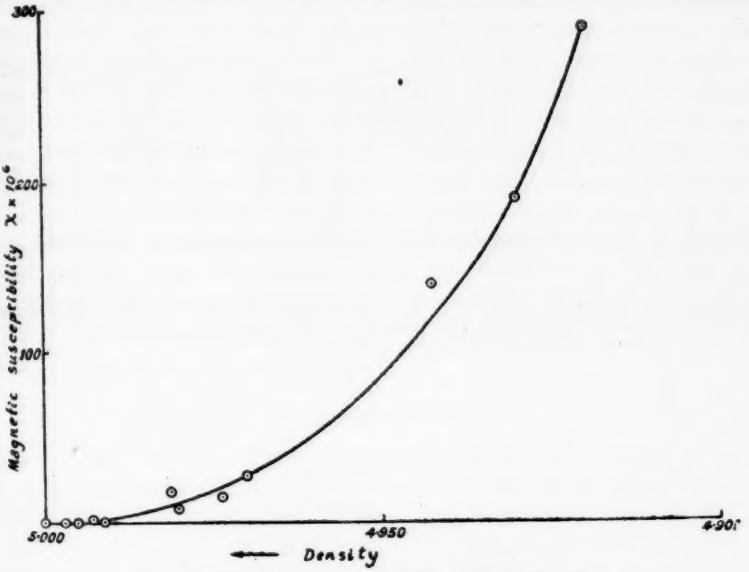

FIG. 1. Variation of magnetic susceptibility with density

conditions of temperature and pressure. The results of their studies on the X-ray structure, magnetic susceptibility and density of these substances are summarised in Table VI. The results of X-ray and magnetic investigations are particularly interesting. Compounds lying between FeS and $FeS_{1\cdot12}$ have the hexagonal crystal structure of Pyrrhotite, while those between $FeS_{1\cdot90}$ and FeS_2 have the cubic structure of iron-pyrites. Compounds having formulæ between $FeS_{1\cdot12}$ and $FeS_{1\cdot90}$ are composed of a mixture of FeS and FeS_2. The magnetic behaviour of these compounds is given in Fig. 2. The susceptibility gradually increases from $0\cdot4 \times 10^{-6}$ to 5500×10^{-6} as the iron: sulphur ratio decreases, but it drops to a very low value when the composition corresponds to $FeS_{1\cdot1}$. The curve given in Fig. 1 corresponds approximately to the part of the curve in Fig. 2 enclosed within dotted lines. As only very few observations of density and susceptibility of compounds having composition very near FeS_2 have been made by Juza and Blitz, no comparison can be made between their results and those obtained in the present work. But a study of Tables V and VI and Figs. 1 and Fig. 2 shows clearly that the phenomenon observed in natural crystals of iron-pyrites

TABLE VI

Preparation	FeS_n n =	X-ray structure	Density	Mol. Vol.	$\chi \times 10^6$
1	1·942	FeS_2	4·978	23·7	0·45
2	1·907	FeS_2	4·975	23·5	283
3	1·720	FeS_2+FeS	4·894	22·7	1220
4	1·450	FeS_2+FeS	4·769	21·4	3180
5	1·345	FeS_2+FeS	4·725	20·9	4170
6	1·187	FeS_2+FeS	4·605	20·4	4930
7	1·118	FeS	4·593	19·95	5590
8	1·060	FeS	4·637	19·4	94·2
9	1·026	FeS	4·736	18·2	14·2

observed in this investigation is generally analogous to that observed by Juza and Blitz in artificially produced sulphides of iron. It may be mentioned here that the slight anisotropy observed in crystals having higher susceptibility may be due to the presence of hexagonal FeS in cubic FeS_2.

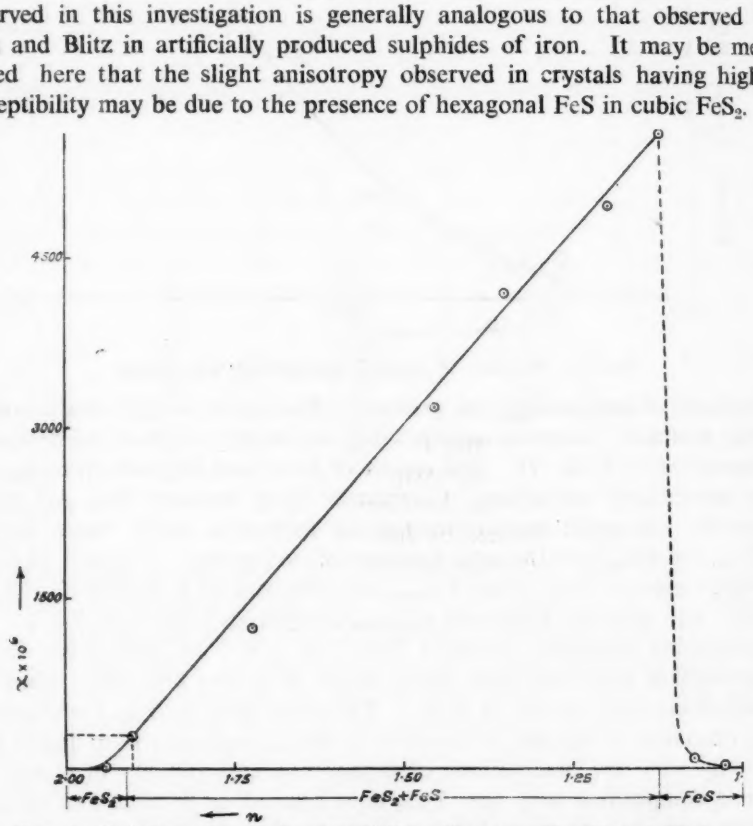

FIG. 2. Variations of magnetic susceptibility with composition (Juza & Blitz)

It is easy to qualitatively understand the appearance of paramagnetism due to the absence of sulphur atoms in the FeS_2 lattice. In the iron-pyrites

structure each iron atom is octahedrally surrounded by six sulphur atoms and each sulphur atom tetrahedrally by three iron and one sulphur atom. If the small residual paramagnetism of FeS_2 ($0{\cdot}2 \times 10^{-6}$) be neglected, one could consider all the spins of the electrons in the Fe—S and S—S bonds to be completely compensated. The removal of one sulphur atom from the FeS_2 structure results in the uncompensation of the spins in three Fe—S and one S—S bond giving rise to paramagnetism. It is hardly likely however that this elementary consideration would be sufficient to explain the high susceptibility values obtained by Juza and Blitz. Approximate computations show that while calculated and observed values are of the same order when the Fe: S ratio is nearly 1 : 2, they are widely different as the ratio increases.

In conclusion, the author wishes to thank Professor Sir C. V. Raman for the loan of the crystals of iron-pyrites and for the keen interest he took during the course of this investigation.

6. Summary

Determination of the magnetic susceptibility of 105 crystals of iron-pyrites have been made and it is found that 95 crystals have values between $0{\cdot}2 \times 10^{-6}$ to $0{\cdot}7 \times 10^{-6}$, seven between $2{\cdot}5 \times 10^{-6}$ and 40×10^{-6} and three between 100×10^{-6} and 300×10^{-6}. A definite correlation between susceptibility and density has been established, crystals with higher susceptibility having lower density. The lowering of the density may be attributed to the absence of iron and sulphur atoms from the crystal lattice. If the number of sulphur atoms missing from the lattice is much greater than the number of iron atoms thus increasing the iron: sulphur ratio, the magnetic data obtained with natural crystals of iron-pyrites in this investigation would be analogous to those obtained by Juza and Blitz with artificially prepared compounds of iron and sulphur having compositions intermediate between FeS_2 and FeS.

References

Allen, E. T., Crensham, J. L., and Johnson, J. .. *Amer. Jour. Sc.*, (4), 1912, **33**, 169.

Dana .. *A System of Mineralogy.*

Hillebrand .. *Applied Inorganic Analysis*, Wiley & Sons, 1929.

Jackson, L. C. .. *Nature*, 1929, **123**, 219.

Juza, R., and Blitz, W. .. *Zeit. anorg. Chem.*, 1932, **305**, 273.

Mellor .. *A Treatise on Inorganic Chemistry.*

Pauling, L., and Huggins, M. L. .. *Zeit. Krist.*, 1934, **87**, 205.

Sigamony, A. .. *Proc. Ind. Acad. Sci.*, 1944, **20A**, 204

PHOTOELASTIC CONSTANTS OF DIAMOND

By G. N. Ramachandran

(From the Department of Physics, Indian Institute of Science, Bangalore)

Received January 23, 1947

(Communicated by Sir C. V. Raman, Kt., F.R.S., N.L.)

1. Introduction

Although the photoelastic constants of various cubic crystals have been determined (Pockels, 1889, 1890, 1906), there appears to be only one observation made on the birefringence produced by pressure in diamond. This was made as early as 1851 by Wertheim (quoted in their book on Photoelasticity by Coker and Filon, 1931). Unfortunately, however, the crystallographic orientation of Wertheim's specimen is unknown. There seems to have been no other attempts at investigating the photoelastic behaviour of diamond. This is probably due to the difficulty of obtaining suitable specimens in the form of rectangular parallelepipeds and also fairly free from natural birefringence. The present investigation has been facilitated by the availability of such specimens in Sir C. V. Raman's collection. The experiments were carried out with three different specimens in each of which different directions of pressure and observation were employed. In this way, it has been possible to determine all the three piezo-optic constants that occur in the theory of photoelasticity (Pockels, 1906) for a cubic crystal. The interesting fact comes out that, for both pressures along the cubic and the octahedral axes, the strained crystal behaves optically as a positive uni-axial crystal. Also, it is found that the refractive index should decrease when subjected to a hydrostatic pressure. In both these respects, diamond stands unique among the cubic crystals that have been studied so far.

2. General Theory of Photoelasticity

Since the notation of the general theory of photoelasticity will have to be used often in later sections, it will be useful to give a brief resumé of its results here.

It is assumed that Fresnel's laws hold good in a homogeneously deformed crystal and that the differences between the optical parameters of the crystal in the deformed and the original states are linear functions of the six deformation components x_x, y_y, z_z, y_z, z_x, x_y or of the six stress components X_x, Y_y, Z_z, Y_z, Z_x, X_y. Thus, if a_{11}, a_{22}, a_{33}, a_{23}, a_{31}, a_{12} are the optical polarisation

constants of the deformed crystal according to an arbitrarily chosen co-ordinate system and if the original values of these are denoted by a superscript°, then we have the following relations:

$$\left.\begin{aligned}
a_{11}-a_{11}^{\circ}=\delta_{11}&=p_{11}\,x_x+p_{12}\,y_y+p_{13}\,z_z+p_{14}\,y_z+p_{15}\,z_x+p_{16}\,x_y\\
a_{22}-a_{22}^{\circ}=\delta_{22}&=p_{21}\,x_x+p_{22}\,y_y+p_{23}\,z_z+p_{24}\,y_z+p_{25}\,z_x+p_{26}\,x_y\\
a_{33}-a_{33}^{\circ}=\delta_{33}&=p_{31}\,x_x+p_{32}\,y_y+p_{33}\,z_z+p_{34}\,y_z+p_{35}\,z_x+p_{36}\,x_y\\
a_{23}-a_{23}^{\circ}=\delta_{23}&=p_{41}\,x_x+p_{42}\,y_y+p_{43}\,z_z+p_{44}\,y_z+p_{45}\,z_x+p_{46}\,x_y\\
a_{31}-a_{31}^{\circ}=\delta_{31}&=p_{51}\,x_x+p_{52}\,y_y+p_{53}\,z_z+p_{54}\,y_z+p_{55}\,z_x+p_{56}\,x_y\\
a_{12}-a_{12}^{\circ}=\delta_{12}&=p_{61}\,x_x+p_{62}\,y_y+p_{63}\,z_z+p_{64}\,y_z+p_{65}\,z_x+p_{66}\,x_y
\end{aligned}\right\} \quad (1)$$

or

$$\left.\begin{aligned}
a_{11}-a_{11}^{\circ}=\delta_{11}&=-\{q_{11}\mathrm{X}_x+q_{12}\mathrm{Y}_y+q_{13}\mathrm{Z}_z+q_{14}\mathrm{Y}_z+q_{15}\mathrm{Z}_x+q_{16}\mathrm{X}_y\}\\
\ldots\quad&\quad\ldots\quad\quad\ldots\quad\quad\ldots\\
\ldots\quad&\quad\ldots\quad\quad\ldots\quad\quad\ldots\\
a_{23}-a_{23}^{\circ}=\delta_{23}&=-\{q_{41}\mathrm{X}_x+q_{42}\mathrm{Y}_y+q_{43}\mathrm{Z}_z+q_{44}\mathrm{Y}_z+q_{45}\mathrm{Z}_x+q_{46}\mathrm{X}_y\}\\
\ldots\quad&\quad\ldots\quad\quad\ldots\quad\quad\ldots\\
\ldots\quad&\quad\ldots\quad\quad\ldots\quad\quad\ldots
\end{aligned}\right\} \quad (2)$$

The first group of constants p_{ij} are called the elasto-optic constants and the second group q_{ij} the piezo-optic constants. Between them, there are the relations:

$$p_{ij}=\sum_{1}^{6} q_{ik}\,c_{kj}; \qquad q_{ij}=\sum_{1}^{6} p_{ik}\,s_{kj}, \quad (3)$$

where $c_{kj}=c_{jk}$ are the elastic constants and $s_{kj}=s_{jk}$ are the elastic moduli. The set of 36 constants composed of the p_{ij}'s or the q_{ij}'s completely define the photoelastic behaviour of a crystal when subjected to known strains or stresses respectively. All the constants are, however, not independent if the crystal possesses elements of symmetry, so that the total number of independent constants is reduced (Pockels, 1906; Bhagavantam, 1942). Thus, in a cubic crystal, there are only three independent constants, *e.g.*, p_{11}, p_{12} and p_{44}, and the scheme of 36 constants will be as follows:

$$\begin{array}{cccccc}
p_{11} & p_{12} & p_{12} & 0 & 0 & 0\\
p_{12} & p_{11} & p_{12} & 0 & 0 & 0\\
p_{12} & p_{12} & p_{11} & 0 & 0 & 0\\
0 & 0 & 0 & p_{44} & 0 & 0\\
0 & 0 & 0 & 0 & p_{44} & 0\\
0 & 0 & 0 & 0 & 0 & p_{44}
\end{array} \quad (4)$$

The piezo-optic constants all follow an exactly similar scheme with only three independent constants, q_{11}, q_{12} and q_{44}. [In isotropic bodies like glasses, we have additional relations $p_{44} = \frac{1}{2}(p_{11} - p_{12})$ or $q_{44} = q_{11} - q_{12}$, so that there are only two independent constants.]

From the above formulæ, the following relations are readily derived for the polarisation constants of a cubic crystal made doubly refracting by an arbitrary stress:

$$\left.\begin{aligned} a_{11} &= a^{\circ 2} - q_1 X_x - q_2(X_x + Y_y + Z_z); \quad a_{23} = -q_3 Y_z \\ a_{22} &= a^{\circ 2} - q_1 Y_y - q_2(X_x + Y_y + Z_z); \quad a_{31} = -q_3 Z_x \\ a_{33} &= a^{\circ 2} - q_1 Z_z - q_2(X_x + Y_y + Z_z); \quad a_{12} = -q_3 X_y \end{aligned}\right\} \qquad (5)$$

where $q_1 = q_{11} - q_{12}$, $q_2 = q_{12}$, $q_3 = q_{44}$ and a° is the velocity of light in the unstrained medium on the basis that the velocity of light *in vacuo* is unity, *i.e.*, $a^\circ = 1/n$, where n is the refractive index of the natural crystal.

From equations (5), it can be shown that, in general, the crystal behaves as a biaxial crystal when subjected to a linear compression or dilatation, except when the stress direction is parallel to a cubic or an octahedral axis, when it behaves as a uniaxial crystal with the optic axis parallel to the direction of the stress. However, for an arbitrary stress direction, the *directions* of the principal axes of polarisations, and consequently those of the two optic axes and the value of the optic axial angle, are *independent of the magnitude of the pressure*. They depend only on the value of the constant q_3/q_1, which may be denoted by χ. Thus, in so far as one is interested in the direction of the principal axes of polarisation and of the optic axes of a deformed cubic crystal, the phenomena can be described in terms of a single constant χ.

Further, the magnitude of the birefringence, *i.e.*, the path difference between the two polarised waves propagated in any direction along the deformed crystal, is a linear function of the pressure and of two constants q_1 and q_3, the constant q_2 not being involved at all. Thus, no observations made on the relative retardation of the rays propagated through the compressed crystal can enable one to determine the value of q_2. For this purpose, one requires also measurements on the absolute retardations of the two components, *i.e.*, the variations in the optical path of a beam of light when the crystal is subjected to strain.

The experimental work thus falls naturally into two stages: (1) the determination of q_1 and q_3 on the basis of measurements made on the relative retardations of the polarised components, for various directions of pressure and of observation and

(2) the determination of q_2, and thus of q_{11} and q_{12} separately, from the measurement of absolute retardations.

3. Determination of the Constants q_1 and q_3

Three specimens of diamond, N.C. 73, N.C. 85 and N.C. 60 from Sir C. V. Raman's collection, were employed for the present studies. Of these, N.C. 73 and N.C. 85 were opaque to the ultra-violet below 3000 Å.U., while N.C. 60 was transparent down to 2250 Å.U. N.C. 73 was particularly suited for the investigation since it exhibited very little natural birefringence. The orientations and the magnitudes of the length, breadth and thickness of the three diamonds are given in Table I below. The orientations were determined by X-rays and are correct to within 1°.

Table I

No. of diamond	Length		Breadth		Thickness	
	mm.	Parallel to	mm.	Parallel to	mm.	Parallel to
N. C. 73	8·05	[01$\bar{1}$]	5·08	[$\bar{2}$11]	0·67	[111]
N. C. 85	7·46	[$\bar{2}$11]	2·70	[01$\bar{1}$]	1·03	[111]
N. C. 60	9·77	[01$\bar{1}$]	6·32	[111]	1·27	[$\bar{2}$11]

A simple apparatus, shown diagrammatically in Fig. 1, was used for subjecting the crystal to a linear compressive stress. The crystal in the form of a rectangular block was placed on a firm plane horizontal support *A* and the load was applied by means of a horizontal movable bar *B*. This bar had two circular holes by which it could be fitted and made to slide smoothly along two cylindrical upright pillars *P* fixed to the base. It rested freely on the crystal and the crystal was compressed by adding weights to two pans hanging from the ends of the bar, the weights in the two pans being always adjusted to be the same. To uniformise the pressure, lead washers about 2 mm. in thickness were placed both above and below the crystal. To prevent any damage to the crystal from the heavy bar falling on it in case it slips and falls flat, two supporting screws *S* were included having locknuts. These could be adjusted such that their height is a little less than that of the crystal, so that normally the loaded bar *B* rested on the crystal, while if the crystal fell down it rested on the supporting screws. No lever arrangement, such as was employed by Pockels, was used in the author's apparatus, for the crystals were all sufficiently small and the requisite stresses of 50 to 100 kg./sq. cm. could be obtained by applying directly loads of the order of 1 to 4 kg.

The measurement of the double refraction generated by pressure was carried out by means of a Babinet compensator for three wavelengths, *viz.*, the radiations of wavelengths 4358 and 5461 Å.U. from the mercury

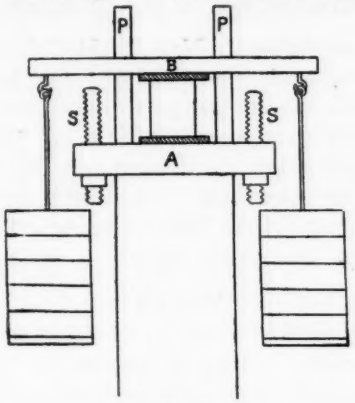

FIG. 1

arc and that of wavelength 5893 Å.U. from the sodium vapour lamp. The experimental set up may be described as follows. The direction of the pressure in the loading apparatus was vertical and this was made parallel to the length, breadth or thickness of the specimen as was necessary. The light from the source was first rendered parallel by means of a lens, and then polarised with its vibration vector exactly at 45° to the vertical, *i.e.*, to the pressure direction. This parallel polarised beam of light then passed through the crystal parallel to one of its two edges at right angles to the direction of the pressure. The emerging light was analysed by the Babinet compensator, which was kept with its principal axes exactly in the horizontal and vertical directions and the analyser at 45° to the vertical, but at right angles to the polariser.

Under these conditions it is obvious that, when the crystal is unstrained and if it possesses no natural birefringence, the central dark fringe of the compensator will be exactly in the zero position. When the load is applied, the fringes should shift and this shift was accurately measured. It is clear that the measured quantity represented the path difference between the two polarised rays having their vibration directions respectively horizontal and vertical. In general, the directions of vibration in the compressed crystal are parallel to these directions so that the measurement directly gives the magnitude of the birefringence. However, there occurred one case where this was not so, *viz.*, with N.C. 85 when the pressure direction was along [$2\bar{1}1$] and observation along [$01\bar{1}$], in which the vibration directions of the two waves in the crystal were inclined to the vertical. The same arrangement

of the Babinet compensator was used in this case also and the shift was measured. The meaning of this shift will be clear when one remembers that the elliptically polarised light emerging from the crystal is resolved into vertical and horizontal components by the compensator itself, and that the difference in phase of these two is what is indicated by the shift. In fact, this measurement served as a useful check on the others as will be seen a little later.

None of the crystals studied were free from birefringence, although N.C. 73 was very nearly so. Consequently, the compensator fringes were not in the zero position with the unstrained crystal. This was corrected for by bringing the fringes to the zero position both with and without the load and taking the difference to be due to the birefringence produced by the stress. This, of course, implies the asssumption that the optical effects of two arbitrary stresses are the same as if they are applied separately and their effects added up. That this is not far from being true is shown by the experiments themselves. As will be seen from Table II, measurements made on different crystals showing different amounts of natural birefringence agree fairly well. So also, observations made with light going through different regions of the same crystal (showing variations in natural birefringence) gave consistent results.

On account of the variations in natural birefringence, it is necessary that the measurements of path retardation must be performed for light passing through a small area of the crystal. In fact, such measurements could be done at different points on the cross-section of the crystal by employing the technique of obtaining the "Babinet pattern" of the crystal, described by the author in a recent paper (Ramachandran, 1946). It consists in focussing the image of the crystal on the plane of the quartz plates of the compensator. It is then possible by shifting the lens to make the central fringe to pass through any desired point of the image and measure the shift at that point. The aperture of the lens should be made small so that the divergence of the rays reaching the compensator is as small as possible, as otherwise the accuracy of the settings is impaired. The measurements were carried out at a number of points (usually 6 or 9) over the area of the crystal and the average shift taken as the correct value. This was done in order to allow for any non-uniformity in the distribution of stress. It was found that the shifts measured with the three different wavelengths did not differ by more than the experimental errors, so that no attempt was made to measure them separately, but an average was made of the measurements with different wavelengths. Hereafter, in talking of the shift, we shall always mean this final average value.

First, it was verified with N.C. 73 that over the range of stresses employed, *viz.*, upto 120 kg./sq. cm. the birefringence was exactly proportional to the stress. Later, measurements were made with only one value of the load. From these, the shift per unit stress per unit thickness was calculated for different directions of pressure and observation. These are given under the heading β in Table II and are expressed in terms of the number of divisions of the compensator. Theoretically, the expressions for this quantity have been worked out and are given in the last column in the same table. These again are not exactly equal to β, but are proportional to it. The full expression for β should contain a factor $2/n^3$ in addition to what is given in the table. The derivation of these expressions is rather cumbersome, but follow the method given by Pockels (1889), and has been omitted here. As already remarked, the expression for β has been calculated to represent the phase difference between the horizontal and vertical components.

TABLE II

Diamond	P along	O along	$\beta \times 10^4$	Expression for β
N.C. 73				
(1)	$[01\bar{1}]$	[111]	0·281	$(q_1+2q_3)/3$
(2)	$[\bar{2}11]$	[111]	0·279	$(q_1+2q_3)/3$
N.C. 85				
(3)	$[\bar{2}11]$	[111]	0·280	$(q_1+2q_3)/3$
(4)	$[01\bar{1}]$	[111]	0·272	$(q_1+2q_3)/3$
(5)	$[01\bar{1}]$	$[\bar{2}11]$	0·222	$(q_1+5q_3)/6$
(6)	[111]	$[\bar{2}11]$	0·178	q_3
(7)	[111]	$[01\bar{1}]$	0·169	q_3
(8)	$[\bar{2}11]$	$[01\bar{1}]$	0·301	$\frac{1}{6}\sqrt{33q_3^2+9q_1^2-6q_1q_3}$
N.C. 60				
(9)	$[01\bar{1}]$	[111]	0·282	$(q_1+2q_3)/3$
(10)	[111]	$[01\bar{1}]$	0·163	q_3
(11)	$[01\bar{1}]$	$[\bar{2}11]$	0·226	$(q_1+5q_3)/6$

It will be noticed that 5 measurements are available for $(q_1+2q_3)/3$, 2 for $(q_1+5q_3)/6$ and 3 for q_3. Of these, two of the first set have been obtained with N.C. 73, which was practically free from natural birefringence. Giving a weightage of 3 for these readings and 1 for the rest, the mean values

for the three quantities come out as 0·279, 0·224 and 0·170. q_1 and q_3 were calculated from these by forming the normal equations from these and solving them. They are $q_1 = 0·503$ and $q_3 = 0·168$. The observed values have been recalculated from these and are compared with the actual data in Table III. The comparison shows that the measurements are consistent. Making use of the observation that 5·39 divisions of the Babinet compensator correspond to 5893 Å.U., the absolute values of q_1, q_3 and χ have been calculated to be

$$q_1 = q_{11} - q_{12} = 7·8 \times 10^{-11},\ q_3 = q_{44} = 2·6 \times 10^{-11},\ \chi = 0·34 \qquad (6)$$

units are $\frac{cm^2}{gm}$

TABLE III

	Observed	Calculated
$(q_1+2q_3)/3$	0·279	0·280
$(q_1+5q_3)/6$	0·224	0·224
q_3	0·170	0·168
$(\sqrt{33q_3^2+9q_1^2-6q_1q_3})/6$	0·301	0·305

The corresponding elasto-optic constants have also been calculated from these, using the elastic constants determined by Bhagavantam and Bhimasenachar (1946), *viz.*, $c_{11} = 9·5 \times 10^{12}$, $c_{12} = 3·9 \times 10^{12}$, $c_{44} = 4·3 \times 10^{12}$.

We have

$$p_{11} - p_{12} = (q_{11} - q_{12}) \cdot (c_{11} - c_{12}) = 0·45 \qquad (7)$$

$$p_{44} = q_{44} \cdot c_{44} = 0·11$$

4. Determination of the Third Photoelastic Constant

As already remarked, it is necessary to measure the absolute retardations of the two polarised waves separately in order to determine all the three photoelastic constants. The method so far used for this purpose (which was first employed by Pockels, *loc. cit.*) was to use plane parallel plates of the crystal and to measure the variations in the path of each polarised wave, as the crystal is compressed, by means of an interferometer. Optically parallel plates of diamond were not available to the author, and therefore a new method was developed which makes use of the crystal itself as an interferometer. The diamond N.C. 73 was used for the purpose and localised interference fringes of the Newtonian type were produced by the interference of light obtained from the two surfaces of the crystal plate. In this particular specimen, the two faces were such that they together formed a convex lens, so that the fringe system consisted of concentric rings. The

surfaces of the diamond were deposited with aluminium by the evaporation process so as to increase the reflectivity and thus render the rings sharp. The surfaces were normal to [111], so that the light passed along this direction. The pressure direction was along [01$\bar{1}$]. The light was polarised with its vibration direction horizontal and vertical respectively and in either case the fringes were photographed with and without the load. The photographs were taken with three different wavelengths, *viz.*, 4358, 5461 and 5893 Å.U.

The fringes were not exactly circular and their spacings did not correspond to a spherical curvature of the surfaces. Consequently, interpolation formulæ had to be used to obtain the actual path change from the measured shift of the fringes. The widths of the fringes were measured along lines through a marked reference point on the surface of the diamond parallel to its length and breadth. Various types of interpolation formulæ were tried, but the simple Newton's formula was found to be most convenient with the available data. This was used and the path difference Δ was deduced by a method of successive approximations. Since the differences were of the order of 1/20 of a wavelength, the first approximation was generally sufficient. The path difference Δ was calculated from the shifts of the first three fringes and they agreed fairly well showing that the interpolation method was fairly satisfactory. For example, we may mention the calculated Δ's for the horizontally polarised beam in two experiments which were

0·050, 0·059, 0·054 ; 0·049, 0·053, 0·062.

Here again, no differences beyond the limits of experimental error were detected in the values of Δ with the different wavelengths of light and their average was taken. The final mean values of the changes in path for the rays with vibrations in the vertical and horizontal directions respectively were $\Delta_1 = +300$ Å.U. and $\Delta_2 = -333$ Å.U., the relative retardation thus coming out to be 633 Å.U. Actually, the relative retardation as deduced from the Babinet compensator measurements is 632 Å.U. checking very well with the result of the interferometric measurement. The remarkably close agreement must however be considered fortuitous. The accuracy of the interference method is only such as to expect an agreement of within $\pm$ 20 Å.U.

The path difference between the interfering beams is $2nt$ when the crystal is unstrained, where t is the thickness of the crystal and n its refractive index. Hence,

$$\Delta = 2(n\,\Delta t + t\Delta n) \qquad (8)$$

We are interested in the quantities Δn_1 and Δn_2, the alterations of the refractive indices for the vertically and horizontally polarised rays. For this

we require to know the change in thickness of the crystal owing to compression. This has been calculated from the theory of elasticity knowing the elastic constants quoted earlier. The contribution to Δ due to the alteration in thickness, *viz.*, $2n\Delta t$ thus comes out to be + 67 Å.U. Making this correction, we obtain the changes in path due to variation in the refractive index to be

$$t\Delta n_1 = +233 \text{ Å.U. and } t\Delta n_2 = -400 \text{ Å.U.} \quad (9)$$

These quantities are respectively proportional to $(3q_1 + 6q_2 + 3q_3)/6$ and $(q_1 + 6q_2 - q_3)/6$. Since q_1 and q_3 are known, $q_2 = q_{12}$ comes out to be $-3{\cdot}6 \times 10^{-11}$. Also, $q_{11} = q_1 + q_{12} = 4{\cdot}2 \times 10^{-11}$.

The values of p_{11} and p_{12} can be calculated from these. They are:

$p_{11} = c_{11}\, q_{11} + 2\, c_{12}\, q_{12} = 0{\cdot}12_5$, $p_{12} = c_{12}\, q_{11} + (c_{11} + c_{12})\, q_{12} = -0{\cdot}32_5$.

5. Discussion of the Results

In Table IV below, the piezo-optic and elasto-optic constants of diamond as determined from the present investigation are shown together with the corresponding constants of other cubic crystals that have been studied so far (Pockels, 1906).

Table IV

	Piezo-optic Constants				Elasto-optic Constants			
	$q_1 \cdot 10^8$	$q_3 \cdot 10^8$	χ	$q_2 \cdot 10^8$	$p_{11} - p_{12}$	p_{44}	p_{11}	p_{12}
Rocksalt ..	−1·183	−0·833	+0·704	+1·43	−0·0408	−0·0108	+0·137	+0·178
Sylvine ..	+1·67	−4·22	−2·525		+0·0595	−0·0276	+0·229*	+0·170*
Fluorspar ..	−1·420	+0·685	−0·482	+1·134	$-0{\cdot}172_2$	+0·0236	$+0{\cdot}055_5$	+0·227
Potassium alum ..	−4·30	−0·455	+0·106					
Ammonium alum ..	−4·462	−0·774	+0·173					
Diamond ..	+0·0078	+0·0026	+0·34	−0·0036	+0·45	+0·11	$+0{\cdot}12_5$	$-0{\cdot}32_5$

* These were not measured photo-elastically, but were deduced from the variation of the refractive index with temperature.

It will be noticed from the table that the piezo-optic constants of diamond are roughly a few hundred times less than those for other crystals, while the elasto-optic constants are of the same order. In other words, when subjected to the same strain, the change in the refractive index of diamond is of the same order as that for other cubic crystals; but when

subjected to the same stress, it is enormously less. This obviously arises from the large values of elastic constants, which are in fact the largest known for any crystal.

Further, both q_1 and q_3 are positive for diamond as distinct from all the other crystals. This means that diamond behaves as a positive uniaxial crystal for unilateral pressures along the cubic and octahedral axes and as a positive biaxial crystal for pressures along the dodecahedral axis or along any other direction.

Another interesting fact follows if we calculate how the refractive index would alter when the crystal is subjected to a uniform hydrostatic pressure. If Δn is the change of the refractive index n, then it can be shown that

$$\Delta n = -\frac{n^3}{2} \cdot \frac{p_{11}+2p_{12}}{3} \cdot e \qquad (10)$$

where e is the volume strain (dv/v), which is positive for a dilatation and negative for a compression. For diamond, $(p_{11}+2p_{12})/3$ is equal to $-0{\cdot}175$ so that *the refractive index decreases when diamond is subjected to a hydrostatic pressure.* It will be noticed from Table IV that $(p_{11}+2p_{12})/3$ is positive for all the other crystals which therefore would be expected to show the usual behaviour, *viz.*, an increase of refractive index under compression. Even in these crystals, however, the numerical value of $dn/d\rho$ is appreciably smaller than the value calculated from the Lorentz-Lorenz equation (Mueller, 1935),

$$viz., \qquad dn/d\rho = (n^2-1)(n^2+2)/6n\rho \qquad (11)$$

Mueller has sought to represent this difference by the addition of a factor $(1-\lambda)$ on the right-hand side. The quantity λ may be called the photoelastic anomaly, which has a value roughly $0{\cdot}4$ for glasses and about $0{\cdot}5$ for NaCl, KCl and CaF_2. In diamond, however, $dn/d\rho$ is negative, so that λ is greater than unity. The value calculated from the data of the present investigation is $1{\cdot}15$. As explained by Mueller, the anomaly arises from the alteration in the polarizabilities of the atoms in the crystal accompanying the strain. A fuller discussion of the question is reserved for a later communication.

In conclusion, I wish to express my sincere thanks to Prof. Sir C. V. Raman for the many discussions I had with him during the course of the investigation.

Summary

All the photoelastic constants of diamond have been determined for the first time. The three stress-optic coefficients are $q_{11} = 4{\cdot}2 \times 10^{-13}$,

$q_{12} = -3{\cdot}6 \times 10^{-11}$, $q_{44} = 2{\cdot}6 \times 10^{-11}$, from which the elasto-optic coefficients have been deduced to be $p_{11} = 0{\cdot}12_5$, $p_{12} = -0{\cdot}32_5$, $p_{44} = 0{\cdot}11$. It is found that $q_{11} - q_{12}$ and q_{44} are both positive and also that the refractive index of the crystal should decrease when subjected to a hydrostatic pressure, both of which are unique for diamond among the cubic crystals studied so far. In the course of the investigation, a new technique has been developed for determining the absolute path retardation, based on the production of localised interference fringes by the light coming from the two surfaces of the crystal.

References

1. Bhagavantam, S. .. *Proc. Ind. Acad. Sci.*, A, 1942, **16**, 359.
2. ——— and Bhimasenachar, J. .. *Proc. Roy. Soc.*, A, 1945, **187**, 381.
3. Coker, E. G., and Filon, L. N. G. "*Photo-elasticity*," 1931, 209.
4. Mueller, H. .. *Phys. Rev.*, 1935, **47**, 947.
5. Pockels, F. .. *Ann. d. Phys.*, 1889, **37**, 144, 372; 1890, **39**, 440.
6. ——— .. "*Lehrbuch der Kristalloptik*," 1906, pp. 467 *et seq.*
7. Ramachandran, G. N. .. *Proc. Ind. Acad. Sci.*, A, 1946, **24**, 68.

254

1371-46 Printed at The Bangalore Press, Mysore Road, Bangalore City, by G. Srinivasa Rao, Superintendent and Published by The Indian Academy of Sciences.